Roles for cell surface glycans in guiding human pluripotent stem cell fate

By
Deena-Al Mahbuba

M.S. Biochemistry
University of Wisconsin-Madison, USA 2017
M.Sc Molecular Medicine
University College London, UK 2013
B. Sc. (2010) and M.S. (2011) in Biochemistry and Molecular Biology,
University of Dhaka, Bangladesh

SUBMITTED TO THE DEPARTMENT OF CHEMISTRY IN PARTIAL FULFILLMENT OF THE REQUIREMENTS FOR THE DEGREE OF

DOCTOR OF PHILOSOPHY IN CHEMISTRY
AT THE

MASSACHUSETTS INSTITUTE OF TECHNOLOGY
May, 2022

Signature of Author: _____
Department of Chemistry
April 25, 2022

Certified By: _____
Laura L. Kiessling
Novartis Professor of Chemistry
Thesis Supervisor

Accepted By: _____
Adam P. Willard
Associate Professor of Chemistry
Chair, Department Committee on Graduate Students

This doctoral thesis has been examined by a committee of professors
from the Department of Chemistry as follows:

Professor Alex Shalek _____

Thesis Committee Chair
Associate Professor of Chemistry

Professor Laura L. Kiessling _____

Thesis Supervisor
Novartis Professor of Chemistry

Professor Angela N. Koehler _____

Thesis Committee Member
Samuel A. Goldblith Career Development Professor in Applied Biology

DEDICATION

Amma
If only you were here!

Roles for cell surface glycans in guiding human pluripotent stem cell fate

By
Deena-Al Mahbuba

Submitted to the Department of Chemistry
on May 6, 2022 in Partial Fulfillment of the
Requirements for the Degree of
Doctor of Philosophy in Chemistry

Abstract

Cell-surface polysaccharides are a fundamental component of the stem cell microenvironment. They are known to modulate developmental signals- critical for pluripotency and differentiation. Nevertheless, the architecture of the cellular glycocalyx and how these structures direct the fate of human pluripotent stem (hPS) cells have not been fully explored. I addressed this gap with a focus on a critical glycan of the hPS cells niche, heparan sulfate (HS). HS is a heterogeneous long-chain cell-surface polysaccharide. The spatial distribution and ultrastructure of this information-rich, signaling polysaccharides are poorly defined. In this work, I aim to understand the interplay between the HS organization and the developmental signal transduction in the hPS cells' microenvironment. We discovered that HS of hPS cells has a dynamic ultrastructure that undergoes changes during lineage-specific differentiation. These changes also correlate with the cells' ability to bind specific growth factor. While variations in HS sequence were thought to be the primary driver of alterations in HS-mediated growth factor signaling, our findings indicate a role for HS ultrastructure in its ability to recruit growth factors in stem cell niche. To advance the understanding of its roles in human development, next we engineered a HS-deficient cell line derived from hPS cells. Parallelly, I set out to develop a synthetic, modular surface-based cell separation strategy that can isolate or enrich cells of interest in a rapid and label-free way. I applied this strategy to isolate genetically engineered HS-deficient hPS cells after a CRISPR modification by engaging the cell surface HS with a small peptide-presenting synthetic surface. These HS-deficient hPS cells aid the investigation further to understand the role of HS in human development. We showed that the multi-lineage commitment of hPS cells depends on HS. Moreover, lack of HS hinders the proper neuronal projections and synaptic vesicle formation in hPS cell-derived neurons, suggesting a specific role of HS in human neural development. Taken together, these results indicate that HS has a highly dynamic ultrastructure that modulates cell fate choices of hPS cells, specifically neuronal connection formation. This work paves the way to a better understanding of HS's role in early human development.

Thesis Supervisor: Laura L. Kiessling
Title: Novartis Professor of Chemistry

Acknowledgments

The last seven years have been an incredible experience for me and this Ph.D. has been quite a journey. I am absolutely grateful for all the relationships I have built and all the experiences I have gathered. I can't write this without saying thank you! To all of you, who supported and encouraged me and helped me to actually make it to the finish line- I owe a debt of gratitude.

First, I want to thank my graduate advisor, Prof. Laura Kiessling. I will forever be grateful to you for your encouragement, guidance, and your patience with me. You have always believed in me and I appreciate truly that you took the time to support me. I would like to thank Prof. Kiessling for providing me the freedom to craft my project to drive it in the direction that I found most interesting. This freedom helped me immensely to grow as an independent and confident scientist. I feel very lucky to have an advisor who always had my back!

I would also like to thank Professors Alex K. Shalek and Angela Koehler for their willingness to serve on my committee. Their support ensured my timely progress in research.

I started my graduate career at UW-Madison with Prof. Alessandro Senes. While I never anticipated transferring to a new school midway through my PhD, but life happened! I feel incredibly blessed to have you as my advisor and would like to thank you for giving me such an enriching experience in Senes lab. Apart from being my advisor, Prof. Senes provided me the support during some very difficult times and helped me to make the choices that were transformative for my professional career. It's already rare to have one true mentor in life I am so lucky to have two! I should also mention my amazing friends from Senes lab, Sam, Sam, Sam (yeah, three Sams that I am friends with), Gladys, and Rika.

One of the best perks of Kiessling lab is the people, they make the lab a great place to live and learn and grow! I am forever grateful to Sayaka for welcoming me to the Kiessling lab. Sayaka, thank you for being my ears for all those years. I absolutely enjoyed learning about sugar and stem cell from you. You are such a kind, hard-working person with amazing organizational skills. I miss all of our hours together in the TC room and thanks to you, now I am a frantic fan of matcha latte! Fima and Jo Klim, you guys never stopped helping a fellow student in the stem cell lounge. Danny, even though we never shared Kiessling lab space together, you are always my 'kiessling-lab-buddy'. You always put your best effort into your friendship which makes you one wonderful kind-hearted friend. Deep, you are one of the most genuine persons I have ever met! I absolutely admire your scientific enthusiasm and your attention to detail. Thank you so much for all the support, I can't ask for a better teammate! I am trying to believe in your mantra 'everything will be ok'! Qiao, my friend, who made my early days in stem cell lounge manageable. Thank you for being my late-night experiment companion! I am very excited about the new additions to our stem cell lounge-Shiwei, a true heparan sulfate enthusiast, so passionate! Carolina, and Ankit for bringing so many great perspectives!

In the last five years in Kiessling lab, I found myself really lucky to make some friends who truly always had my back! Amanda, you are like my long-lost big sister. Living in a foreign country or adjusting to a new lab, or figuring out the overwhelming motherhood, you are my go-

to person with any questions! I admire you so much as a scientist and a person, and I learned so much from you! I am truly grateful for your friendship! Kathrine, the mini-influencer of my life! My go-to person with any random questions, be it about science, fashion, or deeply philosophical! I have so many links in our message thread that I still need to catch up with! And I promise I will finish that needlepoint before the 2022 Christmas! Your warmth, laughter, and brilliance have built a permanent place in my heart. Victoria, I am really out of words for what you mean to me! I am so so blessed to have a friend like you who would stand up for me literally always! I can't imagine getting through MIT without you; you made so many things bearable just by being there with me. You embraced me and my family so wholeheartedly, I can't thank you enough for that. Thank you for such a wholesome friendship. Your constant support (emotional and scientific) literally pulled me out of those difficult moments. Thanks for keeping me sane! I owe you so much!

Marlena-omorfia mou, who I feel deeply connected to even when we are living so far apart, who never fails to remind me how amazing life is. I must have done something really good to have a friend like you! Moon, it's very difficult to put our friendship in words really. Thank you for being so full of kindness, inspiration, and wisdom. You gave me 20 years of friendship where I can actually open my soul! Thanks for everything, thanks for reminding me when it's time to just suck up and move on!

I can't write this without saying thank you to my family for being with me through it all, from halfway across the world. Amma, Abbu- you have shown me the meaning of grit and perseverance and have always encouraged me to go beyond the circle of familiarity in order to make a meaningful impact in the world. I will try my best to keep my efforts going! Dear Ma, who never forgets to cheer me when I am down even a tiny bit. You, Baba always made it sure that I have a happy loving family to support me through all of it! Barpa, Chotpa, Bhaia- I am so lucky, so proud to be your little sister. You three were always there to hold me tight, shielded me from all the darkness out there, and never failed to lend your shoulder to lean on or to stand high. I love you all so so much. Thanks to my nephews and nieces for making life so joyful for me. And, Amma, my hero! Amma, I wish I could turn the time around and just be with you. I wish I could just hug you tight to tell you how much I miss you. I am here only because of you. I love you Ammu and I miss you so much!

By the end of the long graduate school, PhD turned out to be the true type II fun. There were countless moments when I thought I wouldn't do it. Thanks to Murshid, who made sure I keep going and ensured that it's all fun in the end. You are probably my biggest source of feedback but your support and encouragement helped me to grow immensely, I owe you so much for all of those. I am so proud of us as a team, together we can overcome so much. Thank you for being my partner in crime, for being one honest reviewer of my science, thanks for being such a loving baba to our daughter, Aara, and thanks for all the love and laughter!

Last but the most precious, my Aara! Ma, you showed me the meaning of true resilience. Having you in our life is probably one of the most intense experiences. We struggled together, we cried together, we laughed together. We overcame so much. You are my little bundle of joy who motivates me the most! Maa loves you so much Aara!

And with that Alhamdulillah for everything!

Table of Contents

Chapter 1: Human pluripotent stem cells and its microenvironment: from the origin to cell fate choices

Chapter 2: Dynamic changes in heparan sulfate ultrastructure modulate human pluripotent stem cell differentiation

Chapter 3: Heparan sulfate is indispensable for the neuronal differentiation of human pluripotent stem cells

Chapter 4: Ligand-specific synthetic surfaces for label-free enrichment of cell subpopulations

List of Figures

List of Tables

List of Abbreviations

ALK	Activin receptor-like kinase
BDNF	Brain-derived growth factor
BMP	Bone morphogenetic protein
BRET	Bioluminescence resonance energy transfer
Cas	CRISPR-associated
CSPG	Chondroitin sulfate proteoglycan
CRISPR	Clustered regulatory interspaced short palindromic repeats
DMEM/F12	Dulbecco's modified Eagel medium/Nutrient Mixture F-12_
DSPG	Dermatan sulfate proteoglycan
DUSP	Dual-specificity phosphatases
EC	Embryonal carcinoma
E-cadherin	Epithelial cadherin
ECM	Extracellular matrix
EpiS	Epiblast stem
EpCAM	Epithelial cell adhesion molecule
ERK	Extracellular signal-regulated kinase
ES	Embryonic stem
EXT	Exostosin
F-actin	Filamentous actin
FBS	Fetal bovine serum
FGF	Fibroblast growth factor
FN	Fibronectin
GAG	Glycosaminoglycan
GDF	Growth differentiation factor
GDNF	Glial Derived Neurotrophic Factors
HA	Hyaluronan
hES	Human embryonic stem
HEP	Heparin

HGF	Hepatocyte growth factor
HME	Hereditary multiple exostoses
hMS	Human mesenchymal stem
hPS	Human pluripotent stem
HSPG	Heparan sulfate proteoglycan
ICM	Inner cell mass
IP	Immunoprecipiation
iPS	Induced pluripotent stem
IVF	*In vitro* fertilization
Jak/Stat	Janus kinase/signal transducer and activator of transcription
KSPG	Keratan Sulfate proteoglycan
LEF	Lymphoid enhancing factor
LIF	Leukemia inhibitory factor
LM	Laminin
LRRTM	Leucine-rich repeat transmembrane proteins
MAPK	Mitogen-activated protein kinase
MEF	Mouse embryonic fibroblast
mES	Mouse embryonic stem
NCAM	Neuronal cell adhesion molecule
NEUROG	Neurogenin
NSC	Neural stem cell
PI3K	Phosphoinositide 3-kinase
PLCγ	Phosphoinositide phospholipase C
ROCK	Rho-associated kinase
SCNT	Somatic cell nuclear transfer
SEF	similar expression to FGF
SMAD	*C. elegans* Sma and Drosphila mothers against dpp (Mad)
SSEA	Stage specific embryonic antigen
TCF	T-cell factor
TSP	Thrombospondins
TGF-β	Transforming Growth Factor-β
TUJ1	Neuron-specific class III β-tubulin
TN	Tenascin
VHBD	Vitronectin heparin-binding domain
VN	Vitronectin

Chapter 1

Human pluripotent stem cells and its microenvironment: from the origin to cell fate choices

1.1 Overview

Pluripotent stem cells are unspecialized yet unique cells that are remarkable for their ability to self-renew and differentiate into specialized cell types under optimal conditions (*1*). These unique properties make them an excellent tool for studying mammalian development and disease. To exploit the full potential of stem cells to understand human development, the first step is to elucidate the origin of cellular pluripotency. To this end, determining the role of the stem cell microenvironment is crucial.

The stem cell microenvironment comprises soluble and insoluble factors that modulate the cell fate choices of pluripotent stem cells. While glycans are some of the most ubiquitous factors of this environment, they are the least explored. This chapter will cover advances in our understanding of the role of glycan and highlight unaddressed questions in the field.

1.2. States of pluripotency

Pluripotent cells can self-renew and differentiate to generate all the tissues of an organism (*2*). This self-renewal property defines the power of stem cells to go through numerous cycles of cell division while maintaining the undifferentiated state. Pluripotency refers to the ability of the cells to differentiate into derivatives of the three embryonic germ layers: mesoderm, endoderm, and ectoderm (*3*). The ectoderm derivatives are precursors to the nervous system (the brain and spinal cord, the peripheral nervous system); the sensory epithelia of the eye, ear, and nose; the epidermis, among other tissues. Mesoderm cells give rise to connective tissue, cartilage, bone; muscles; blood and lymph vessels and cells; the kidneys; the gonads and genital ducts. All the internal organs (e.g., liver, thymus, thyroid, pancreas, etc.) are derived from the innermost layer, called the endoderm. Their interaction with the cellular niche maintains stem cell pluripotency.

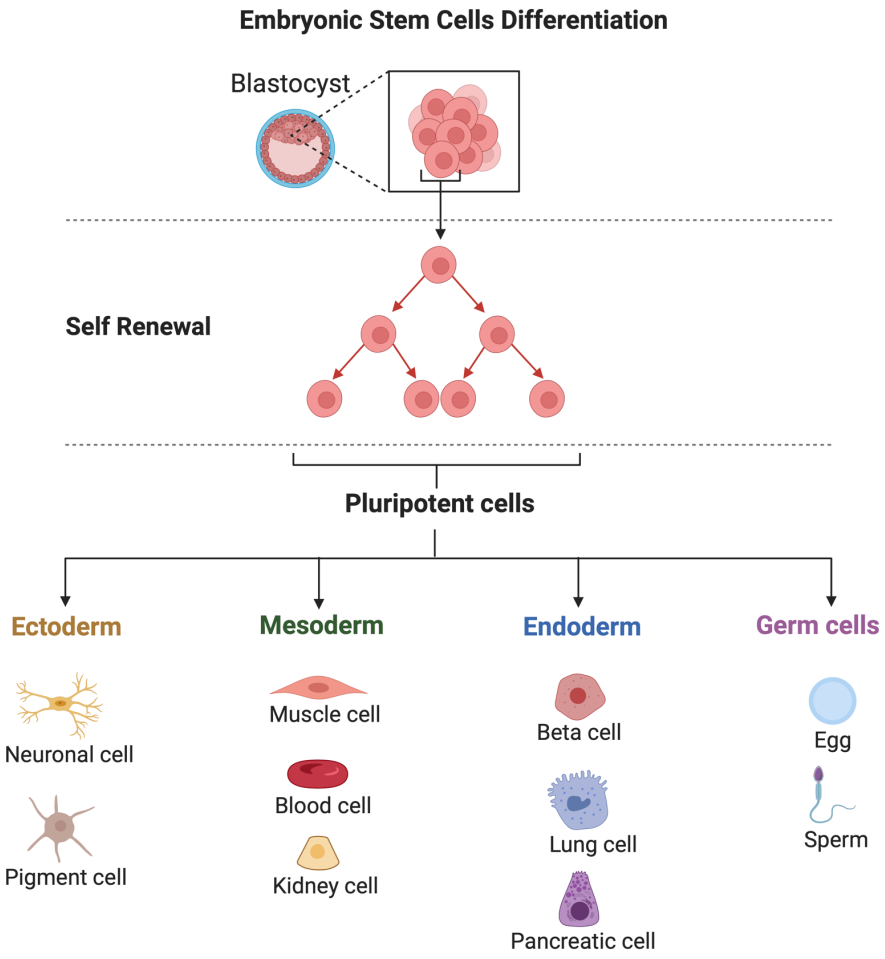

Fig.1.1. Embryonic stem cells can self-renew and give rise to all different cell types of the organism. Created with Biorender.com

1.2.1 Pluripotency during mammalian embryogenesis

Mammalian development begins with the formation of a totipotent single-cell zygote after the successful fertilization of an oocyte by a spermatozoon. Upon multiple successive divisions of blastomeres, the morula stage emerges with 32-64 totipotent cells (*4*). The cell's totipotency at this stage of embryogenesis is manifested by their ability to differentiate into all types of the organism's cells, including both the embryonic and extra-embryonic lineages (*5*). Right after this stage, the morula develops into a blastocyst, the first differentiation event of mammalian embryogenesis. The peripheral cells of the blastocyst (a hollow ball of cells) are the trophectoderm that forms the

embryonic membrane and placenta to nourish the growing embryo. The inner cell mass (ICM) gives rise to the epiblast that develops into the fetus. In 1968, Gardner *et al*. identified that these ICM cells are pluripotent, when they generated the first mouse chimera by injecting the extracted ICM into a receipt blastocyst (*6*). These resulting embryos survived to term with identified mosaicism in several tissues. These epiblast cells of ICM exist transiently during the early stages of embryogenesis and can differentiate into all the cell types of the adult organism.

Understanding stem cell pluripotency was advanced with the identification of embryonic carcinoma (EC) cells derived from gonadal tumors, termed teratomas. In the late 1950s, Stevens *et al*. identified the spontaneous testicular teratomas (*7*). Findings a decade later revealed that a single cell from this tumor can give rise to all the cell types found in the teratoma (*8*). These findings led to the isolation of the first mammalian pluripotent stem cell line (*9*) followed by the isolation of an EC line derived from the human teratoma (*10*). These discoveries were further expanded upon by uncovering a panel of glycan cell surface markers: stage-specific embryonic antigen 1 (SSEA1) for mouse-derived EC cells (*11*), and stage-specific embryonic antigen 3 (SSEA3) and 4 (SSEA4) for human EC cells (*12, 13*).

Though isolation of EC cells significantly advanced the study of pluripotency in the early age of stem cells, its malignant nature had limitations (*14, 15*), including its abnormal karyotype (*16*). This led to further research focused on deriving a nonmalignant pluripotent stem cell line.

1.2.2 Mouse embryonic stem (mES) cells

With the need for a cell culture system that could serve as a platform to study early embryonic development, a mouse embryonic stem (mES) cell line was derived from mouse blastocysts in the early 1980s. Many of the technological advancements used in the isolation of mES cells were established through the early studies using mouse EC cell lines. The first report of

mES cell isolation by Evans and Kaufman (1981) demonstrated that stem cells with normal karyotype could be cultured (*17*). Moreover, these cells formed teratomas when injected into the syngeneic mice, thus demonstrating pluripotency.

A more refined technique was employed by Martin *et al.* (*18*) who isolated mES cells without any *in vivo* alteration. They demonstrated the mES cells could be cultured by using a conditioned medium. They also noted that the conditioned media used to culture the cells contained a 'growth factor' that stimulate the proliferation of the normal pluripotent stem cells (*18*). These cells were the first line of 'embryonic stem cells' that could be maintained in an undifferentiated state for longer period. They demonstrated pluripotency by showing that the cells form teratomas. In addition, they demonstrated these cells could differentiate into multiple lineages. The remarkable discovery of mES cells ushered in a new era of stem cell biology and laid the foundation for the derivation of ES cell from the human embryo.

1.2.3 Human embryonic stem (hES)cells

The isolation of stem cells from pre-implantation human embryos was a major breakthrough in the stem cell history. After the derivation of mES cells, it took almost two decades before a human ES (hES) cell line was successfully generated (*19*). Many crucial advancements in science and technology were integrated into this endeavor. First, in *vitro* fertilization (IVF) was critical to hES isolation. The first successful mammalian IVF with rabbit gametes in 1959 (*20*) steadily led the scientific path to the birth of the first human child via IVF (*21*). With these advancements, hES cells were finally isolated from the surplus human embryos after the IVF treatment (*19, 22, 23*). The disclosure that hES cells had been isolated led to ethical and emotional concerns. Moreover, the rarity of human donors made it difficult to obtain cell lines that would be best suited to explore distinct diseases.

The first human ES cell line was derived by Thomson *et al.* 1998 (*19*). They isolated the ICM from the blastocyst by exposing the trophectoderm to antiserum followed by complement. In this approach, they used mouse embryonic fibroblast (MEF) as the feeder cell layer. With these aids, the blastocyst-stage embryos gave rise to the first line of hES cells that were karyotypically normal and demonstrated the full potential of pluripotency.

Over the last two decades, significant progress has been through the study of hES cell biology. For cell therapies, however, hurdles were identified. First, culture conditions that meet with FDA safety standards were needed. For example, hES cells were first cultured using mouse embryonic fibroblast feeder cells and fetal bovine serum (FBS). The addition of these agents induces the cell surface display of an immunogenic nonhuman sialic acid, Neu5Gc (*24*), which makes it challenging to use for clinical trials. Second, an expandable hES cell line was required that could generate enough number of different differentiated cell types for the downstream applications. Over the last decade, novel chemically defined cultural conditions have been developed that allowed the derivation of hES cells under the xeno-free conditions (*25*). Multiple differentiation protocols have been developed for generating a wide variety of cell types, including neural cells, blood cells, cardiac cells, and islet cells to name but a few (*26*). Together, these developments have added to the promise of the human pluripotent stem (hPS) cells as a potential solution to degenerative diseases including spinal cord injury, macular degeneration, diabetes, cardiac ischemia, and Parkinson's disease (*27, 28*).

1.2.4 Reprogramming somatic cells to a pluripotent state

To alleviate the ethical concerns associated with the hES cells, alternative strategies have been developed to attain pluripotent stem cells. The field was revolutionized by the generation of

induced pluripotent stem cells (iPSC) by reprogramming the adult somatic cells pioneered by Sir John Gurdon and Shinya Yamanaka (*29*).

Gurdon's studies of frog development showed that a differentiated somatic cell can be reprogrammed to ultimately generate a tadpole (*30*). These results indicate that pluripotency is not limited to the embryonic cells, but can be attained through reprogramming. This reprogramming approach through somatic cell nuclear transfer (SCNT) was further refined with the discovery of a transcription factor-based reprogramming (*31*). In 2006, Yamanaka and colleagues identified four crucial transcription factors (OCT4, SOX2, KLF4, and MYC) enough to reprogram the mouse embryonic fibroblast into pluripotent cells. Within a year of discovery, this technology was used for the derivation of human iPS cells from adult human fibroblasts (*29, 32*), contemporaneously with a similar report by Thomson and colleagues who used a slightly different set of 4 factors (*32*). Together they provided an alternative source of pluripotent stem cells without the need of human embryos (*28*).

The initial methods for cellular reprogramming used lentivirus or retroviral vectors to deliver the transcription factors with the possible risk of insertional mutagenesis. Over the years, many non-integrating methods have been developed including episomal DNA plasmids, Sendai virus, Adenovirus, synthesized modified mRNAs, and proteins (*28*). The pluripotency of mouse iPS cells has been thoroughly validated by demonstrating their ability to produce viable fertile mice (*33*). Eventually, it has been confirmed through genetically matched cell lines that iPS and ES cells are functionally and molecularly equivalent (*34*).

The major advantage of iPS cells is their ability to model disease *in vitro*. Human iPS cells have emerged as exciting tools for disease modeling, drug discovery, and cell therapy development (*35*). As human iPS cells are now successfully derived from a wide variety of different adult cell

types, including blood cells (*36*), they offer an unlimited source for studying the genotype-phenotype relationship. For example, the derivation of iPSCs from a patient with spinal muscular atrophy demonstrated the disease-specific deficits in iPS-derived motor neurons (*37*). A number of diseases have been subsequently modeled using iPS cells, including monogenic diseases, such as Rett syndrome (*38*) and type 2 long QT syndrome (*39*), and genetically complex diseases, such as Alzheimer's disease (*40*) and Parkinson's disease (*41*). Furthermore, iPS cells are used as an autologous cell source or as an HLA-matched allogeneic cell source that can minimize the risk of transplantation rejection. These features suggest that they can become a promising route for the immunologically compatible cell transplantation (*42*).

1.3 Stem cell microenvironment

The fate decisions of human pluripotent stem (hPS) cells are regulated by the signals that they receive from their microenvironment known as the stem cell niche. The signaling factors in the stem cell niche include both the soluble factors (receptors-growth factors (*43*) cytokines, cell-cell contact (*44*)) and the insoluble cues from the extracellular matrices with characteristic structure, compositions, and physiochemical properties (*45-47*). Precise control over stem cell differentiation *in vivo* is maintained by synchronizing these signals in the stem cell microenvironment. Replicating these cues *in vitro* can aid in regenerative medicine by boosting the effectiveness of differentiation protocols. Nevertheless, the mechanisms by which hPS cells respond to signals within the niche are still not completely understood.

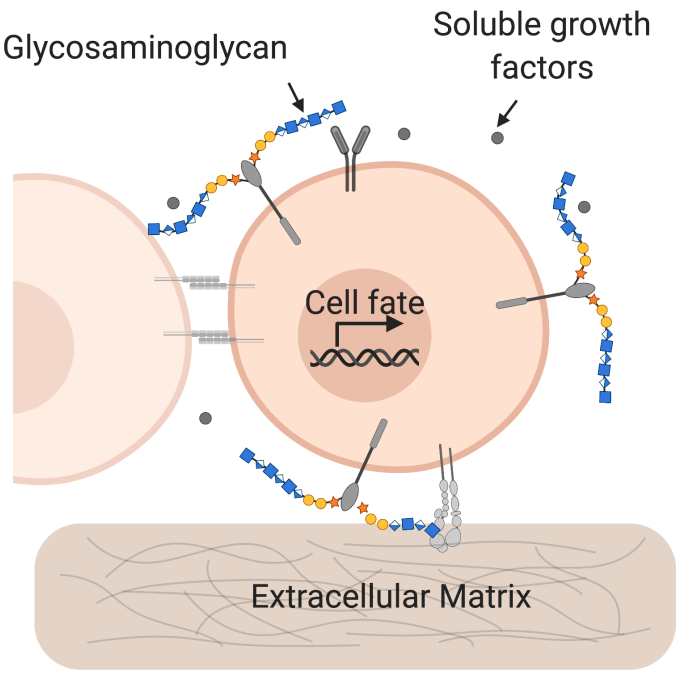

Fig.1.2. The stem cell microenvironment is composed of soluble and insoluble niche signals that govern the fate decision of ES cells. Created with Biorender.com

1.3.1 Soluble factors modulating stem cell fate choices

1.3.1.1 FGF signaling pathway

Fibroblast growth factor (FGF) signaling was identified as an important regulator of human ES cell pluripotency. Early studies identified a significant upregulation of FGF signaling in human ES cells (*48*). These findings corroborated the past observations of the benefit of adding exogenous FGF when maintaining human ES cells *in vitro* on an MEF feeder layer (*49*). Further characterization of the FGF signal alongside with others (*47*) enabled the development of chemically-defined standard cultural conditions currently in use for human ES cells.

FGFs comprise a family of 22 proteins that elicit mitogenesis and non-mitogenic effects through their binding to four specific receptors tyrosine kinases (FGFRs) (*50*). The signaling is initiated when an FGF ligand binds to an FGF receptor, resulting in autophosphorylation of the tyrosine residing in the intracellular domain of the receptor. The activated receptors transduce the

downstream signal through four dominant pathways: the Janus kinase/signal transducer and activator of transcription (Jak/Stat), phosphoinositide phospholipase C (PLCγ), phosphatidylinositol 3-kinase (PI3K), and Erk pathways (*51-54*).

Both extracellular and intracellular factors tightly regulate FGF signaling. All 22 ligands have two conserved cysteine residues that employ a high affinity to extracellular matrix sugar, heparin/heparan sulfate (HS). The extracellular heparan sulfate proteoglycan can bind the secreted FGF ligands and regulate its bioavailability. Thus, HSPGs act as important co-receptors in FGF signaling by facilitating the assembly of activated ligand-receptor complexes (*55*). Furthermore, the FGF signal can also be regulated intracellularly via a negative feedback loop; mostly through dual-specificity phosphatases (DUSPs), similar expression to FGF (Sef), Spred, and Sprouty proteins (*51*).

FGF signaling is crucial for maintaining pluripotency as well as the proliferation, differentiation, and migration of cells during mammalian cell development. In mES cells, the FGF/Erk signaling instructs the cells to exit the self-renewal phase and induce the differentiation (*56*); therefore, the inhibition of this signaling pathway increases the efficiency of ES cell maintenance. In contrast to mES cells, human ES cells exhibit a higher tendency to undergo spontaneous differentiation into extraembryonic lineages (*57-59*), and FGF signaling can block such spontaneous differentiation (*60-62*). In contrast to mES cells, FGF preserves the undifferentiated state of hES cells through PI3K/AKT, PLCγ, ERK1/2, and JAK/STAT pathways by inducing the activin and TGFβ signaling pathways (*63-65*) (discussed in section 1.3.1.4). Although the FGF and TGF-β signaling cooperatively regulate the human ES cell self-renewal, the molecular contribution of the FGF pathway to this process is not fully understood. Small molecule inhibitors of the MAPK/ERK pathway lead to differentiation, whereas inhibiting the

PI3K-AKT signaling route results in loss of proliferation and cell survival (*61*). FGF signaling is also vital for mesoderm and neural lineage-specific differentiation (*66, 67*). These findings indicate that FGF signaling in hES cells may play different roles in different contexts depending on the downstream activated pathway. This fine-tuned balance can be achieved through the regulation of FGF ligand-receptor expression. Furthermore, other extracellular signals including BMP, WNT, that are interconnected with the FGF pathway can influence outcomes.

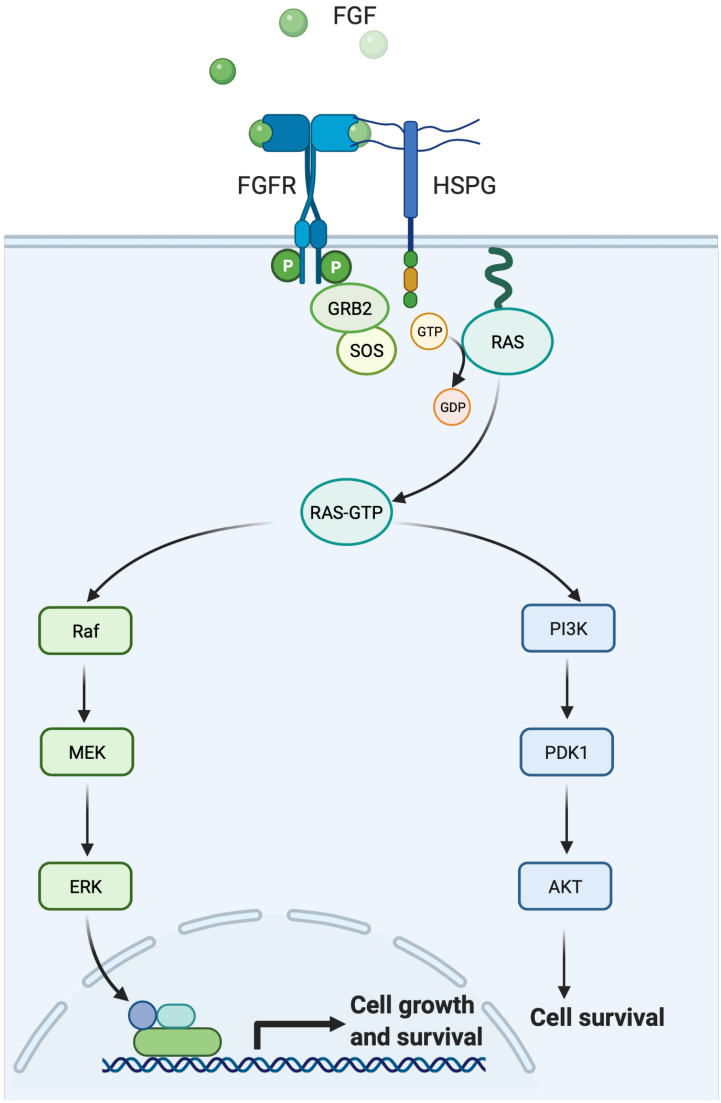

Fig.1.3. The overview of FGF singling. Created with Biorender.com

In summary, elucidating the critical contribution of the FGF signaling pathway to ES cell pluripotency and differentiation efficiency paved the way for developing defined culture conditions for human ES cell propagation. The delicate balance amongst interconnected signaling pathways modulates the cell fate choices of ES cells; thus, a more complete understanding of each pathway could significantly impact our knowledge early development and the fields of cell reprogramming and regenerative medicine.

1.3.1.2 BMP signaling pathways

Bone morphogenetic protein (BMP) is a vital extrinsic signal that directs both ES self-renewal and differentiation. BMP signaling, in conjunction with other extrinsic factors, intrinsic transcription factors, and epigenetic regulators delicately controls the cell fate of stem cells in a context-dependent manner.

There are 20 homodimeric or heterodimeric BMP ligands encoded by the human genome. These ligands induce downstream signaling by binding to the type I and type II BMP receptor (BMPRI, BMPRII) and forming a ternary complex (*68-70*). This complex elicits activation of the serine/threonine kinase in the intracellular domain of the type I receptors, which is followed by phosphorylation of BMP signal mediators, the receptor-activated Smads (R-Smads, Smad1/5/8). The phosphorylated Smads form a complex with the common-mediator Smad (Smad4) and translocate to the nucleus to elicit a transcriptional response (*71-74*).

BMPs are part of the transforming growth factor-β (TGF-β) superfamily of proteins, which includes TGF-βs, activins, inhibins, growth differentiation factors (GDFs), glial-derived neurotrophic factors (GDNFs), nodal, lefty, and anti-Müllerian hormone (*75*). All of these signaling agents are help regulate cell proliferation, differentiation, and therefore early embryogenesis (*76*). BMP signaling maintains the self-renewal of mES cells in cooperation with

leukemia inhibitory factor (LIF) signaling (*77, 78*). BMP signaling enhances the self-renewal propensity of mES cells by inducing the inhibitor of differentiation (Id) protein, downregulating several developmental regulators, and activating the LIF-induced ERK pathway. In human ES cells, BMP signaling plays a reverse role by inducing differentiation. Human ES cell differentiation into extraembryonic lineages, such as trophoblasts, was shown to be mediated by BMP signaling (*79*). Additionally, BMP signaling promotes the mesendoderm commitment of ES cells, in a temporal and context-dependent manner. Short-time stimulation with BMP4 ligand induces the expression of mesodermal genes such as Brachyury and MIXL1, resulting in the generation of the multipotent progenitor lineage, mesendoderm, that can further differentiate into lineages that include cardiac, hematopoietic, pancreatic, and liver cells. More specifically, BMP signaling contributes to mesoderm differentiation in the hematopoietic (*80, 81*) and cardiac (*82, 83*) lineages, and also endoderm derivatives in the hepatic lineage (*84*). Time-dependent inhibition is necessary for the differentiation into insulin-expressing pancreatic cells (*85*) and anterior foregut endoderm (*86*).

BMP signaling has long been established as an inhibitory factor for ectoderm-specific differentiation. In both mouse and human ES cells, this process is critical for the neural commitment (*87*). BMP directly induces the downstream signaling molecules, including Id family proteins (*78*), Dusp9 (*77*), Dpysl2, and Jmjd3 (*88*). However, the inhibitory effect of BMP signaling is phase and context-dependent. The delineation of neural vs. non-neural fate choice in the ectoderm specific differentiation route relies on dose-dependent treatment with BMPs. For the non-neural ectodermal lineage (neural crest (NC), cranial placode (CP), and non-neural ectoderm (NNE)), a precise pulse of BMP signal is required. In these cases, BMP directly induces the upregulation of the intrinsic factor, TFAP2A, which then acts in conjunction with another signal

(such as with WNT activation to generate neural crest, FGF activation to generate CP, and FGF inhibition to generate NNE) to determine the final ES fate choice (*89*).

Overall, BMP signaling directs a wide variety of cell fate choices in hES cells, both in the ectodermal and mesendodermal lineages. There are gaps in our current understanding of the signaling mechanism. Therefore, further investigations to elaborate the balance between BMP signaling and its partners, namely FGF and WNT, are needed.

1.3.1.3 Activin/Nodal/TGF-β signaling pathway

Activin/Nodal/TGF-β are ligands of the transforming growth factor (TGF)-β superfamily. These growth factors were identified as critical to maintain the human ES cells *in vitro*. They share this superfamily with other crucial intrinsic factors, such as BMP.

The downstream signaling of TGF-β superfamily ligands is transduced through cell surface receptor complexes composed of two distinct types of transmembrane kinases, the type I and type II receptors. The downstream SMAD responses subdivide the TGF-β superfamily signaling pathway in two categories: BMP/GDF ligand and Activin/Nodal/TGF-β ligands (*72, 74*). TGF-β and activin primarily activate the type I receptors TβRI/ALK-5 and ActRIB/ALK-4, respectively, while nodal functions through ActRIB/ALK-4 and ALK-7. The TGF-β/activin/nodal receptors induce the downstream signaling by activating the Smad2 and Smad3 through phosphorylation. Once phosphorylated, the SMADs form a complex with SMAD4, and translocate to the nucleus where they bind DNA to modulate transcription.

The activin/nodal/TGF- β signaling branch can promote the self-renewal or direct cell differentiation, findings that emphasize the complexity of the role of these extrinsic signals on stem cell fate choices. As mentioned, these growth factors identified from the cell culture conditions are essential for maintaining the ES cell pluripotency. Likewise, transcriptome analysis

at early time points showed gene enrichment of the nodal signaling pathway in undifferentiated cells (*48*). Later, it was discovered that the addition of external activin can maintain human ES cell pluripotency (*90*). Singh *et al*. discovered that the level of activated SMAD2/3 determines which downstream genes are activated. For example, a limited SMAD2/3 signal accelerates the self-renewal state whereas, increased SMAD2/3 phosphorylation activates the genes involved in the differentiation route (*91*). Interestingly, diverse effects of TGF-β signaling on ES cell differentiation have also been reported (*62, 83, 92-95*). The inhibition of TGF-β signaling with the small molecule SB431542 (through blocking ALK receptor kinase activity) promotes differentiation into neuroectoderm (*96*). At the same time, activation of activin/Nodal and BMP induces the primitive streak differentiation. The effects of promoting activin/nodal signaling in mesendoderm lineage-specific differentiation are context-dependent. For mesoderm differentiation, a moderate level of activin/nodal signals, along with BMP signaling, is required, whereas endodermal differentiation demands a high level of activin/nodal signals in the absence of serum (*97*) (*98*). These differences exemplify the dual functions of activin/nodal/TGF-β signal, which warrants further investigation into the underlying mechanism.

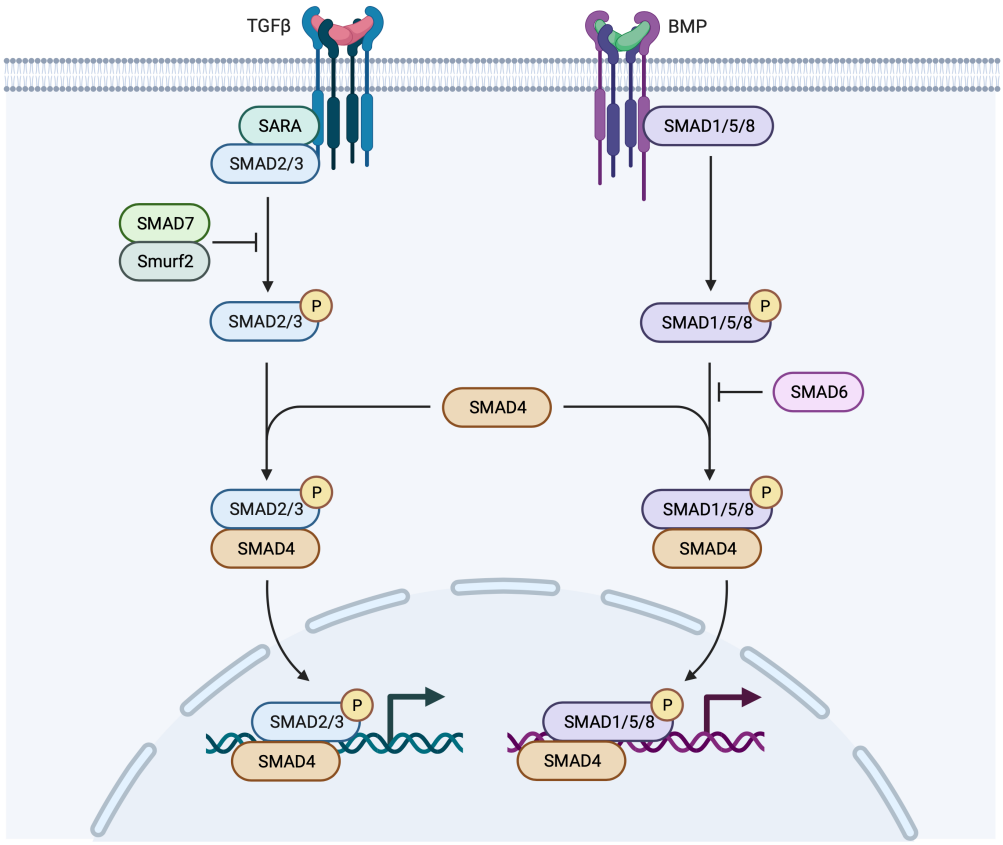

Fig.1.4. Overview of BMP and TGF-β signaling pathways. Created with Biorender.com

The Activin/Nodal/TGF-β pathway was the first of many regulators of hES cells pluripotency that was discovered and characterized. Its ability to promote both self-renewal and direct differentiation highlights the complexity of cell signaling and the importance of interplay between different pathways.

1.3.1.4 WNT signaling pathway

The Wnt signaling pathway, along with those mediated by FGF, BMP, and TGF-β (discussed in section 1.3.1.4), has a pivotal role in hES cell differentiation and self-renewal. Historically Wnt signaling was attributed to the maintenance of stem cells of various lineages.

Over the years, the dominant role of the Wnt signaling pathway in hES stem cell differentiation and self-renewal has become apparent.

Wnt ligands are cysteine-rich secreted glycoproteins that function in autocrine and paracrine cell signaling. These evolutionarily conserved proteins have as many as 19 different homologs that (https://web.stanford.edu/~rnusse/wntwindow.html) are expressed in a temporal-spatial pattern. The Wnt pathway is classified into two branches: canonical (β-catenin-dependent) and noncanonical (β-catenin-independent); however, in both cases the Wnt ligand binds to the Frizzled receptors in tandem with other co-receptors. In absence of Wnt ligands, the cytosolic proteins glycogen synthase kinase 3 (GSK3), AXIN, adenomatous polyposis coli (APC) protein, and casein kinase 1α form a "destruction complex" that phosphorylates β-catenin. The phosphorylated β-catenin is ubiquitylated and thereby targeted to the proteasome for degradation. When Wnt ligands bind to the Frizzled and co-receptors LRP5 or LRP6, the kinase GSK3 inhibited as is the "destruction complex". This inhibition enables the accumulation of β-catenin in the cytoplasm where it can translocate to the nucleus to act as transcriptional coactivator for the T-cell factor (TCF) and lymphoid enhancing factor (LEF) family of DNA-binding transcription factors (*99, 100*).

Wnt/β-catenin signaling is considered a positive regulator of human naïve pluripotency. The levels of the genes involved in Wnt signaling change early during the naïve-to-primed transition in hES cells (*48, 101*). Small molecule inhibition of GSK3 (thus activating Wnt pathway) could maintain self-renewal and pluripotency gene expression in human ES cells cultured under feeder-free conditions (*102*). Multiple studies revealed that the autocrine Wnt/β-catenin signaling promotes self-renewal a conserved feature of naïve-state hES cells and mES cells. However, these observations remain controversial. Specifically, Ullmann *et al*. (*103*) found that though GSK3

inhibitor promoted undifferentiated cellular morphology and maintained expression of pluripotency markers in short-term assays, it was not sufficient to expand undifferentiated hES cells over multiple passages. Additionally, two other studies showed Wnt3A or GSK3 inhibitors lead to hESC differentiation toward the primitive streak and definitive endoderm lineages (*104, 105*).

Later, studies revealed that Wnt/β-catenin signaling plays a dominant role in driving differentiation rather than self-renewal. Davidson *et al.* showed with the β-catenin human ES cell reporter cell line that in the undifferentiated state of the human ES cells the β-catenin signaling is repressed, whereas its activation leads to mesoderm differentiation (*106*). The β-catenin may possess an opposite dual function-where the cytoplasmic β-catenin can promote self-renewal, but nuclear β-catenin induces differentiation (*107*) . Also, in hES cells, the endogenous Wnt signaling activity can be heterogeneous (*108*). This spatial expression pattern can also direct the fate of the cells. For example, the Wnt-high cells differentiate preferentially toward mesoderm/endoderm whereas the Wnt-low cells primarily differentiate toward neuroectoderm. Moreover, Wnt signaling plays an important role in the cell fate choice in conjunction with BMP signal. During BMP treatment, presence of endogenous Wnt signal mediate mesendoderm differentiation whereas, in absence it directs cells towards trophoblast lineage (*109*).

In summary, Wnt signaling may act as a niche factor to maintain the pluripotent state of the ES cells. In addition to maintaining the self-renewal state, it can direct the differentiation of hES cells towards all three primary germ layers. These together exemplify the role of endogenous signaling in cell fate choice of hES cells.

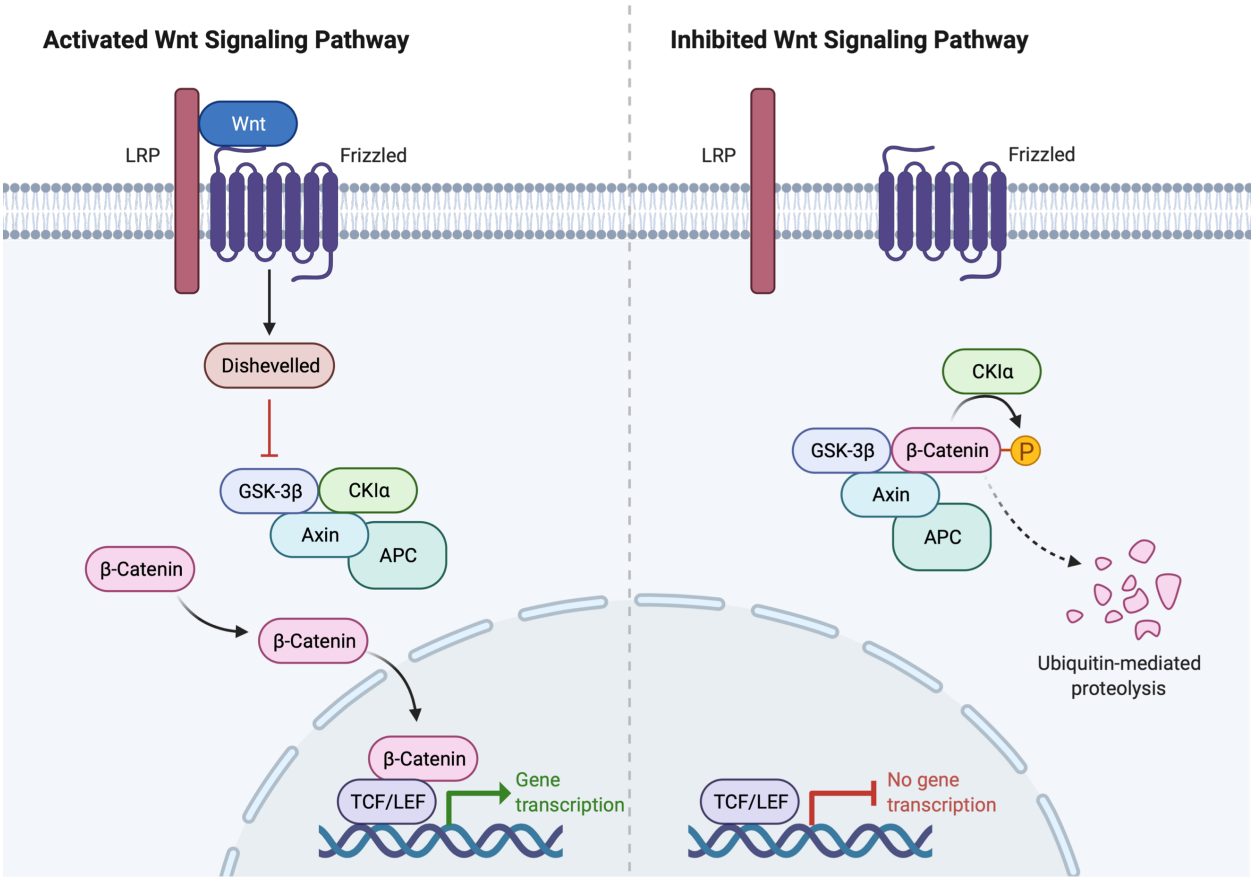

Fig.1.5. Overview of Wnt signaling pathways. Created with Biorender.com

1.3.2 Insoluble factors modulating stem cell fate choices

The precise balance between stem cell self-renewal and differentiation is essential for proper organogenesis and tissue homeostasis maintenance. In addition to all the soluble factors described in the above sections, the stem cell niche also comprises several insoluble factors that greatly contribute to the cell fate choices of hES cells.

1.3.2.1 Cell to cell interaction

The stem cell microenvironment comprises several niche cells that hPS cells contact. These cell-cell interactions could be between pluripotent cells or between hPS and other types of cells. We envision these interactions exert a profound influence over the cell fate decisions.

The original *in vitro* ES cell culture was carried out using an MEF feeder cell layer (*19*). In this system, the feeder layer provides both the extracellular matrix and the soluble factor Activin A to maintain ES cell pluripotency. These co-culture strategies provide supportive signals that greatly accelerate hPS cell differentiation. For example, the glial cell support layer significantly improves neuronal maturation during the hPS cell differentiation (*110*) and astrocytes enhance synaptic transmission in differentiated cells.

In addition to the heterotypic cellular interactions, hPS cells also receive insoluble cues from the interactions with other hPS cells. In this regard, the most significant discovery was the understanding of the underlying mechanism of Rho-associated kinase (ROCK)-dependent apoptotic cell death in hES cells (*111*). It was found that ROCK activation and loss of E-cadherin-dependent cell-cell interaction in hPS colonies induce cellular blebbing and apoptosis (*112*). These findings further led to the discovery of a ROCK inhibitor that significantly improved the hPS cell culture survival *in vitro*.

1.3.2.2 The extracellular matrix of stem cells

The extracellular matrix (ECM) is a complex and dynamic network of macromolecules with different physical and biochemical properties (*113, 114*). The ECM can act as an insoluble cue to influence stem cell states. As a key component of the stem cell niche, the ECM was once considered an inert supportive scaffold, but its fundamental role during development, morphogenesis, and organogenesis has become increasingly evident. Indeed, the ECM can facilitate cell adhesion, proliferation, migration, specification, differentiation, and survival (*115-117*). By modulating the complex signaling pathways, the ECM can afford phenotypic outcomes that supersede genotypic effects (*118, 119*).

A unique contribution of the ECM to the stem cell microenvironment is its bulk mechanical properties. Cell adhesion to the ECM can alter the cellular actin cytoskeleton to yield focal adhesions. Thus, the cell can sense changes in mechanical properties and respond accordingly. For example, Discher and colleagues showed the human bone-marrow-derived mesenchymal stem (hMS) cells can sense the substrate elasticity and can differentiate into different lineages in reponse (*120*). With regard to hPS cells, their culture on a hydrogel with an elastic modulus close to the 1 kPa (similar to the brain stiffness) results in their differentiation into a neural lineage-even without soluble cues, such as growth factors or small molecules (*121*). While an elastic surface promotes neural differentiation, a stiffer surface can help induce cardiomyocyte differentiation (*122*). Thus, the ECM plays a crucial role in the differentiation of hPS cells to different lineages.

In addition to ECM mechanics, other components also contribute to cell fate. The ECM is composed of fibrous proteins, glycoproteins, and proteoglycans. Other proteins that modulate the ECM's structural organization and biochemical roles, include mucins, lectins, semaphorins, and plexins (*123*). Collagen is a major component. Among non-collagenous components of the ECM, there is fibronectin (FN), laminin (LM), vitronectin (VN), thrombospondins (TSPs), and tenascin (TN). The cell fate choices of hPS can be controlled through the differential engagement of cell-surface molecules to various ECM components.

A major ECM partner is the cellular glycocalyx, the exterior coat of the cell membrane. For many decades, it was considered only as an inert protective layer on the cell surface without any regulative properties. In recent years, novel tools have revealed that this dense cellular coat is not a passive; rather it is involved in fundamental cellular events such as leukocyte adhesion, viral and bacterial infections, blastocyst implantation, embryonic development (*124-129*). To elaborate

the role of glycan in human pluripotent stem cell biology, the following sections provide a general introduction and a summary of the roles of specific glycans.

1.4 The cellular glycocalyx in stem cell microenvironment

The glycocalyx of the cell is composed of the glycan conjugates that reside on cell membranes and surround them like a cloak. Glycans are either free (e.g., polysaccharides) or conjugated to a protein (glycoproteins or proteoglycans) or lipid (glycolipids). Generally (though not exclusively), glycoproteins can bear *N*-glycans (the glycan is attached to the nitrogen atom of an asparagine side chain), *O*-glycans (the glycan is attached to the side chain oxygen atom of a serine or threonine residue), or both.

The biosynthesis of glycoproteins or glycolipids is complex. Depending on the type of glycan, the process occurs in ER or Golgi apparatus: the core *N*-glycosylation occurs through the attachment of preassembled oligosaccharide that is transferred to the protein core. Further glycan tailoring takes place in the Golgi. The O-glycosylation modifications start with a single sugar attachment in the ER and are further elaborated in the Golgi with additional sugar residues appended. The latter type of stepwise assembly is involved in glycolipid formation(*130*). Notably, the identity of the glycan is regulated developmentally and with tissue-specifically which signifies their contribution during the mammalian developmental processes.

The differences in the glycan sequences between different tissues are consistent with the use of glycans as cellular IDs that reflect a cell's state. For example, the stage-specific embryonic antigen-1 (SSEA-1), SSEA-3, SSEA-5, TRA-1-60 antigen, and TRA-1-81 antigen (*131*) are used as ES cell markers; all are glycans. As the outermost layer of the stem cells, glycocalyx components are optimally positioned to help these specialized cells to communicate with the neighboring cells and molecules of the extracellular milieu. In particular, the sulfated glycans can

act a coactivator or stabilizing factors of multiple signaling molecules, including FGF, BMP, Wnt, and Hh. Thus, glycans can modulate the pluripotency to cell fate choices of stem cells.

1.4.1 Proteoglycans and glycosaminoglycans

Proteoglycans consist of a core protein that is covalently attached to one or more glycosaminoglycan (GAG) chains (*132*). The glycosaminoglycan substituents are long, linear polysaccharides composed of repeating disaccharide building blocks. The disaccharide unit is composed of N-acetylated or N-sulfated hexosamine and either a uronic acid (glucuronic acid or iduronic acid) or galactose. The identity of the amino sugar is either a variant of *N*-acetylglucosamine, (glucosamine with N-substituents) or *N*-acetylgalactosamine. Based on the composition of the repeating disaccharide unit, GAGs are subdivided into chondroitin sulfate (CS), dermatan sulfate (DS), keratan sulfate (KS), heparan sulfate (HS) or hyaluronan (HA). A secreted polysaccharide similar to GAG chains of heparan sulfate proteoglycans is heparin. One prominent feature of GAGs, with the exception of hyaluronan is that they are highly sulfated (*133*).

1.4.1.1 Keratan sulfate proteoglycans (KSPGs)

Keratan sulfate (KS) is composed of a repeating disaccharide unit consisting of a sequence of GlcNAc and Gal, more specifically 3Galβ1-4GlcNAcβ1. The 6 position hydroxyl group of either the Gal or GlcNAc saccharide can be sulfated. The three types of KS can be distinguished by their linkage to the protein core. KS I has the GAG chain linked to protein core through an asparagine residue. The glycan chain of KS II is appended as an O-glycan linkage wherein the first residue is an N-acetylgalactosamine attached to serine or threonine (*134*). Finally, in the type III KS, a mannosylated glycan is linked to a serine side chain. The highest level of KS in humans is in the cornea tissue. KS chains are mostly enriched with type I (*135-138*). KS has a critical role in

disease, as illustrated by macular corneal dystrophy, which is characterized by a decrease in sulfated KS (*139*). Moreover, KS null mice have total corneal thinning (*140*).

1.4.1.2 Chondroitin sulfate proteoglycans (CSPGs)

Chondroitin sulfate (CS) is a repeating disaccharide of GlcA and GalNAc with sulfation at various positions. CS is classified in 4 different forms that are based on sulfation sites: CS A is sulfated at carbon 4 of the GalNAc sugar, CS C is sulfated at carbon 6 of the GalNAc sugar, CS D is sulfated at carbon 2 of the GlcA and 6 of the GalNAc sugar, and CS E is sulfated at carbons 4 and 6 of the GalNAc sugar (*141*). Like HS, CS is also anchored to a serine residue of a core protein via xylose.

The functions of CS chain are multifaceted, including physiological (cytokinesis, morphogenesis, and neuronal plasticity), and pathological (skeletal disorders, glial scar formation after brain injury, and infections with viruses and bacteria) events (*142-144*). The level of variation of CS chains directly affects multiple differentiation and regeneration processes during embryonic development. For example, a lack of CS results in abnormal multinucleation leading to cellular death (*145-147*). In retrospect down-regulation of CS induce myogenic differentiation *in vitro*. In neuronal culture, CS can activate the cytokines mediated signaling to stimulate the neurite outgrowth and/or proliferation/ maintenance of neural stem/progenitor cells (*148-151*). Not only the differential expression of CS, the sulfation pattern of CS chain is also variable depending on the developmental stages (*145-147*). For example, the accumulation of 4S sulfation over 6S in CS chains modulates the maturation of the interneurons in the perineuronal nets. Also, CS E and CS C variants can exert a stimulatory effect for neurite outgrowth (*143, 148, 152, 153*) and axonal regeneration (*143, 154*) respectively, whereas, CSA negatively regulates axonal guidance and growth of cerebellar granule neurons (*155*).

More broadly, the structural heterogeneity of CS allows it to bind with a number of humoral factors, such as PTN, midkine (MK), FGFs, hepatocyte growth factor (HGF), and brain-derived growth factor (BDNF) (*142, 143, 151, 153, 156*) to modulate a variety of signaling pathways. Thus, CS plays a diverse and significant role in the extracellular regulatory milieu of the stem cells.

1.4.1.3 Dermatan sulfate proteoglycans (DSPGs)

Dermatan sulfate (DS), previously known as chondroitin sulfate B, has the same basic composition as CS. The exception is that the glucuronic acid is epimerized to iduronic acid by glucuronyl C5-epimerase (*157*). DS is predominantly present in the skin and plays an important role in wound healing (*158*).

1.4.1.4 Heparan sulfate proteoglycans (HSPGs)

Heparan sulfate (HS) is a major class of GAGs that can be produced by cells that are found in simple invertebrates to humans. The presence of a rudimentary HS biosynthetic machinery in a unicellular organism at the root of the metazoan lineage confirmed the presence of HS as early as in the metazoan evolution (*159*). This ancient and ubiquitous polysaccharide chain can possess sequence and therefore structural heterogeneity. This diversity contributes to its critical functions as a cell surface signaling co-receptor and as an essential scaffolding component in the surrounding microenvironment. In the stem cell microenvironment, HS appears to be perhaps the most influential GAG. It has been shown that GAGs on the surface of hES cells help attachment of cells to the substratum. Specifically, it has been found that the surface presenting heparin-binding peptides (GKKQRFRHRNRKG, FHRRIKA and GWQPPARARI) consistently mediate hES cell adhesion and support long-term hES cell propagation *in vitro* (*47*).

1.5 Structure, biosynthesis, and diversity of HSPGs

HS is a long polymer made of repeating disaccharide units composed of uronic acid (D-glucuronic acid [GlcA] or its C5-epimer, l-iduronic acid [IdoA]) connected to β1,4 linked to D-glucosamine (GlcN) which may be *N*-acetylated, *N*-sulfated or, in rare circumstances, a free amine (*160*). The uronic acid can be sulfated at the C2 position while sulfation of the glucosamine can occur at the *N*, C6, and rarely, C3 positions. Eleven biosynthetic enzymes carry out the synthesis of HS chain. The initial glycosylation generates a tetrasaccharide unit (glucuronosyl–galactosyl–galactosyl–xylosyl) attached to a serine residue of the core protein. This linker sequence is common for proteoglycan carrying HS, CS, or DS. The next glycosylation step determines the specificity of the gag chain: β1,4-linked N-acetylgalactosamine (GalNAc) for CS/DS, or an α1,4-linked N-acetylglucosamine (GlcNAc) for HS. After this sequence is established, further elongation occurs by polymerization of alternating GlcA and GlcNAc residues, yielding a (GlcA-(β1,4)-GlcNAc-(α1,4)-)$_n$ HS precursor polysaccharide. This polymerization is catalyzed by a Golgi-located heterodimeric complex of two glycosyltransferase enzymes (referred to as exotosin or EXT) EXT1 and EXT2 (*161*). The long polymer chain is then modified by further epimerization, acetylation (catalyzed by one or more of the four NDST isoenzymes), and sulfation (by glucosaminyl O- sulfotransferase). These steps within the Golgi apparatus rely on nucleotide sugar building blocks (such as UDP-glucosamine) and the sulfate donor 3′-phosphoadenosine-5′-phosphosulfate (PAPS) (*162*).

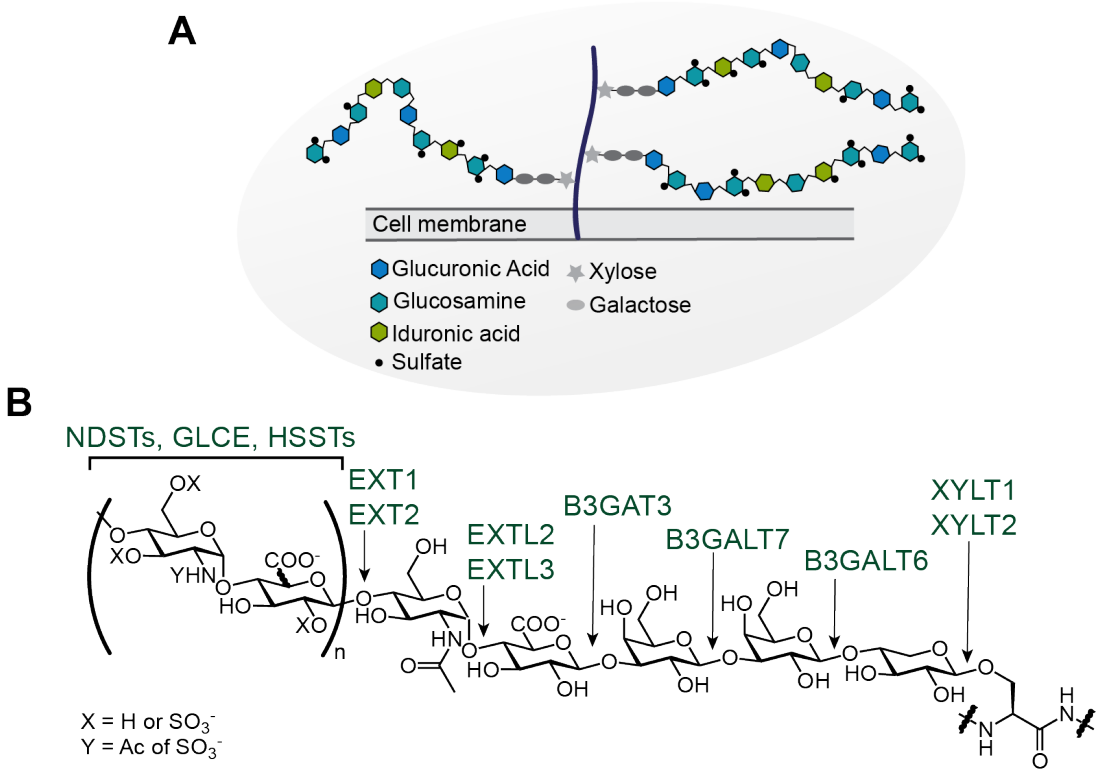

Fig. 1.6. (A) An example heparan sulfate proteoglycan. (B) Enzymes involved in the biosynthesis of heparan sulfate

The modifications that generate heparan sequence variation endow HS with a wide range of structural and functional diversity. The basic structural disaccharide precursor appears to be ancient, but the relative content of the modification varies quantitatively. For example, the disaccharide GlcA-GlcNS3S occurs predominantly in endothelial cells and connective tissue mast cells, where a pentasaccharide encompassing this motif within the polysaccharide heparin binds to antithrombin (*163, 164*). In contrast, kidney HS contains a many IdoA2S-GlcNS3S (*165*) sequences. The relative distribution of different substituted GlcN residues also introduces HS diversity. Contiguous N-acetylated disaccharide units (NA domains), contiguous N-sulfated sequences of variable length (NS domains), and alternating N-acetylated and N-sulfated units (NA/NS domains) are characteristic of the cells/tissues from which the HS was obtained. The *N*-sulfation of the GlcN units also tends to direct other modifications, such as *O*-sulfation and

epimerization of GlcA to l-IdoA, therefore, the modified disaccharide units tend to cluster in the NS or NA/NS domains (*166*). Moreover, the non-template-driven incomplete nature of the HS biosynthesis can introduce these heterogeneities at the HS chain levels (*167-169*).

Heterogeneity at the HS chain level can arise from the activity of multiple biosynthetic enzyme isoforms that differ in their substrate specificities and the products they generate (*167, 169, 170*). Post-biosynthetic alterations to sulfation and chain length are also known to contribute to the structural diversity and associated functional variability in HS. For example, selective removal of 6-*O*-sulfate groups by the sulfatase SULF2 leads to domain reorganization within the HS chain, preventing the binding of HS to signaling factors and consequently, a decrease in the ligand–receptor interactions that influence stem cell or progenitor cell fate decisions. Moreover, the biodistribution of signaling molecules in the ECM may be altered as a result of HS chain cleavage by the single copy heparanase enzyme (HPSE). In this case, cleavage releases biologically active HS fragments that can bind and sequester signaling factors within the extracellular space (*171-173*).

The core protein to which the HS chain is covalently attached can introduce additional variety. Based on primary amino acid sequence homology the plasma-membrane-bound core proteins are subdivided in two superfamilies: syndecans and glypicans (*174*). There are four syndecans, each of them has the variable ectodomain exposed to the extracellular space, a short hydrophobic transmembrane region, and a small cytoplasmic tail. HS chains (typically three to five) are attached to the ectodomains, and on occasion, a chondroitin sulfate chain can also be present. The cytoplasmic tail contains a specific sequence that interacts with intracellular proteins involved in the endocytosis (*175*). Syndecans also contain a peptide sequence that interacts with cytoskeletal proteins to enable syndecans to signal (*176, 177*). With regard to glypicans there are

six members with cysteine-rich globular ectodomains and a glycosylphosphatidylinositol moiety that anchors the protein to the outer leaflet of the plasma membrane (*178*). Usually, two to three HS chains are attached between the globular domain and glycosylphosphatidylinositol moiety. Cells also have minor proteoglycans that contain HS chains (epican, betaglycan, and others) (*174*). Other proteoglycans include those secreted in the basement membranes, such as perlecan, agrin, and collagen XVIII (*179, 180*), which have tissue-specific expression. The heterogeneity at the core protein level can result from the differential expression of the encoding genes. Lower organisms such as *Drosophila melanogaster* and *Caenorhabditis elegans* carry homologs of glypican, syndecan, and perlecan (*179*). Thus, these proteoglycans are evolutionarily conserved and are present even in the ancient organism *Hydra (181)*.

In summary, HSPGs have structural and functional heterogeneities that are controlled by physiological location and vary dynamically with cell state (*182, 183*). The dynamic alterations of these proteoglycans can have distinct consequences on cell signaling.

1.6 Heterogeneity in HS composition influencing stem cell fate

The heterogeneity of HSPG can directly affect its roles in the stem cell microenvironment. Changes in the sulfation pattern of HS through post-biosynthetic alteration can alter its interaction with growth factors that influence stem cell or progenitor cell fate. For example, SULF2-catalyzed hydrolysis of 6-*O*-sultate groups can prevent HS-FGF binding and thereby modulate hES cell lineage specificity (*184-186*). Similar desulfation in MM14 myoblast culture prevents FGF signaling and leads to myoblast differentiation (*187*). Similarly, heparanase-mediated cleavage can yield fragments that bind and sequester signaling factors to modulate the cell fate choices (*172, 173, 188*). Moreover, during the development and wound healing the spatiotemporal expression of the core proteins can vary, which can modulate stem cell responses to their surroundings. The

shedding of bioactive HSPG induced by sheddases can change the morphogen gradient in the stem cell microenvironment that directs the stem cell response (*189, 190*).

In summary, the heterogeneity in the HS chain, core protein, and the cell and tissue-specific expression can all influence HS function. These variables allow HS to modulate the signaling events in the stem cell microenvironment and directly affect cell fate. Despite its critical roles, the specific function of HS in human pluripotent stem cell differentiation cannot yet be fully harnessed. A major barrier is the limited tools available to probe the unique compositional characteristics and mechanism of action of specific HSPGs. The advent of new approaches would significantly advance the field.

1.7 HS in development and stem cell differentiation

Over the past two decades, ample evidence has emerged revealing the significant role of HS in tuning cellular response to growth factors, cytokines, chemokines, and morphogens which can modulate the stem cell fate during development and differentiation. In pioneering studies, Lin *et al.* developed the first HS-deficient mouse by knocking out the HS co-polymerase enzyme *Ext1*$^{-/-}$ (*191*). The HS-null mouse embryos failed to develop beyond the blastocyst stage, indicating the essential role of HS in gastrulation and embryogenesis. Subsequently, Johnson *et al*. developed HS-null mouse embryonic stem (mES) cells to investigate the role of HS in development. Several studies came together to show that HS is essential for mES cell to exit the pluripotent state; thus, in absence of HS, mES cells fail to differentiate either to neuroectoderm or mesendoderm lineage (*192-196*). Later, it was discovered that the complete absence of HS in the mES cells results in defects in the FGF and BMP signaling pathways, key signals (discussed in section 1.3 1.1 and 1.3 1.2) for mES cell differentiation (*197, 198*). The development of conditional *Ext1* knockout in the nervous system of the murine embryo showed the direct effect of HS in the development of

cerebral cortices. Specifically, deficiencies in HS biosynthetic enzymes cause defects in the forebrain development, cerebral hypoplasia, and hydrocephalus. These findings corroborate earlier observations, showing that concentrated expression of HSPGs at the dendritic spine is critical for synapse maturation (*199-201*).

More recently, HS has been identified as a synapse organizer (*202*). HSPGs (GPC4, neurexins) of the presynaptic neuron interact with the leucine-rich repeat transmembrane proteins (LRRTM), Neurologin of the post-synaptic neurons to modulate the excitatory synaptogenesis *in vivo*, and in cultural rodent dentate gyrus neurons (*203, 204*). In parallel, Narin *et al.* (*205*) showed that during mES cell differentiation into embryoid bodies and extra-embryonic endoderm lineage HS synthesis is upregulated, as is the sulfation of HS, particularly, in the level of N-sulfated HS disaccharides. Another group also identified that specific HS sulfation patterns (*N*, 6- and 2-*O*-sulfated disaccharides) are upregulated in the mES-derived neural progenitor cells (*196*) to facilitate the binding of FGF2 and therefore ectodermal differentiation. Similarly, during mesodermal differentiation towards haemangioblasts as well as the primitive streak stage of the mouse embryo are accompanied by upregulation of 3-*O*-sulfation of HS (*195*). The specific change in the HS sulfation is key to facilitating the Fas-signaling required for the differentiation (*206*). These observations corroborate the previous findings that a lack of HS *N*-sulfation hinders mES cell exit from the pluripotent state by directly downregulating the FGF signal. The change in HS sequence also perturbs angiogenesis by interfering with VEGF signaling (*207*). However, loss of N-sulfation does not hinder BMP signaling, which explains why the *Ndst1/2*$^{-/-}$ mESCs can differentiate toward osteoblastic lineages. These findings reflect the context-dependent role of HS and its structure in influencing mES cell fate choices. Intriguingly, hES cells are significantly different from mES cells. Because of the relative ease of culture and the possibility of genetic

modifications, many studies focused solely on mES cells. A 2014 study by Gasimli *et al.* with hES cells showed that differentiation to splanchnic mesoderm and immature hepatocytes afforded a significant upregulation of N-sulfation and 6-*O*-sulfation of HS respectively (*208*). However, a deeper understanding of how HS sequence varies in hES cells during lineage commitment is needed.

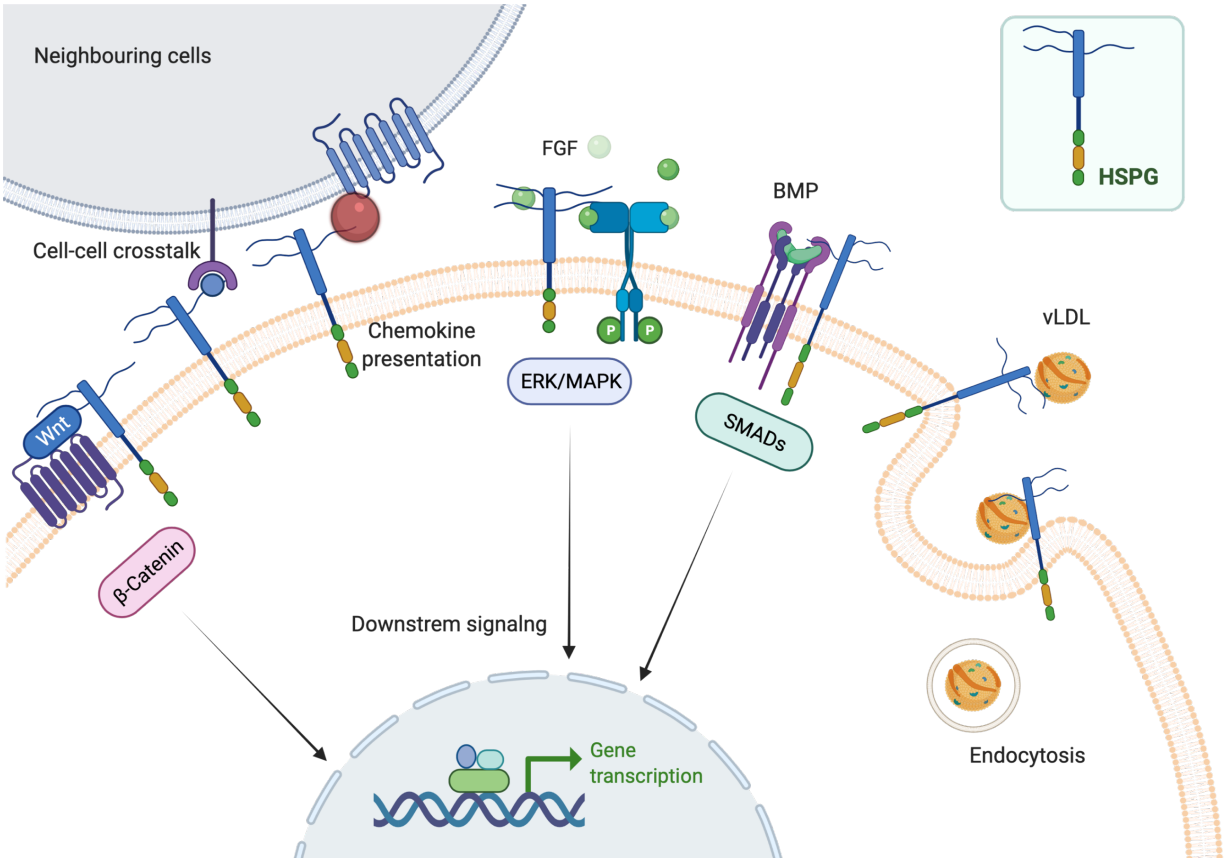

Fig 1.7. Heparan sulfate proteoglycans have many roles in cell physiology including but not limited to cellular signaling, cell-cell crosstalk, or endocytosis. Created with Biorender.com

1.8 Approaches to understand the HSPG-stem cell relationship

The investigation of glycans, in general, is complicated because glycans are secondary gene products. How they are linked to genetic information is not well understood. They are made from multiple interdependent biosynthetic pathways, and the cell's metabolic state can direct

glycan biosynthesis (*209*). This non-template-driven glycan biosynthesis is a major roadblock to understanding the role of specific sugar in the development or diseases.

A number of strategies have been developed to exploit the roles of HSPGs in stem cell fate. First, exogenous heparan sulfate and heparin were used to stabilize the growth factor (e.g., FGF) to the respective receptor to promote the growth factor activity. Second, a heparin-conjugate was used to develop an affinity-based controlled release system in which heparin interacts with growth factors, prevents degradation and facilitates the sustained interaction of the growth factors to its receptor. Third, a synthetic glycopolymer has been developed that acts as a HS mimetic and can be appended onto the cell surface via lipid or protein anchors. These GAG-mimicking polymers (*210*) or synthetic neoproteoglycans (*211*) tweak the FGF signal to modulate the cell fate choice of the stem cells.

The specific composition of HSPG and the associated functional features mediate stem cell fate, though the current knowledge regarding this is limited. A multi-omics approach (combination of glycomic, genomic, chemical, and proteomic methods) is on-demand to address this gap. It is essential to identify the fine structural features of HS (including length, domain organization, sulfate modifications, and protein binding sites). Liquid chromatography-tandem mass spectrometry (LC-MS/MS) and high-resolution visualization with efficient labeling would facilitate the temporal changes of HSPG in lineage-specific differentiation.

Perturbation and loss-of-function is another strategy to investigate the role of a specific structural feature of HS in progenitors of stem cells and their differentiation state. Despite residing in the stem cell niche, this cell surface glycan and its contributions to fate decisions of human stem cells are not well understood. This can be achieved through genetic manipulation, chemical inhibitions (xylosides, heparan sulfate antagonist surfen, sodium chlorate) or heparinase mediate

inhibition (*212-216*). A hPS cell line without HS would be an excellent tool to investigate the roles of HS in human diseases and development.

Overall, these strategies can be used to probe the roles of the heparan sulfate polysaccharide and exploit its immense promise in modulating the stem cell fate choices as well as in regenerative medicine. Furthermore, modulating the expression and distribution of HSPG, as well as the function of HS should be adopted to improve the stem cell microenvironment *in vitro* and the fate choice decisions of stem cells.

1.9 Conclusion and perspectives

Because of their unique abilities to proliferate, differentiate and self-renew, human pluripotent stem cells are heralded as an attractive tool for regenerative medicine. In an uncontrolled environment, however, tumor formation may ensue. This danger demands an extensive understanding of the stem cell niche, including the glycans, for developing and deploying strategies to guide and control stem cell fate choices.

Heparan sulfate functions as a scaffolding component of the ECM and a critical cell surface signaling co-activator. The emerging evidence that HSPGs play central roles in regulating stem cell fate choices in mammalian cells prompted my investigation of the role of HS in hPS cells, as outlined in this thesis. Unfolding the structural variability of HS during hPS cell differentiation and its role in lineage-specific differentiation would significantly advance our understanding of the roles of the cellular glycome in development and diseases.

1.10 References

1. K. A. Moore, I. R. Lemischka, Stem cells and their niches. *Science* **311**, 1880-1885 (2006).
2. I. L. Weissman, D. J. Anderson, F. Gage, Stem and progenitor cells: origins, phenotypes, lineage commitments, and transdifferentiations. *Annu Rev Cell Dev Biol* **17**, 387-403 (2001).
3. G. Keller, Embryonic stem cell differentiation: emergence of a new era in biology and medicine. *Genes & development* **19**, 1129-1155 (2005).
4. P. C. Chagastelles, N. B. Nardi, Biology of stem cells: an overview. *Kidney Int Suppl (2011)* **1**, 63-67 (2011).
5. R. Jaenisch, R. Young, Stem cells, the molecular circuitry of pluripotency and nuclear reprogramming. *Cell* **132**, 567-582 (2008).
6. R. L. Gardner, Mouse chimeras obtained by the injection of cells into the blastocyst. *Nature* **220**, 596-597 (1968).
7. L. C. Stevens, C. C. Little, Spontaneous Testicular Teratomas in an Inbred Strain of Mice. *Proc Natl Acad Sci U S A* **40**, 1080-1087 (1954).
8. L. J. Kleinsmith, G. B. Pierce, Jr., Multipotentiality of Single Embryonal Carcinoma Cells. *Cancer Res* **24**, 1544-1551 (1964).
9. G. R. Martin, M. J. Evans, The morphology and growth of a pluripotent teratocarcinoma cell line and its derivatives in tissue culture. *Cell* **2**, 163-172 (1974).
10. B. Hogan, M. Fellous, P. Avner, F. Jacob, Isolation of a human teratoma cell line which expresses F9 antigen. *Nature* **270**, 515-518 (1977).
11. D. Solter, B. B. Knowles, Monoclonal antibody defining a stage-specific mouse embryonic antigen (SSEA-1). *Proc Natl Acad Sci U S A* **75**, 5565-5569 (1978).
12. B. A. Fenderson, P. W. Andrews, E. Nudelman, H. Clausen, S. Hakomori, Glycolipid core structure switching from globo- to lacto- and ganglio-series during retinoic acid-induced differentiation of TERA-2-derived human embryonal carcinoma cells. *Dev Biol* **122**, 21-34 (1987).
13. R. Kannagi, N. A. Cochran, F. Ishigami, S. Hakomori, P. W. Andrews, B. B. Knowles, D. Solter, Stage-specific embryonic antigens (SSEA-3 and -4) are epitopes of a unique globo-series ganglioside isolated from human teratocarcinoma cells. *EMBO J* **2**, 2355-2361 (1983).
14. J. Rossant, M. W. McBurney, The developmental potential of a euploid male teratocarcinoma cell line after blastocyst injection. *J Embryol Exp Morphol* **70**, 99-112 (1982).
15. V. E. Papaioannou, M. W. McBurney, R. L. Gardner, M. J. Evans, Fate of teratocarcinoma cells injected into early mouse embryos. *Nature* **258**, 70-73 (1975).
16. R. H. Blelloch, K. Hochedlinger, Y. Yamada, C. Brennan, M. Kim, B. Mintz, L. Chin, R. Jaenisch, Nuclear cloning of embryonal carcinoma cells. *Proc Natl Acad Sci U S A* **101**, 13985-13990 (2004).
17. M. J. Evans, M. H. Kaufman, Establishment in culture of pluripotential cells from mouse embryos. *Nature* **292**, 154-156 (1981).
18. G. R. Martin, Isolation of a pluripotent cell line from early mouse embryos cultured in medium conditioned by teratocarcinoma stem cells. *Proc Natl Acad Sci U S A* **78**, 7634-7638 (1981).

19. J. A. Thomson, J. Itskovitz-Eldor, S. S. Shapiro, M. A. Waknitz, J. J. Swiergiel, V. S. Marshall, J. M. Jones, Embryonic stem cell lines derived from human blastocysts. *Science* **282**, 1145-1147 (1998).
20. M. C. Chang, Fertilization of rabbit ova in vitro. *Nature* **184(Suppl 7)**, 466-467 (1959).
21. P. C. Steptoe, R. G. Edwards, Birth after the reimplantation of a human embryo. *Lancet* **2**, 366 (1978).
22. B. E. Reubinoff, M. F. Pera, C. Y. Fong, A. Trounson, A. Bongso, Embryonic stem cell lines from human blastocysts: somatic differentiation in vitro. *Nat Biotechnol* **18**, 399-404 (2000).
23. A. Bongso, C. Y. Fong, S. C. Ng, S. Ratnam, Isolation and culture of inner cell mass cells from human blastocysts. *Hum Reprod* **9**, 2110-2117 (1994).
24. M. J. Martin, A. Muotri, F. Gage, A. Varki, Human embryonic stem cells express an immunogenic nonhuman sialic acid. *Nat Med* **11**, 228-232 (2005).
25. T. E. Ludwig, M. E. Levenstein, J. M. Jones, W. T. Berggren, E. R. Mitchen, J. L. Frane, L. J. Crandall, C. A. Daigh, K. R. Conard, M. S. Piekarczyk, R. A. Llanas, J. A. Thomson, Derivation of human embryonic stem cells in defined conditions. *Nat Biotechnol* **24**, 185-187 (2006).
26. V. Tabar, L. Studer, Pluripotent stem cells in regenerative medicine: challenges and recent progress. *Nat Rev Genet* **15**, 82-92 (2014).
27. A. Trounson, N. D. DeWitt, Pluripotent stem cells progressing to the clinic. *Nat Rev Mol Cell Biol* **17**, 194-200 (2016).
28. C. Eguizabal, B. Aran, S. M. Chuva de Sousa Lopes, M. Geens, B. Heindryckx, S. Panula, M. Popovic, R. Vassena, A. Veiga, Two decades of embryonic stem cells: a historical overview. *Hum Reprod Open* **2019**, hoy024 (2019).
29. K. Takahashi, K. Tanabe, M. Ohnuki, M. Narita, T. Ichisaka, K. Tomoda, S. Yamanaka, Induction of pluripotent stem cells from adult human fibroblasts by defined factors. *Cell* **131**, 861-872 (2007).
30. J. B. Gurdon, The developmental capacity of nuclei taken from intestinal epithelium cells of feeding tadpoles. *J Embryol Exp Morphol* **10**, 622-640 (1962).
31. R. L. Davis, H. Weintraub, A. B. Lassar, Expression of a single transfected cDNA converts fibroblasts to myoblasts. *Cell* **51**, 987-1000 (1987).
32. J. Yu, M. A. Vodyanik, K. Smuga-Otto, J. Antosiewicz-Bourget, J. L. Frane, S. Tian, J. Nie, G. A. Jonsdottir, V. Ruotti, R. Stewart, Slukvin, II, J. A. Thomson, Induced pluripotent stem cell lines derived from human somatic cells. *Science* **318**, 1917-1920 (2007).
33. X. Y. Zhao, W. Li, Z. Lv, L. Liu, M. Tong, T. Hai, J. Hao, C. L. Guo, Q. W. Ma, L. Wang, F. Zeng, Q. Zhou, iPS cells produce viable mice through tetraploid complementation. *Nature* **461**, 86-90 (2009).
34. J. Choi, S. Lee, W. Mallard, K. Clement, G. M. Tagliazucchi, H. Lim, I. Y. Choi, F. Ferrari, A. M. Tsankov, R. Pop, G. Lee, J. L. Rinn, A. Meissner, P. J. Park, K. Hochedlinger, A comparison of genetically matched cell lines reveals the equivalence of human iPSCs and ESCs. *Nat Biotechnol* **33**, 1173-1181 (2015).
35. Y. Shi, H. Inoue, J. C. Wu, S. Yamanaka, Induced pluripotent stem cell technology: a decade of progress. *Nat Rev Drug Discov* **16**, 115-130 (2017).

36. Y. H. Loh, S. Agarwal, I. H. Park, A. Urbach, H. Huo, G. C. Heffner, K. Kim, J. D. Miller, K. Ng, G. Q. Daley, Generation of induced pluripotent stem cells from human blood. *Blood* **113**, 5476-5479 (2009).
37. A. D. Ebert, J. Yu, F. F. Rose, Jr., V. B. Mattis, C. L. Lorson, J. A. Thomson, C. N. Svendsen, Induced pluripotent stem cells from a spinal muscular atrophy patient. *Nature* **457**, 277-280 (2009).
38. M. C. Marchetto, C. Carromeu, A. Acab, D. Yu, G. W. Yeo, Y. Mu, G. Chen, F. H. Gage, A. R. Muotri, A model for neural development and treatment of Rett syndrome using human induced pluripotent stem cells. *Cell* **143**, 527-539 (2010).
39. I. Itzhaki, L. Maizels, I. Huber, L. Zwi-Dantsis, O. Caspi, A. Winterstern, O. Feldman, A. Gepstein, G. Arbel, H. Hammerman, M. Boulos, L. Gepstein, Modelling the long QT syndrome with induced pluripotent stem cells. *Nature* **471**, 225-229 (2011).
40. M. A. Israel, S. H. Yuan, C. Bardy, S. M. Reyna, Y. Mu, C. Herrera, M. P. Hefferan, S. Van Gorp, K. L. Nazor, F. S. Boscolo, C. T. Carson, L. C. Laurent, M. Marsala, F. H. Gage, A. M. Remes, E. H. Koo, L. S. Goldstein, Probing sporadic and familial Alzheimer's disease using induced pluripotent stem cells. *Nature* **482**, 216-220 (2012).
41. H. N. Nguyen, B. Byers, B. Cord, A. Shcheglovitov, J. Byrne, P. Gujar, K. Kee, B. Schule, R. E. Dolmetsch, W. Langston, T. D. Palmer, R. R. Pera, LRRK2 mutant iPSC-derived DA neurons demonstrate increased susceptibility to oxidative stress. *Cell Stem Cell* **8**, 267-280 (2011).
42. R. G. Rowe, G. Q. Daley, Induced pluripotent stem cells in disease modelling and drug discovery. *Nat Rev Genet* **20**, 377-388 (2019).
43. K. G. Chen, B. S. Mallon, R. D. McKay, P. G. Robey, Human pluripotent stem cell culture: considerations for maintenance, expansion, and therapeutics. *Cell Stem Cell* **14**, 13-26 (2014).
44. L. Li, S. A. Bennett, L. Wang, Role of E-cadherin and other cell adhesion molecules in survival and differentiation of human pluripotent stem cells. *Cell Adh Migr* **6**, 59-70 (2012).
45. P. J. Wrighton, J. R. Klim, B. A. Hernandez, C. H. Koonce, T. J. Kamp, L. L. Kiessling, Signals from the surface modulate differentiation of human pluripotent stem cells through glycosaminoglycans and integrins. *Proc Natl Acad Sci U S A* **111**, 18126-18131 (2014).
46. W. L. Murphy, T. C. McDevitt, A. J. Engler, Materials as stem cell regulators. *Nat Mater* **13**, 547-557 (2014).
47. J. R. Klim, L. Li, P. J. Wrighton, M. S. Piekarczyk, L. L. Kiessling, A defined glycosaminoglycan-binding substratum for human pluripotent stem cells. *Nat Methods* **7**, 989-994 (2010).
48. R. Brandenberger, H. Wei, S. Zhang, S. Lei, J. Murage, G. J. Fisk, Y. Li, C. Xu, R. Fang, K. Guegler, M. S. Rao, R. Mandalam, J. Lebkowski, L. W. Stanton, Transcriptome characterization elucidates signaling networks that control human ES cell growth and differentiation. *Nat Biotechnol* **22**, 707-716 (2004).
49. M. Amit, M. K. Carpenter, M. S. Inokuma, C. P. Chiu, C. P. Harris, M. A. Waknitz, J. Itskovitz-Eldor, J. A. Thomson, Clonally derived human embryonic stem cell lines maintain pluripotency and proliferative potential for prolonged periods of culture. *Dev Biol* **227**, 271-278 (2000).
50. Q. Hui, Z. Jin, X. Li, C. Liu, X. Wang, FGF Family: From Drug Development to Clinical Application. *Int J Mol Sci* **19**, (2018).

51. L. Dailey, D. Ambrosetti, A. Mansukhani, C. Basilico, Mechanisms underlying differential responses to FGF signaling. *Cytokine Growth Factor Rev* **16**, 233-247 (2005).
52. X. Li, C. Wang, J. Xiao, W. L. McKeehan, F. Wang, Fibroblast growth factors, old kids on the new block. *Semin Cell Dev Biol* **53**, 155-167 (2016).
53. Y. R. Yun, J. E. Won, E. Jeon, S. Lee, W. Kang, H. Jo, J. H. Jang, U. S. Shin, H. W. Kim, Fibroblast growth factors: biology, function, and application for tissue regeneration. *J Tissue Eng* **2010**, 218142 (2010).
54. Y. Nakashima, T. Omasa, What Kind of Signaling Maintains Pluripotency and Viability in Human-Induced Pluripotent Stem Cells Cultured on Laminin-511 with Serum-Free Medium? *Biores Open Access* **5**, 84-93 (2016).
55. D. M. Ornitz, N. Itoh, Fibroblast growth factors. *Genome Biol* **2**, REVIEWS3005 (2001).
56. T. Kunath, M. K. Saba-El-Leil, M. Almousailleakh, J. Wray, S. Meloche, A. Smith, FGF stimulation of the Erk1/2 signalling cascade triggers transition of pluripotent embryonic stem cells from self-renewal to lineage commitment. *Development* **134**, 2895-2902 (2007).
57. R. H. Xu, R. M. Peck, D. S. Li, X. Feng, T. Ludwig, J. A. Thomson, Basic FGF and suppression of BMP signaling sustain undifferentiated proliferation of human ES cells. *Nat Methods* **2**, 185-190 (2005).
58. P. J. Tesar, J. G. Chenoweth, F. A. Brook, T. J. Davies, E. P. Evans, D. L. Mack, R. L. Gardner, R. D. McKay, New cell lines from mouse epiblast share defining features with human embryonic stem cells. *Nature* **448**, 196-199 (2007).
59. I. G. Brons, L. E. Smithers, M. W. Trotter, P. Rugg-Gunn, B. Sun, S. M. Chuva de Sousa Lopes, S. K. Howlett, A. Clarkson, L. Ahrlund-Richter, R. A. Pedersen, L. Vallier, Derivation of pluripotent epiblast stem cells from mammalian embryos. *Nature* **448**, 191-195 (2007).
60. C. W. Lu, A. Yabuuchi, L. Chen, S. Viswanathan, K. Kim, G. Q. Daley, Ras-MAPK signaling promotes trophectoderm formation from embryonic stem cells and mouse embryos. *Nat Genet* **40**, 921-926 (2008).
61. J. Li, G. Wang, C. Wang, Y. Zhao, H. Zhang, Z. Tan, Z. Song, M. Ding, H. Deng, MEK/ERK signaling contributes to the maintenance of human embryonic stem cell self-renewal. *Differentiation* **75**, 299-307 (2007).
62. K. A. D'Amour, A. D. Agulnick, S. Eliazer, O. G. Kelly, E. Kroon, E. E. Baetge, Efficient differentiation of human embryonic stem cells to definitive endoderm. *Nat Biotechnol* **23**, 1534-1541 (2005).
63. B. Greber, H. Lehrach, J. Adjaye, Fibroblast growth factor 2 modulates transforming growth factor beta signaling in mouse embryonic fibroblasts and human ESCs (hESCs) to support hESC self-renewal. *Stem Cells* **25**, 455-464 (2007).
64. D. Besser, Expression of nodal, lefty-a, and lefty-B in undifferentiated human embryonic stem cells requires activation of Smad2/3. *J Biol Chem* **279**, 45076-45084 (2004).
65. G. S. Feng, Shp2-mediated molecular signaling in control of embryonic stem cell self-renewal and differentiation. *Cell Res* **17**, 37-41 (2007).
66. P. Yu, G. Pan, J. Yu, J. A. Thomson, FGF2 sustains NANOG and switches the outcome of BMP4-induced human embryonic stem cell differentiation. *Cell Stem Cell* **8**, 326-334 (2011).

67. M. P. Stavridis, J. S. Lunn, B. J. Collins, K. G. Storey, A discrete period of FGF-induced Erk1/2 signalling is required for vertebrate neural specification. *Development* **134**, 2889-2894 (2007).
68. M. S. Rahman, N. Akhtar, H. M. Jamil, R. S. Banik, S. M. Asaduzzaman, TGF-beta/BMP signaling and other molecular events: regulation of osteoblastogenesis and bone formation. *Bone Res* **3**, 15005 (2015).
69. G. P. Allendorph, W. W. Vale, S. Choe, Structure of the ternary signaling complex of a TGF-beta superfamily member. *Proc Natl Acad Sci U S A* **103**, 7643-7648 (2006).
70. A. L. Balboni, J. A. Hutchinson, A. J. DeCastro, P. Cherukuri, K. Liby, M. B. Sporn, G. N. Schwartz, W. A. Wells, L. F. Sempere, P. B. Yu, J. DiRenzo, DeltaNp63alpha-mediated activation of bone morphogenetic protein signaling governs stem cell activity and plasticity in normal and malignant mammary epithelial cells. *Cancer Res* **73**, 1020-1030 (2013).
71. A. Moustakas, S. Souchelnytskyi, C. H. Heldin, Smad regulation in TGF-beta signal transduction. *J Cell Sci* **114**, 4359-4369 (2001).
72. C. H. Heldin, K. Miyazono, P. ten Dijke, TGF-beta signalling from cell membrane to nucleus through SMAD proteins. *Nature* **390**, 465-471 (1997).
73. X. H. Feng, R. Derynck, Specificity and versatility in tgf-beta signaling through Smads. *Annu Rev Cell Dev Biol* **21**, 659-693 (2005).
74. Y. Shi, J. Massague, Mechanisms of TGF-beta signaling from cell membrane to the nucleus. *Cell* **113**, 685-700 (2003).
75. R. N. Wang, J. Green, Z. Wang, Y. Deng, M. Qiao, M. Peabody, Q. Zhang, J. Ye, Z. Yan, S. Denduluri, O. Idowu, M. Li, C. Shen, A. Hu, R. C. Haydon, R. Kang, J. Mok, M. J. Lee, H. L. Luu, L. L. Shi, Bone Morphogenetic Protein (BMP) signaling in development and human diseases. *Genes Dis* **1**, 87-105 (2014).
76. J. Massague, TGF-beta signal transduction. *Annu Rev Biochem* **67**, 753-791 (1998).
77. Z. Li, T. Fei, J. Zhang, G. Zhu, L. Wang, D. Lu, X. Chi, Y. Teng, N. Hou, X. Yang, H. Zhang, J. D. Han, Y. G. Chen, BMP4 Signaling Acts via dual-specificity phosphatase 9 to control ERK activity in mouse embryonic stem cells. *Cell Stem Cell* **10**, 171-182 (2012).
78. Q. L. Ying, J. Nichols, I. Chambers, A. Smith, BMP induction of Id proteins suppresses differentiation and sustains embryonic stem cell self-renewal in collaboration with STAT3. *Cell* **115**, 281-292 (2003).
79. R. H. Xu, X. Chen, D. S. Li, R. Li, G. C. Addicks, C. Glennon, T. P. Zwaka, J. A. Thomson, BMP4 initiates human embryonic stem cell differentiation to trophoblast. *Nat Biotechnol* **20**, 1261-1264 (2002).
80. M. Pick, L. Azzola, A. Mossman, E. G. Stanley, A. G. Elefanty, Differentiation of human embryonic stem cells in serum-free medium reveals distinct roles for bone morphogenetic protein 4, vascular endothelial growth factor, stem cell factor, and fibroblast growth factor 2 in hematopoiesis. *Stem Cells* **25**, 2206-2214 (2007).
81. S. W. Park, Y. Jun Koh, J. Jeon, Y. H. Cho, M. J. Jang, Y. Kang, M. J. Kim, C. Choi, Y. Sook Cho, H. M. Chung, G. Y. Koh, Y. M. Han, Efficient differentiation of human pluripotent stem cells into functional CD34+ progenitor cells by combined modulation of the MEK/ERK and BMP4 signaling pathways. *Blood* **116**, 5762-5772 (2010).
82. L. Yang, M. H. Soonpaa, E. D. Adler, T. K. Roepke, S. J. Kattman, M. Kennedy, E. Henckaerts, K. Bonham, G. W. Abbott, R. M. Linden, L. J. Field, G. M. Keller, Human

cardiovascular progenitor cells develop from a KDR+ embryonic-stem-cell-derived population. *Nature* **453**, 524-528 (2008).
83. S. J. Kattman, A. D. Witty, M. Gagliardi, N. C. Dubois, M. Niapour, A. Hotta, J. Ellis, G. Keller, Stage-specific optimization of activin/nodal and BMP signaling promotes cardiac differentiation of mouse and human pluripotent stem cell lines. *Cell Stem Cell* **8**, 228-240 (2011).
84. J. Cai, Y. Zhao, Y. Liu, F. Ye, Z. Song, H. Qin, S. Meng, Y. Chen, R. Zhou, X. Song, Y. Guo, M. Ding, H. Deng, Directed differentiation of human embryonic stem cells into functional hepatic cells. *Hepatology* **45**, 1229-1239 (2007).
85. M. C. Nostro, F. Sarangi, S. Ogawa, A. Holtzinger, B. Corneo, X. Li, S. J. Micallef, I. H. Park, C. Basford, M. B. Wheeler, G. Q. Daley, A. G. Elefanty, E. G. Stanley, G. Keller, Stage-specific signaling through TGFbeta family members and WNT regulates patterning and pancreatic specification of human pluripotent stem cells. *Development* **138**, 861-871 (2011).
86. M. D. Green, A. Chen, M. C. Nostro, S. L. d'Souza, C. Schaniel, I. R. Lemischka, V. Gouon-Evans, G. Keller, H. W. Snoeck, Generation of anterior foregut endoderm from human embryonic and induced pluripotent stem cells. *Nat Biotechnol* **29**, 267-272 (2011).
87. Q. L. Ying, M. Stavridis, D. Griffiths, M. Li, A. Smith, Conversion of embryonic stem cells into neuroectodermal precursors in adherent monoculture. *Nat Biotechnol* **21**, 183-186 (2003).
88. T. Fei, K. Xia, Z. Li, B. Zhou, S. Zhu, H. Chen, J. Zhang, Z. Chen, H. Xiao, J. D. Han, Y. G. Chen, Genome-wide mapping of SMAD target genes reveals the role of BMP signaling in embryonic stem cell fate determination. *Genome Res* **20**, 36-44 (2010).
89. J. Tchieu, B. Zimmer, F. Fattahi, S. Amin, N. Zeltner, S. Chen, L. Studer, A Modular Platform for Differentiation of Human PSCs into All Major Ectodermal Lineages. *Cell Stem Cell* **21**, 399-410 e397 (2017).
90. G. M. Beattie, A. D. Lopez, N. Bucay, A. Hinton, M. T. Firpo, C. C. King, A. Hayek, Activin A maintains pluripotency of human embryonic stem cells in the absence of feeder layers. *Stem Cells* **23**, 489-495 (2005).
91. A. M. Singh, D. Reynolds, T. Cliff, S. Ohtsuka, A. L. Mattheyses, Y. Sun, L. Menendez, M. Kulik, S. Dalton, Signaling network crosstalk in human pluripotent cells: a Smad2/3-regulated switch that controls the balance between self-renewal and differentiation. *Cell Stem Cell* **10**, 312-326 (2012).
92. M. Yasunaga, S. Tada, S. Torikai-Nishikawa, Y. Nakano, M. Okada, L. M. Jakt, S. Nishikawa, T. Chiba, T. Era, S. Nishikawa, Induction and monitoring of definitive and visceral endoderm differentiation of mouse ES cells. *Nat Biotechnol* **23**, 1542-1550 (2005).
93. P. Gadue, T. L. Huber, P. J. Paddison, G. M. Keller, Wnt and TGF-beta signaling are required for the induction of an in vitro model of primitive streak formation using embryonic stem cells. *Proc Natl Acad Sci U S A* **103**, 16806-16811 (2006).
94. T. Sumi, N. Tsuneyoshi, N. Nakatsuji, H. Suemori, Defining early lineage specification of human embryonic stem cells by the orchestrated balance of canonical Wnt/beta-catenin, Activin/Nodal and BMP signaling. *Development* **135**, 2969-2979 (2008).
95. X. Xu, V. L. Browning, J. S. Odorico, Activin, BMP and FGF pathways cooperate to promote endoderm and pancreatic lineage cell differentiation from human embryonic stem cells. *Mech Dev* **128**, 412-427 (2011).

96. J. R. Smith, L. Vallier, G. Lupo, M. Alexander, W. A. Harris, R. A. Pedersen, Inhibition of Activin/Nodal signaling promotes specification of human embryonic stem cells into neuroectoderm. *Dev Biol* **313**, 107-117 (2008).
97. T. Watabe, K. Miyazono, Roles of TGF-beta family signaling in stem cell renewal and differentiation. *Cell Res* **19**, 103-115 (2009).
98. A. B. McLean, K. A. D'Amour, K. L. Jones, M. Krishnamoorthy, M. J. Kulik, D. M. Reynolds, A. M. Sheppard, H. Liu, Y. Xu, E. E. Baetge, S. Dalton, Activin a efficiently specifies definitive endoderm from human embryonic stem cells only when phosphatidylinositol 3-kinase signaling is suppressed. *Stem Cells* **25**, 29-38 (2007).
99. R. T. Moon, Wnt/beta-catenin pathway. *Sci STKE* **2005**, cm1 (2005).
100. Z. Xu, A. M. Robitaille, J. D. Berndt, K. C. Davidson, K. A. Fischer, J. Mathieu, J. C. Potter, H. Ruohola-Baker, R. T. Moon, Wnt/beta-catenin signaling promotes self-renewal and inhibits the primed state transition in naive human embryonic stem cells. *Proc Natl Acad Sci U S A* **113**, E6382-E6390 (2016).
101. H. Sperber, J. Mathieu, Y. Wang, A. Ferreccio, J. Hesson, Z. Xu, K. A. Fischer, A. Devi, D. Detraux, H. Gu, S. L. Battle, M. Showalter, C. Valensisi, J. H. Bielas, N. G. Ericson, L. Margaretha, A. M. Robitaille, D. Margineantu, O. Fiehn, D. Hockenbery, C. A. Blau, D. Raftery, A. A. Margolin, R. D. Hawkins, R. T. Moon, C. B. Ware, H. Ruohola-Baker, The metabolome regulates the epigenetic landscape during naive-to-primed human embryonic stem cell transition. *Nat Cell Biol* **17**, 1523-1535 (2015).
102. N. Sato, L. Meijer, L. Skaltsounis, P. Greengard, A. H. Brivanlou, Maintenance of pluripotency in human and mouse embryonic stem cells through activation of Wnt signaling by a pharmacological GSK-3-specific inhibitor. *Nat Med* **10**, 55-63 (2004).
103. U. Ullmann, C. Gilles, M. De Rycke, H. Van de Velde, K. Sermon, I. Liebaers, GSK-3-specific inhibitor-supplemented hESC medium prevents the epithelial-mesenchymal transition process and the up-regulation of matrix metalloproteinases in hESCs cultured in feeder-free conditions. *Mol Hum Reprod* **14**, 169-179 (2008).
104. M. Nakanishi, A. Kurisaki, Y. Hayashi, M. Warashina, S. Ishiura, M. Kusuda-Furue, M. Asashima, Directed induction of anterior and posterior primitive streak by Wnt from embryonic stem cells cultured in a chemically defined serum-free medium. *FASEB J* **23**, 114-122 (2009).
105. H. K. Bone, A. S. Nelson, C. E. Goldring, D. Tosh, M. J. Welham, A novel chemically directed route for the generation of definitive endoderm from human embryonic stem cells based on inhibition of GSK-3. *J Cell Sci* **124**, 1992-2000 (2011).
106. K. C. Davidson, A. M. Adams, J. M. Goodson, C. E. McDonald, J. C. Potter, J. D. Berndt, T. L. Biechele, R. J. Taylor, R. T. Moon, Wnt/beta-catenin signaling promotes differentiation, not self-renewal, of human embryonic stem cells and is repressed by Oct4. *Proc Natl Acad Sci U S A* **109**, 4485-4490 (2012).
107. H. Kim, J. Wu, S. Ye, C. I. Tai, X. Zhou, H. Yan, P. Li, M. Pera, Q. L. Ying, Modulation of beta-catenin function maintains mouse epiblast stem cell and human embryonic stem cell self-renewal. *Nat Commun* **4**, 2403 (2013).
108. T. A. Blauwkamp, S. Nigam, R. Ardehali, I. L. Weissman, R. Nusse, Endogenous Wnt signalling in human embryonic stem cells generates an equilibrium of distinct lineage-specified progenitors. *Nat Commun* **3**, 1070 (2012).
109. D. Kurek, A. Neagu, M. Tastemel, N. Tuysuz, J. Lehmann, H. J. G. van de Werken, S. Philipsen, R. van der Linden, A. Maas, I. W. F. J. van, M. Drukker, D. Ten Berge,

Endogenous WNT signals mediate BMP-induced and spontaneous differentiation of epiblast stem cells and human embryonic stem cells. *Stem Cell Reports* **4**, 114-128 (2015).
110. M. A. Johnson, J. P. Weick, R. A. Pearce, S. C. Zhang, Functional neural development from human embryonic stem cells: accelerated synaptic activity via astrocyte coculture. *J Neurosci* **27**, 3069-3077 (2007).
111. K. Watanabe, M. Ueno, D. Kamiya, A. Nishiyama, M. Matsumura, T. Wataya, J. B. Takahashi, S. Nishikawa, S. Nishikawa, K. Muguruma, Y. Sasai, A ROCK inhibitor permits survival of dissociated human embryonic stem cells. *Nat Biotechnol* **25**, 681-686 (2007).
112. M. Ohgushi, M. Matsumura, M. Eiraku, K. Murakami, T. Aramaki, A. Nishiyama, K. Muguruma, T. Nakano, H. Suga, M. Ueno, T. Ishizaki, H. Suemori, S. Narumiya, H. Niwa, Y. Sasai, Molecular pathway and cell state responsible for dissociation-induced apoptosis in human pluripotent stem cells. *Cell Stem Cell* **7**, 225-239 (2010).
113. F. M. Watt, W. T. Huck, Role of the extracellular matrix in regulating stem cell fate. *Nat Rev Mol Cell Biol* **14**, 467-473 (2013).
114. S. Ozbek, P. G. Balasubramanian, R. Chiquet-Ehrismann, R. P. Tucker, J. C. Adams, The evolution of extracellular matrix. *Mol Biol Cell* **21**, 4300-4305 (2010).
115. K. Y. Tsang, M. C. Cheung, D. Chan, K. S. Cheah, The developmental roles of the extracellular matrix: beyond structure to regulation. *Cell and tissue research* **339**, 93-110 (2010).
116. F. Gattazzo, A. Urciuolo, P. Bonaldo, Extracellular matrix: a dynamic microenvironment for stem cell niche. *Biochimica et Biophysica Acta (BBA)-General Subjects* **1840**, 2506-2519 (2014).
117. R. O. Hynes, The extracellular matrix: not just pretty fibrils. *Science* **326**, 1216-1219 (2009).
118. M. J. Domingues, H. Cao, S. Y. Heazlewood, B. Cao, S. K. Nilsson, Niche extracellular matrix components and their influence on HSC. *Journal of cellular biochemistry* **118**, 1984-1993 (2017).
119. L. C. Ceafalan, A.-M. Enciu, T. E. Fertig, B. O. Popescu, M. Gherghiceanu, M. E. Hinescu, E. Radu, Heterocellular molecular contacts in the mammalian stem cell niche. *European journal of cell biology* **97**, 442-461 (2018).
120. A. J. Engler, S. Sen, H. L. Sweeney, D. E. Discher, Matrix elasticity directs stem cell lineage specification. *Cell* **126**, 677-689 (2006).
121. S. Musah, S. A. Morin, P. J. Wrighton, D. B. Zwick, S. Jin, L. L. Kiessling, Glycosaminoglycan-binding hydrogels enable mechanical control of human pluripotent stem cell self-renewal. *ACS Nano* **6**, 10168-10177 (2012).
122. L. B. Hazeltine, M. G. Badur, X. Lian, A. Das, W. Han, S. P. Palecek, Temporal impact of substrate mechanics on differentiation of human embryonic stem cells to cardiomyocytes. *Acta Biomater* **10**, 604-612 (2014).
123. J. Nicolas, S. Magli, L. Rabbachin, S. Sampaolesi, F. Nicotra, L. Russo, 3D Extracellular Matrix Mimics: Fundamental Concepts and Role of Materials Chemistry to Influence Stem Cell Fate. *Biomacromolecules* **21**, 1968-1994 (2020).
124. C. Formosa-Dague, M. Castelain, H. Martin-Yken, K. Dunker, E. Dague, M. Sletmoen, The role of glycans in bacterial adhesion to mucosal surfaces: how can single-molecule techniques advance our understanding? *Microorganisms* **6**, 39 (2018).

125. P. Stanley, R. D. Cummings, Structures common to different glycans. (2017).
126. P. E. Constantinou, M. Morgado, D. D. Carson, Transmembrane mucin expression and function in embryo implantation and placentation. *Regulation of Implantation and Establishment of Pregnancy in Mammals*, 51-68 (2015).
127. T. Weber, V. Chandrasekaran, I. Stamer, M. B. Thygesen, A. Terfort, T. K. Lindhorst, Switching of bacterial adhesion to a glycosylated surface by reversible reorientation of the carbohydrate ligand. *Angewandte Chemie International Edition* **53**, 14583-14586 (2014).
128. H. H. Lipowsky, The endothelial glycocalyx as a barrier to leukocyte adhesion and its mediation by extracellular proteases. *Annals of biomedical engineering* **40**, 840-848 (2012).
129. M. N. Matrosovich, T. Y. Matrosovich, T. Gray, N. A. Roberts, H.-D. Klenk, Neuraminidase is important for the initiation of influenza virus infection in human airway epithelium. *Journal of virology* **78**, 12665-12667 (2004).
130. L. Mockl, The Emerging Role of the Mammalian Glycocalyx in Functional Membrane Organization and Immune System Regulation. *Front Cell Dev Biol* **8**, 253 (2020).
131. J. S. Draper, C. Pigott, J. A. Thomson, P. W. Andrews, Surface antigens of human embryonic stem cells: changes upon differentiation in culture. *J Anat* **200**, 249-258 (2002).
132. R. A. Smith, K. Meade, C. E. Pickford, R. J. Holley, C. L. Merry, Glycosaminoglycans as regulators of stem cell differentiation. *Biochem Soc Trans* **39**, 383-387 (2011).
133. H. E. Bulow, O. Hobert, The molecular diversity of glycosaminoglycans shapes animal development. *Annu Rev Cell Dev Biol* **22**, 375-407 (2006).
134. S. Puri, Y. M. Coulson-Thomas, T. F. Gesteira, V. J. Coulson-Thomas, Distribution and Function of Glycosaminoglycans and Proteoglycans in the Development, Homeostasis and Pathology of the Ocular Surface. *Front Cell Dev Biol* **8**, 731 (2020).
135. A. J. Quantock, R. D. Young, T. O. Akama, Structural and biochemical aspects of keratan sulphate in the cornea. *Cellular and molecular life sciences* **67**, 891-906 (2010).
136. J. L. Funderburgh, MINI REVIEW Keratan sulfate: structure, biosynthesis, and function. *Glycobiology* **10**, 951-958 (2000).
137. M. SUZUKI, BIOCHEMICAL STUDIES ON CARBOHYDRATES L. Prosthetic Group of Corneamucoid. *The Journal of biochemistry* **30**, 185-191 (1939).
138. A. H. Plaas, L. A. West, E. J. Thonar, Z. A. Karcioglu, C. J. Smith, G. K. Klintworth, V. C. Hascall, Altered fine structures of corneal and skeletal keratan sulfate and chondroitin/dermatan sulfate in macular corneal dystrophy. *Journal of Biological Chemistry* **276**, 39788-39796 (2001).
139. N. Hasegawa, T. Torii, T. Kato, H. Miyajima, A. Furuhata, K. Nakayasu, A. Kanai, O. Habuchi, Decreased GlcNAc 6-O-sulfotransferase activity in the cornea with macular corneal dystrophy. *Investigative ophthalmology & visual science* **41**, 3670-3677 (2000).
140. S. L. Littlechild, R. D. Young, B. Caterson, H. Yoshida, M. Yamazaki, K. Sakimura, A. J. Quantock, T. O. Akama, Keratan sulfate phenotype in the β-1, 3-N-acetylglucosaminyltransferase-7–null mouse cornea. *Investigative ophthalmology & visual science* **59**, 1641-1651 (2018).
141. T. Mikami, H. Kitagawa, Biosynthesis and function of chondroitin sulfate. *Biochimica et Biophysica Acta (BBA)-General Subjects* **1830**, 4719-4733 (2013).

142. S. Yamada, K. Sugahara, S. Ozbek, Evolution of glycosaminoglycans: Comparative biochemical study. *Commun Integr Biol* **4**, 150-158 (2011).
143. K. Sugahara, T. Mikami, T. Uyama, S. Mizuguchi, K. Nomura, H. Kitagawa, Recent advances in the structural biology of chondroitin sulfate and dermatan sulfate. *Curr Opin Struct Biol* **13**, 612-620 (2003).
144. K. Sugahara, H. Kitagawa, Recent advances in the study of the biosynthesis and functions of sulfated glycosaminoglycans. *Curr Opin Struct Biol* **10**, 518-527 (2000).
145. C. Mitsunaga, T. Mikami, S. Mizumoto, J. Fukuda, K. Sugahara, Chondroitin sulfate/dermatan sulfate hybrid chains in the development of cerebellum. Spatiotemporal regulation of the expression of critical disulfated disaccharides by specific sulfotransferases. *J Biol Chem* **281**, 18942-18952 (2006).
146. H. Kitagawa, K. Tsutsumi, Y. Tone, K. Sugahara, Developmental regulation of the sulfation profile of chondroitin sulfate chains in the chicken embryo brain. *J Biol Chem* **272**, 31377-31381 (1997).
147. F. Properzi, D. Carulli, R. A. Asher, E. Muir, L. M. Camargo, T. H. van Kuppevelt, G. B. ten Dam, Y. Furukawa, T. Mikami, K. Sugahara, T. Toida, H. M. Geller, J. W. Fawcett, Chondroitin 6-sulphate synthesis is up-regulated in injured CNS, induced by injury-related cytokines and enhanced in axon-growth inhibitory glia. *Eur J Neurosci* **21**, 378-390 (2005).
148. K. Akita, A. von Holst, Y. Furukawa, T. Mikami, K. Sugahara, A. Faissner, Expression of multiple chondroitin/dermatan sulfotransferases in the neurogenic regions of the embryonic and adult central nervous system implies that complex chondroitin sulfates have a role in neural stem cell maintenance. *Stem Cells* **26**, 798-809 (2008).
149. M. Ida, T. Shuo, K. Hirano, Y. Tokita, K. Nakanishi, F. Matsui, S. Aono, H. Fujita, Y. Fujiwara, T. Kaji, A. Oohira, Identification and functions of chondroitin sulfate in the milieu of neural stem cells. *J Biol Chem* **281**, 5982-5991 (2006).
150. C. I. Gama, S. E. Tully, N. Sotogaku, P. M. Clark, M. Rawat, N. Vaidehi, W. A. Goddard, 3rd, A. Nishi, L. C. Hsieh-Wilson, Sulfation patterns of glycosaminoglycans encode molecular recognition and activity. *Nat Chem Biol* **2**, 467-473 (2006).
151. R. Raman, V. Sasisekharan, R. Sasisekharan, Structural insights into biological roles of protein-glycosaminoglycan interactions. *Chem Biol* **12**, 267-277 (2005).
152. J. M. Brown, J. Xia, B. Zhuang, K. S. Cho, C. J. Rogers, C. I. Gama, M. Rawat, S. E. Tully, N. Uetani, D. E. Mason, M. L. Tremblay, E. C. Peters, O. Habuchi, D. F. Chen, L. C. Hsieh-Wilson, A sulfated carbohydrate epitope inhibits axon regeneration after injury. *Proc Natl Acad Sci U S A* **109**, 4768-4773 (2012).
153. K. Sugahara, T. Mikami, Chondroitin/dermatan sulfate in the central nervous system. *Curr Opin Struct Biol* **17**, 536-545 (2007).
154. R. Lin, T. W. Rosahl, P. J. Whiting, J. W. Fawcett, J. C. Kwok, 6-Sulphated chondroitins have a positive influence on axonal regeneration. *PLoS One* **6**, e21499 (2011).
155. H. Wang, Y. Katagiri, T. E. McCann, E. Unsworth, P. Goldsmith, Z. X. Yu, F. Tan, L. Santiago, E. M. Mills, Y. Wang, A. J. Symes, H. M. Geller, Chondroitin-4-sulfation negatively regulates axonal guidance and growth. *J Cell Sci* **121**, 3083-3091 (2008).
156. A. Purushothaman, K. Sugahara, A. Faissner, Chondroitin sulfate "wobble motifs" modulate maintenance and differentiation of neural stem cells and their progeny. *J Biol Chem* **287**, 2935-2942 (2012).

157. A. Malmstrom, L. A. Fransson, Biosynthesis of dermatan sulfate. I. Formation of L-iduronic acid residues. *J Biol Chem* **250**, 3419-3425 (1975).
158. S. F. Penc, B. Pomahac, T. Winkler, R. A. Dorschner, E. Eriksson, M. Herndon, R. L. Gallo, Dermatan sulfate released after injury is a potent promoter of fibroblast growth factor-2 function. *J Biol Chem* **273**, 28116-28121 (1998).
159. A. Ori, M. C. Wilkinson, D. G. Fernig, A systems biology approach for the investigation of the heparin/heparan sulfate interactome. *J Biol Chem* **286**, 19892-19904 (2011).
160. J. Kreuger, L. Kjellen, Heparan sulfate biosynthesis: regulation and variability. *J Histochem Cytochem* **60**, 898-907 (2012).
161. M. Busse, A. Feta, J. Presto, M. Wilen, M. Gronning, L. Kjellen, M. Kusche-Gullberg, Contribution of EXT1, EXT2, and EXTL3 to heparan sulfate chain elongation. *J Biol Chem* **282**, 32802-32810 (2007).
162. J. D. Esko, U. Lindahl, Molecular diversity of heparan sulfate. *J Clin Invest* **108**, 169-173 (2001).
163. R. D. Rosenberg, N. W. Shworak, J. Liu, J. J. Schwartz, L. Zhang, Heparan sulfate proteoglycans of the cardiovascular system. Specific structures emerge but how is synthesis regulated? *J Clin Invest* **99**, 2062-2070 (1997).
164. M. C. Bourin, U. Lindahl, Glycosaminoglycans and the regulation of blood coagulation. *Biochem J* **289 (Pt 2)**, 313-330 (1993).
165. A. S. Edge, R. G. Spiro, Characterization of novel sequences containing 3-O-sulfated glucosamine in glomerular basement membrane heparan sulfate and localization of sulfated disaccharides to a peripheral domain. *J Biol Chem* **265**, 15874-15881 (1990).
166. U. Lindahl, M. Kusche-Gullberg, L. Kjellen, Regulated diversity of heparan sulfate. *J Biol Chem* **273**, 24979-24982 (1998).
167. J. E. Turnbull, D. G. Fernig, Y. Ke, M. C. Wilkinson, J. T. Gallagher, Identification of the basic fibroblast growth factor binding sequence in fibroblast heparan sulfate. *J Biol Chem* **267**, 10337-10341 (1992).
168. H. Habuchi, M. Tanaka, O. Habuchi, K. Yoshida, H. Suzuki, K. Ban, K. Kimata, The occurrence of three isoforms of heparan sulfate 6-O-sulfotransferase having different specificities for hexuronic acid adjacent to the targeted N-sulfoglucosamine. *J Biol Chem* **275**, 2859-2868 (2000).
169. J. Liu, N. W. Shworak, P. Sinay, J. J. Schwartz, L. Zhang, L. M. Fritze, R. D. Rosenberg, Expression of heparan sulfate D-glucosaminyl 3-O-sulfotransferase isoforms reveals novel substrate specificities. *J Biol Chem* **274**, 5185-5192 (1999).
170. J. Aikawa, J. D. Esko, Molecular cloning and expression of a third member of the heparan sulfate/heparin GlcNAc N-deacetylase/ N-sulfotransferase family. *J Biol Chem* **274**, 2690-2695 (1999).
171. I. Vlodavsky, N. Ilan, A. Naggi, B. Casu, Heparanase: structure, biological functions, and inhibition by heparin-derived mimetics of heparan sulfate. *Curr Pharm Des* **13**, 2057-2073 (2007).
172. M. D. Hulett, J. R. Hornby, S. J. Ohms, J. Zuegg, C. Freeman, J. E. Gready, C. R. Parish, Identification of active-site residues of the pro-metastatic endoglycosidase heparanase. *Biochemistry* **39**, 15659-15667 (2000).
173. P. H. Kussie, J. D. Hulmes, D. L. Ludwig, S. Patel, E. C. Navarro, A. P. Seddon, N. A. Giorgio, P. Bohlen, Cloning and functional expression of a human heparanase gene. *Biochem Biophys Res Commun* **261**, 183-187 (1999).

174. M. Bernfield, M. Gotte, P. W. Park, O. Reizes, M. L. Fitzgerald, J. Lincecum, M. Zako, Functions of cell surface heparan sulfate proteoglycans. *Annu Rev Biochem* **68**, 729-777 (1999).
175. K. J. Williams, I. V. Fuki, Cell-surface heparan sulfate proteoglycans: dynamic molecules mediating ligand catabolism. *Curr Opin Lipidol* **8**, 253-262 (1997).
176. A. C. Rapraeger, Syndecan-regulated receptor signaling. *J Cell Biol* **149**, 995-998 (2000).
177. S. Tumova, A. Woods, J. R. Couchman, Heparan sulfate proteoglycans on the cell surface: versatile coordinators of cellular functions. *Int J Biochem Cell Biol* **32**, 269-288 (2000).
178. J. Filmus, Glypicans in growth control and cancer. *Glycobiology* **11**, 19R-23R (2001).
179. W. Halfter, S. Dong, B. Schurer, G. J. Cole, Collagen XVIII is a basement membrane heparan sulfate proteoglycan. *J Biol Chem* **273**, 25404-25412 (1998).
180. R. V. Iozzo, Matrix proteoglycans: from molecular design to cellular function. *Annu Rev Biochem* **67**, 609-652 (1998).
181. M. P. Sarras, Jr., M. E. Madden, X. M. Zhang, S. Gunwar, J. K. Huff, B. G. Hudson, Extracellular matrix (mesoglea) of Hydra vulgaris. I. Isolation and characterization. *Dev Biol* **148**, 481-494 (1991).
182. B. L. Allen, M. S. Filla, A. C. Rapraeger, Role of heparan sulfate as a tissue-specific regulator of FGF-4 and FGF receptor recognition. *J Cell Biol* **155**, 845-858 (2001).
183. J. E. Turnbull, J. T. Gallagher, Oligosaccharide mapping of heparan sulphate by polyacrylamide-gradient-gel electrophoresis and electrotransfer to nylon membrane. *Biochem J* **251**, 597-608 (1988).
184. E. Hammond, A. Khurana, V. Shridhar, K. Dredge, The Role of Heparanase and Sulfatases in the Modification of Heparan Sulfate Proteoglycans within the Tumor Microenvironment and Opportunities for Novel Cancer Therapeutics. *Front Oncol* **4**, 195 (2014).
185. J. Lai, J. Chien, J. Staub, R. Avula, E. L. Greene, T. A. Matthews, D. I. Smith, S. H. Kaufmann, L. R. Roberts, V. Shridhar, Loss of HSulf-1 up-regulates heparin-binding growth factor signaling in cancer. *J Biol Chem* **278**, 23107-23117 (2003).
186. X. Ai, A. T. Do, O. Lozynska, M. Kusche-Gullberg, U. Lindahl, C. P. Emerson, Jr., QSulf1 remodels the 6-O sulfation states of cell surface heparan sulfate proteoglycans to promote Wnt signaling. *J Cell Biol* **162**, 341-351 (2003).
187. A. C. Rapraeger, A. Krufka, B. B. Olwin, Requirement of heparan sulfate for bFGF-mediated fibroblast growth and myoblast differentiation. *Science* **252**, 1705-1708 (1991).
188. I. Vlodavsky, O. Goldshmidt, E. Zcharia, R. Atzmon, Z. Rangini-Guatta, M. Elkin, T. Peretz, Y. Friedmann, Mammalian heparanase: involvement in cancer metastasis, angiogenesis and normal development. *Semin Cancer Biol* **12**, 121-129 (2002).
189. P. Olczyk, L. Mencner, K. Komosinska-Vassev, Diverse Roles of Heparan Sulfate and Heparin in Wound Repair. *Biomed Res Int* **2015**, 549417 (2015).
190. J. Capdevila, R. L. Johnson, Endogenous and ectopic expression of noggin suggests a conserved mechanism for regulation of BMP function during limb and somite patterning. *Dev Biol* **197**, 205-217 (1998).
191. X. Lin, G. Wei, Z. Shi, L. Dryer, J. D. Esko, D. E. Wells, M. M. Matzuk, Disruption of gastrulation and heparan sulfate biosynthesis in EXT1-deficient mice. *Dev Biol* **224**, 299-311 (2000).

192. K. A. Meade, K. J. White, C. E. Pickford, R. J. Holley, A. Marson, D. Tillotson, T. H. van Kuppevelt, J. D. Whittle, A. J. Day, C. L. Merry, Immobilization of heparan sulfate on electrospun meshes to support embryonic stem cell culture and differentiation. *J Biol Chem* **288**, 5530-5538 (2013).
193. C. E. Pickford, R. J. Holley, G. Rushton, M. P. Stavridis, C. M. Ward, C. L. Merry, Specific glycosaminoglycans modulate neural specification of mouse embryonic stem cells. *Stem Cells* **29**, 629-640 (2011).
194. R. J. Holley, C. E. Pickford, G. Rushton, G. Lacaud, J. T. Gallagher, V. Kouskoff, C. L. Merry, Influencing hematopoietic differentiation of mouse embryonic stem cells using soluble heparin and heparan sulfate saccharides. *J Biol Chem* **286**, 6241-6252 (2011).
195. R. J. Baldwin, G. B. ten Dam, T. H. van Kuppevelt, G. Lacaud, J. T. Gallagher, V. Kouskoff, C. L. Merry, A developmentally regulated heparan sulfate epitope defines a subpopulation with increased blood potential during mesodermal differentiation. *Stem Cells* **26**, 3108-3118 (2008).
196. C. E. Johnson, B. E. Crawford, M. Stavridis, G. Ten Dam, A. L. Wat, G. Rushton, C. M. Ward, V. Wilson, T. H. van Kuppevelt, J. D. Esko, A. Smith, J. T. Gallagher, C. L. Merry, Essential alterations of heparan sulfate during the differentiation of embryonic stem cells to Sox1-enhanced green fluorescent protein-expressing neural progenitor cells. *Stem Cells* **25**, 1913-1923 (2007).
197. D. C. Kraushaar, S. Rai, E. Condac, A. Nairn, S. Zhang, Y. Yamaguchi, K. Moremen, S. Dalton, L. Wang, Heparan sulfate facilitates FGF and BMP signaling to drive mesoderm differentiation of mouse embryonic stem cells. *J Biol Chem* **287**, 22691-22700 (2012).
198. D. C. Kraushaar, Y. Yamaguchi, L. Wang, Heparan sulfate is required for embryonic stem cells to exit from self-renewal. *J Biol Chem* **285**, 5907-5916 (2010).
199. Q. Wang, L. Yang, C. Alexander, S. Temple, The niche factor syndecan-1 regulates the maintenance and proliferation of neural progenitor cells during mammalian cortical development. *PLoS One* **7**, e42883 (2012).
200. A. Dityatev, G. Dityateva, V. Sytnyk, M. Delling, N. Toni, I. Nikonenko, D. Muller, M. Schachner, Polysialylated neural cell adhesion molecule promotes remodeling and formation of hippocampal synapses. *J Neurosci* **24**, 9372-9382 (2004).
201. Y. Yamaguchi, Heparan sulfate proteoglycans in the nervous system: their diverse roles in neurogenesis, axon guidance, and synaptogenesis. *Semin Cell Dev Biol* **12**, 99-106 (2001).
202. P. Zhang, H. Lu, R. T. Peixoto, M. K. Pines, Y. Ge, S. Oku, T. J. Siddiqui, Y. Xie, W. Wu, S. Archer-Hartmann, K. Yoshida, K. F. Tanaka, A. R. Aricescu, P. Azadi, M. D. Gordon, B. L. Sabatini, R. O. L. Wong, A. M. Craig, Heparan Sulfate Organizes Neuronal Synapses through Neurexin Partnerships. *Cell* **174**, 1450-1464 e1423 (2018).
203. T. J. Siddiqui, P. K. Tari, S. A. Connor, P. Zhang, F. A. Dobie, K. She, H. Kawabe, Y. T. Wang, N. Brose, A. M. Craig, An LRRTM4-HSPG complex mediates excitatory synapse development on dentate gyrus granule cells. *Neuron* **79**, 680-695 (2013).
204. J. de Wit, M. L. O'Sullivan, J. N. Savas, G. Condomitti, M. C. Caccese, K. M. Vennekens, J. R. Yates, 3rd, A. Ghosh, Unbiased discovery of glypican as a receptor for LRRTM4 in regulating excitatory synapse development. *Neuron* **79**, 696-711 (2013).
205. A. V. Nairn, A. Kinoshita-Toyoda, H. Toyoda, J. Xie, K. Harris, S. Dalton, M. Kulik, J. M. Pierce, T. Toida, K. W. Moremen, R. J. Linhardt, Glycomics of proteoglycan

biosynthesis in murine embryonic stem cell differentiation. *J Proteome Res* **6**, 4374-4387 (2007).
206. K. Hirano, T. H. Van Kuppevelt, S. Nishihara, The transition of mouse pluripotent stem cells from the naive to the primed state requires Fas signaling through 3-O sulfated heparan sulfate structures recognized by the HS4C3 antibody. *Biochem Biophys Res Commun* **430**, 1175-1181 (2013).
207. L. Jakobsson, J. Kreuger, K. Holmborn, L. Lundin, I. Eriksson, L. Kjellen, L. Claesson-Welsh, Heparan sulfate in trans potentiates VEGFR-mediated angiogenesis. *Dev Cell* **10**, 625-634 (2006).
208. L. Gasimli, A. M. Hickey, B. Yang, G. Li, M. dela Rosa, A. V. Nairn, M. J. Kulik, J. S. Dordick, K. W. Moremen, S. Dalton, R. J. Linhardt, Changes in glycosaminoglycan structure on differentiation of human embryonic stem cells towards mesoderm and endoderm lineages. *Biochim Biophys Acta* **1840**, 1993-2003 (2014).
209. K. S. Lau, E. A. Partridge, A. Grigorian, C. I. Silvescu, V. N. Reinhold, M. Demetriou, J. W. Dennis, Complex N-glycan number and degree of branching cooperate to regulate cell proliferation and differentiation. *Cell* **129**, 123-134 (2007).
210. Q. Liu, Z. Lyu, Y. Yu, Z. A. Zhao, S. Hu, L. Yuan, G. Chen, H. Chen, Synthetic Glycopolymers for Highly Efficient Differentiation of Embryonic Stem Cells into Neurons: Lipo- or Not? *ACS Appl Mater Interfaces* **9**, 11518-11527 (2017).
211. M. L. Huang, R. A. Smith, G. W. Trieger, K. Godula, Glycocalyx remodeling with proteoglycan mimetics promotes neural specification in embryonic stem cells. *J Am Chem Soc* **136**, 10565-10568 (2014).
212. B. I. Ayerst, R. A. Smith, V. Nurcombe, A. J. Day, C. L. Merry, S. M. Cool, Growth Differentiation Factor 5-Mediated Enhancement of Chondrocyte Phenotype Is Inhibited by Heparin: Implications for the Use of Heparin in the Clinic and in Tissue Engineering Applications. *Tissue Eng Part A* **23**, 275-292 (2017).
213. R. J. Weiss, P. L. Gordts, D. Le, D. Xu, J. D. Esko, Y. Tor, Small molecule antagonists of cell-surface heparan sulfate and heparin-protein interactions. *Chem Sci* **6**, 5984-5993 (2015).
214. D. R. Garud, V. M. Tran, X. V. Victor, M. Koketsu, B. Kuberan, Inhibition of heparan sulfate and chondroitin sulfate proteoglycan biosynthesis. *J Biol Chem* **283**, 28881-28887 (2008).
215. D. E. Humphries, J. E. Silbert, Chlorate: a reversible inhibitor of proteoglycan sulfation. *Biochem Biophys Res Commun* **154**, 365-371 (1988).
216. M. L. Huang, A. L. Michalak, C. J. Fisher, M. Christy, R. A. A. Smith, K. Godula, Small Molecule Antagonist of Cell Surface Glycosaminoglycans Restricts Mouse Embryonic Stem Cells in a Pluripotent State. *Stem Cells* **36**, 45-54 (2018).

Chapter 2

Dynamic changes in heparan sulfate ultrastructure modulate human pluripotent stem cell differentiation

Portions of the work presented in this chapter have been adapted from the following manuscript in preparation:
Deena Al Mahbuba, Sayaka Masuko, Shiwei Wang, Deepsing Syangtan, Jeong Seuk Kang, Yuefan Song, Tay Won Shin, Ke Xia, Fuming Zhang, Robert J. Linhardt, Edward S. Boyden, and Laura L. Kiessling**.** Dynamic changes in heparan sulfate ultrastructure modulate human pluripotent stem cell differentiation.

2.1 Abstract

Heparan sulfate (HS) is a heterogeneous, cell-surface polysaccharide essential for mammalian development. Imaging of developmental growth factors has revealed the interplay between their localization and signal transduction, but the spatial distribution and ultrastructure of information-rich, signaling polysaccharides like HS is unknown. We used expansion microscopy (ExM) to reveal the dramatic changes in HS ultrastructure during human pluripotent stem (hPS) cell differentiation. These studies reveal that undifferentiated hPS cells are densely coated with HS displayed as hair-like protrusions. This ultrastructure can recruit fibroblast growth factor for signaling. Unexpectedly, when the hPS cells differentiate into the ectoderm lineage, HS is localized into dispersed puncta. This dramatic change in HS distribution corresponds to a decrease in fibroblast growth factor binding to neural cells. While developmental variations in HS sequence were thought to be the primary driver of alterations in HS-mediated growth factor signaling, our high-resolution images of HS indicate a role for HS ultrastructure. Our study highlights the utility of high-resolution glycan imaging using ExM to uncover changes in HS localization, which plays a profound role in its ability to engage growth factors.

2.2 Introduction

All mammalian cells are covered with a dense layer of carbohydrates. This glycan coat is critical for numerous biological processes, including cell-cell recognition, cancer initiation and progression, and embryonic development. An integral part of this coat's ability to mediate information transfer is the extracellular polysaccharide heparan sulfate (HS), a ubiquitous and critical component of the mammalian glycocalyx (*1*). HS is a highly sulfated, polyanionic glycosaminoglycan whose sequence can vary. Distinct HS sequences determine how HS interacts with diverse binding partners, ranging from growth factors, lipid particles, to synaptic proteins. Although the chemical composition of purified HS sequences can be used to understand the role of this information-rich glycan, the molecular diversity of HS in its native environment is challenging to probe. Thus, approaches for visualizing endogenous cell-surface complex glycans, such as HS, are needed, especially to elucidate the interplay between their distribution and roles in the signal transduction pathways critical for human development and disease.

Human pluripotent stem (hPS) cells can self-renew and generate specialized cells through differentiation. Stem cell differentiation is tightly regulated by cues from growth factors and chemokines in the extracellular matrix (ECM). HS is present in the ECM and on the surface of cells, where it interacts with signaling molecules and facilitates ligand-receptor interactions that govern cell fate (*2, 3*). The HS sulfation pattern of embryonic stem cells changes significantly as cells switch from a proliferative state to lineage differentiation to all three germ layers (*4-8*). These observations suggest that the adaptive and dynamic nature of HS fine-tune its ability to transduce signals. Still, we lack a complete understanding of how HS structure changes and how these alterations modulate its function in cell fate commitment.

HS assembly occurs by the copolymerization of a repeating disaccharide unit consisting of *N*-acetyl-D-glucosamine (GlcNAc) and D-glucuronic acid (GlcA). As the chain assembles, the polysaccharide undergoes multiple enzymatic modifications, including deacetylation, epimerization, and sulfation. Elongated HS chains (40–300 sugar residues, 20–150 nm) demonstrate enormous structural variability that stems from differences in the number and length of the chains (*9*), degree and pattern of sulfation, the extent of uronic acid epimerization, and the sequence of the modified residues. The structural and compositional heterogeneity of HS underlies its role in regulating cell signaling, turnover, and tissue distribution in response to many secreted signaling molecules such as growth factors and morphogens (*10*). Still, much remains unknown about the role of HS in human development, especially regarding how HS nanostructure changes in response to differentiation cues in the stem cell microenvironment.

New insight into temporal-spatial variations in HS expression can elucidate the basis for differential responses of lineage-specific signaling molecules in the stem cell microenvironment. Analytical methods for examining HS composition and its functional consequence typically require extraction of HS from cell culture or tissue samples, losing all spatial information related to various cell types and subcellular locations. The liquid chromatography-tandem mass spectrometry (LC-MS/MS) is beginning to identify HS sequences within the whole sample and its associated temporal changes (*11-15*). Additionally, chemoenzymatically synthesized HS microarrays are now revealing insight into how the sulfation pattern influences protein recognition (*16*). Assessing HS variation at the cell surface would complement these approaches. Thus, we set out to visualize changes in cell surface HS as pluripotent stem cells differentiate into distinct lineages.

High-resolution visualization of endogenous glycans could guide our understanding of their structures and functions (*17-22*), yet glycan imaging has been challenging. Visualization of polysaccharide arrangement at the requisite nanometer length scale is underdeveloped. We reasoned high-resolution imaging could unravel structural and functional features of polysaccharides like HS. We, therefore, tested the utility of expansion microscopy (ExM), a powerful imaging method in which nanoscale features of a cell are resolved by physically expanding the sample in polyacrylate/acrylamide gel (*23-26*), for revealing glycan organization. Although it has been widely applied to image biomolecules such as proteins and nucleic acids with nanoscale precision, its potential for glycobiology is unclear (*27*).

We applied ExM imaging to HS in hPS cells to test whether changes in this polysaccharide could be detected visually throughout the lineage progression. We found that HS nanostructure undergoes striking changes during differentiation. At the proliferative stage, the HS of hPS cells appears on hair-like extensions from the cell surface. This extended structure then morphs into discrete puncta during ectoderm but not mesendoderm differentiation. These lineage-specific changes in HS ultrastructure correlate with the cells' ability to bind fibroblast growth factor (FGF). Cells displaying HS as cell surface protusions showed increased binding to the FGF. In comparison, differentiated neuronal cells have a highly sulfated variant of HS but this polysaccharide is distributed within localized puncta on the cell surface. These cells showed decreased binding to FGF. These findings suggest a role for HS nanostructure in modulating HS-ligand interactions in early stages of human development. Thus, our findings highlight how nanoscale imaging of complex glycans can reveal their structure-function relationship. We anticipate that ExM-empowered glycan imaging can identify specific glycan–ligand interactions, and dynamic changes in cellular glycome in development and disease.

2.3 Results

2.3.1 Visualizing heparan sulfate on human pluripotent stem cells by expansion microscopy

We first visualized HS in human pluripotent stem (hPS) cells using conventional microscopy. Undifferentiated hPS cells were exposed to an anti-HS primary antibody (10E4) that binds glucosamine N-sulfate. The deacetylation and N-sulfation is a critical step in the biosynthesis of HS, and other modification enzymes act subsequently, rendering 10E4 a general tool for visualizing HS. Immunofluorescence microscopy indicated bright and uniform HS staining on the surface of the cells at the edges of the colonies. These data suggest that the cells at the colony center lacked HS. Still, hPS cell colonies are tightly packed, and we postulated that conventional microscopy might fail to capture the range of cell surface markers, including HS. We therefore employed super resolution imaging using protein-retention expansion microscopy (pro-ExM). We postulated that pro-ExM might provide insight into HS localization beyond that detectable with conventional immunocytochemistry.

A pro-ExM protocol was applied to anchor the formaldehyde-fixed cells to a swellable polyacrylamide gel to expand hPS cells (*24*) (**Fig. 2.1**). Historically, pro-ExM has been used for protein imaging, and this protocol is not expected to result in gel-glycan links directly. Still, HS is appended to proteoglycans, and the protein core provides a means to preserve spatial information. Additionally, we employed a fluorescent antibody that recognizes HS as the readout for the spatial distribution of the polysaccharide chain (*24*). Using pro-ExM, we observed a long and elongated hair-like structure displaying HS on the cell surface (**Fig. 2.2A**). These data indicate that HS is not restricted to the outer cells of the colony but is present throughout the hPS colony. A comparison of the pre- and post-expansion nuclear DAPI signal indicated that pro-ExM afforded 4-4.5x linear expansion. We used an amine-reactive membrane dye and confirmed that hPS cells have uniform

cell membrane morphology with no apparent filopodia. These findings suggest the long extensions are not standard filopodial protrusions **(Supp fig. 1A).** Using phalloidin staining in pro-ExM, we also verified that the elongated HS structure extends from the base of the actin cytoskeleton **(Supp fig. 1B)**

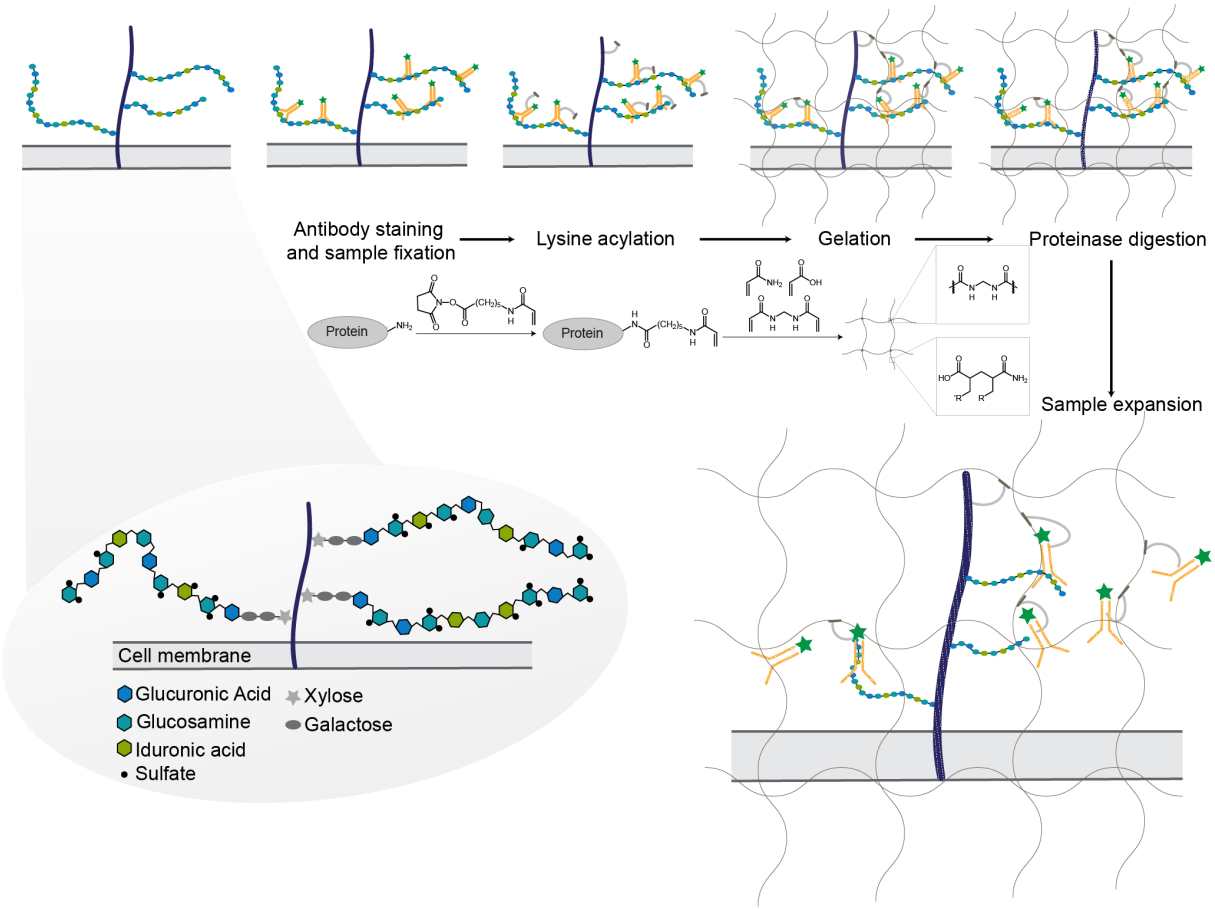

Fig. 2.1. Workflow of protein-retention expansion microscopy (pro-ExM) adapted for visualizing HS.

We used 3D-structured illumination microscopy (3D-SIM) to test whether the HS nanostructure observed by pro-ExM is consistent with unexpanded structures and is not an artifact of distortion during gel formation. The application of 3D-SIM revealed a similar pattern of HS

distribution (**Fig. 2.2B**) throughout the colony. These results highlight the advantages of using ExM to visualize cell surface features of hPS cell colonies and underscore that ExM can provide insight into polysaccharides such as HS.

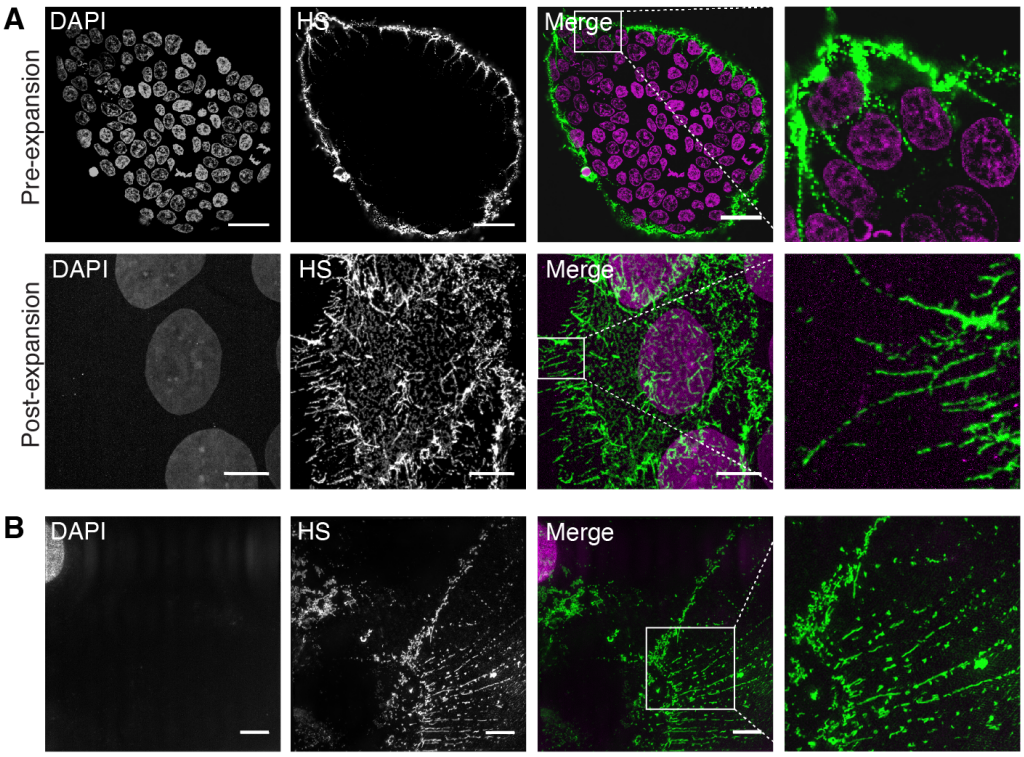

Fig. 2.2. Expansion microscopy enables antibody-mediated visualization of heparan sulfate on the cell surface. (A) Representative confocal images of HS in pre-expansion and post-expansion of hPS cells. HS is labeled using the 10E4 antibody, and the nucleus is stained with DAPI. The scale bar is 30 μm. (B) 3D-SIM images of HS in super-resolution. The scale bar is 5 μm.

2.3.2 Changes in heparan sulfate content and structure in ectoderm cells

Changes in HS can coincide with cell lineage (*28*). HS sulfation pattern and chain length can vary across cell types (*4, 10*), and we sought to visualize these changes directly with pro-ExM. We therefore differentiated hPS cells into multipotent mesendoderm cells using a chemically-defined protocol with 90% differentiation efficiency (*29*). The imaging data indicate that

mesendoderm cells have long and extended HS similar to that of undifferentiated cells (**Fig. 2.3A**). For a quantitative comparison of HS differences between undifferentiated hPS cells and mesendoderm cells, we used LC-MS to analyze glycosaminoglycans (GAGs) isolated from each cell type (*30*). The mean percentages of HS content of total GAGs in hPS cells and mesendoderm cells were 74% and 69%, respectively (**Fig. 2.3B**). Flow cytometry data collected using an anti-HS antibody further supported a comparable HS content between the hPS and mesendoderm cells (**Fig. 2.3C**). We next assessed the molecular weights of HS using polyacrylamide gel electrophoresis (PAGE) to probe whether HS length changes during mesendoderm differentiation (**Fig. 2.3D**). HS from hPS and mesendoderm cells gave rise to similar band distributions with average molecular weights of 16.2 kDa and 15.8 kDa, respectively. These results suggest that no major changes occur in HS length and distribution during mesendoderm differentiation.

We differentiated hPS cells to neural crest cells (*31*), which are ectoderm-derived multipotent migratory cells, to probe HS changes in the ectoderm. The HS of neural crest cells was distributed in discrete puncta on the cell surface (**Fig. 2.3E**). Because the differentiation yielded a heterogenous population (**Supp fig. 3**), we employed flow cytometry to analyze the relevant population. Consistently, we observed that neural crest cells have lower HS levels than undifferentiated hPS or mesendoderm cells (**Fig. 2.3C**). These data highlight the utility of high-resolution imaging for capturing the dynamic changes in HS: The morphology and distribution of cell surface HS changes dramatically upon differentiation to the ectoderm lineage.

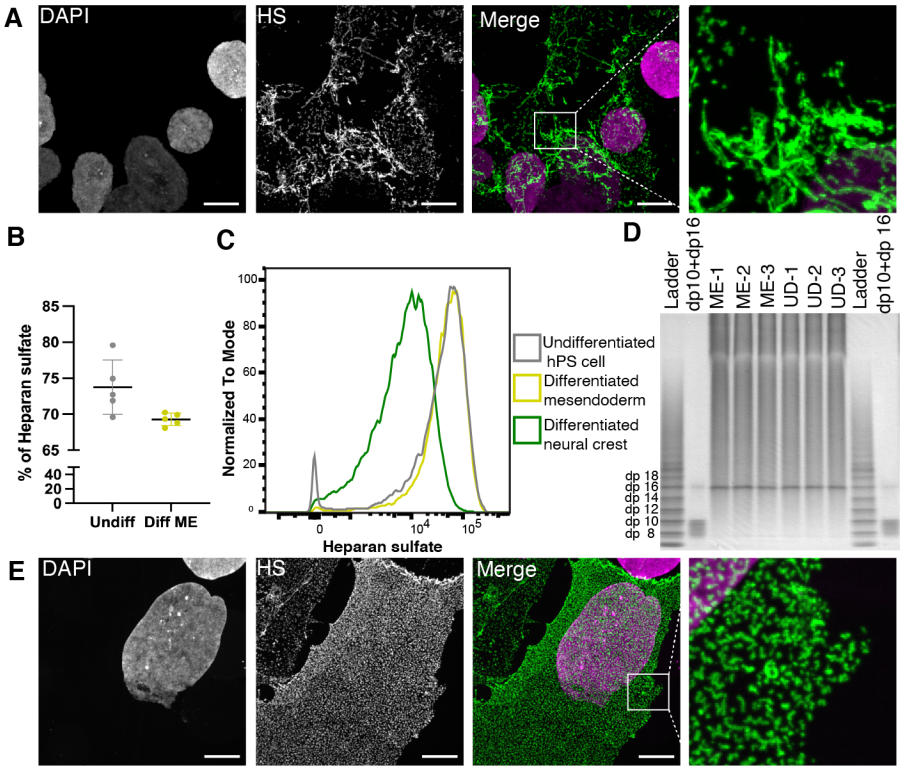

Fig. 2.3. Heparan sulfate content and structure changes in ectodermal cells. (A) Representative pro-ExM image of HS on the surface of the hPS cell-derived mesendoderm cells. (B) LC-MS-based disaccharide analysis was performed to quantify the percentage of HS of total isolated GAGs in hPS cells (Undiff) and mesendoderm cells (Diff ME) (n=6). (C) Flow cytometry analysis of surface HS in hPS cells, mesendoderm cells, and neural crest cells. (D) PAGE analysis of undifferentiated hPS cells (lanes 4-6) and differentiated mesendoderm cells (lanes 3-5) (n=3) showing HS from undifferentiated hPS cells (UD) and mesendoderm (ME) samples. After the PAGE analysis, the gels were visualized with 0.5% (w/v) Alcian blue in a 2% (v/v) aqueous acetic acid solution. The average molecular weights were determined based on heparin oligosaccharides (partially digested) with various degrees of polymerization (dp). (e) Representative image of HS puncta on the surface of hPS cells-derived neural crest cells (A,E) Scale bar, 30 μm.

2.3.3 Heparan sulfate of terminally differentiated neuronal cells

The changes in HS observed as hPS differentiate to neural crest cells led us to examine the distribution of the glycan in terminally differentiated hPS-derived neurons. To this end, we used a dual-SMAD inhibition protocol to convert hPS cells to spinal motor neurons (*32, 33*) **(Supp fig. 4A)**. In this approach, hPS cells differentiate into neural progenitor (NP) cells by day six and then

into spinal motor neuron (hMN) cells by day thirteen. The application of pro-ExM revealed NP and hMN cells had lower levels of HS than hPS cells (**Fig. 2.4A and 2.4B**). The gradual decrease (**Supp fig. 4C**) in cell surface HS during neuronal differentiation could be readily detected with the anti-HS antibody (**Fig. 2.4C**). We observed a diffuse distribution of HS on NP cells, but HS in hMN cells was localized in discrete puncta along the neuronal processes. The punctate HS in hMN cells appeared to be shorter than the HS in the hPS cells.

The differentiation efficiency complicates (**Supp fig. 4B**) the use of biochemical approaches such as PAGE for HS characterization. We therefore used HS-specific antibodies (10E4 and 3G10) to conduct an optical analysis of HS distribution per chain. The 10E4 antibody recognizes the *N*-sulfated domains in HS, a proxy for total HS, whereas the 3G10 antibody recognizes the unsaturated uronic acid generated after heparinase digestion. Thus, the ratio of 10E4 antibody to 3G10 antibody staining is an on-cell estimate of HS chain length. The 3G10 signal of hMN cells was decreased relative that of hPS cells, as was staining from the 10E4 antibody **(Supp fig. 4D)**. Moreover, the ratio of 10E4 to 3G10 staining in hMN cells (1.8) was significantly lower than that of hPS cells (3.09), which indicates that HS chains in MNs are relatively shorter than those of hPS cells (**Fig. 2.4D**).

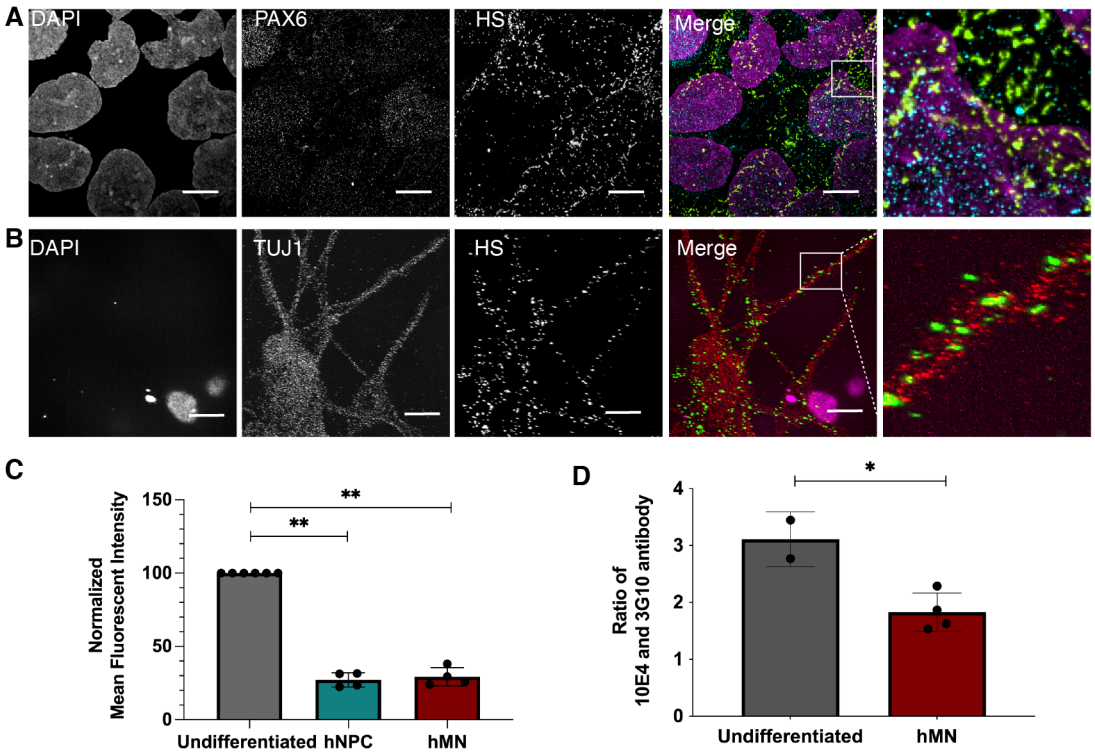

Fig. 2.4. Imaging heparan sulfate in spinal motor neuron differentiation. (A) Representative pro-ExM images of HS on the surface of PAX6^{+} NP cells (B) Representative pro-ExM images of HS on the surface of TUJ1^{+} hMN cells. (C) Flow cytometry of cell surface HS of hPS cells, NP cells, and hMN cells (n=4). Mean fluorescence intensity (MFI; arbitrary units) was calculated using the geometric mean and normalized to that of the undifferentiated hPS cells. (D) hMN cells show a decrease in the ratio of 10E4 antibody to 3G10 antibody binding (n=4). Scale bars, (A, B) 30 μm. *****p<0.000000xx, **p<0.05, unpaired t-test in (C, D).

2.3.4 Differential binding of growth factor in response to changes in cell-surface HS

HS interacts with many growth factors and cytokines at the cell surface. We hypothesized that the changes in HS length and distribution during neuronal differentiation would influence the polysaccharide's interactions with growth factors. We probed the binding of FGF2, a HS-interacting growth factor critical for hPS self-renewal. We compared the cell-surface binding of recombinant FGF2 to hPS, mesendoderm, and hMN cells. When hPS cells and mesendoderm cells were compared, no differences in FGF2 binding were detected, consistent with the similarity of

HS in these different cell types (**Fig. 2.5A**). In contrast, hMN cells' ability to bind FGF2 was reduced. Gene expression data could not predict this difference. Specifically, FGF2 binds to sulfated HS, yet the HS biosynthetic genes that lead to HS sulfation are upregulated in hMN cells, including those encoding sulfotransferases (*HS6ST1, HS6ST1, HS6ST2, HS6ST3, NDST1, NDST2, NDST3, NDST4*) (**Fig. 2.5B**). The upregulation of expression of these genes would be predicted to lead to enhanced FGF2 binding. For example, HS sequences with IdoA2S and GlcNS residues have been reported to bind FGF2 (*16, 34*) . Additionally, the 6-*O*-sulfated residues of HS bridge FGF2 and FGFR in mouse embryonic fibroblast models promote the formation of the ternary complexes that signal. Similarly, in breast cancer cell-line models (*35*), *2OST1* gene expression promotes the acquisition of cancer stem cell like properties by activating FGF signaling pathways (*36*). Nevertheless, hMN cells show reduced binding to FGF2. Thus, methods to visualize detailed HS interactions can uncover changes in HS nanostructure and their consequences for growth factor interactions. We next tested growth factor binding to the HS chains on the different cell types. ExM enabled high-resolution imaging that revealed FGF2 interacting with the HS chains protruding from on the hPS cell surface (**Fig. 2.5C).** These data suggest that the protruding glycans are readily accessible for growth factor binding.

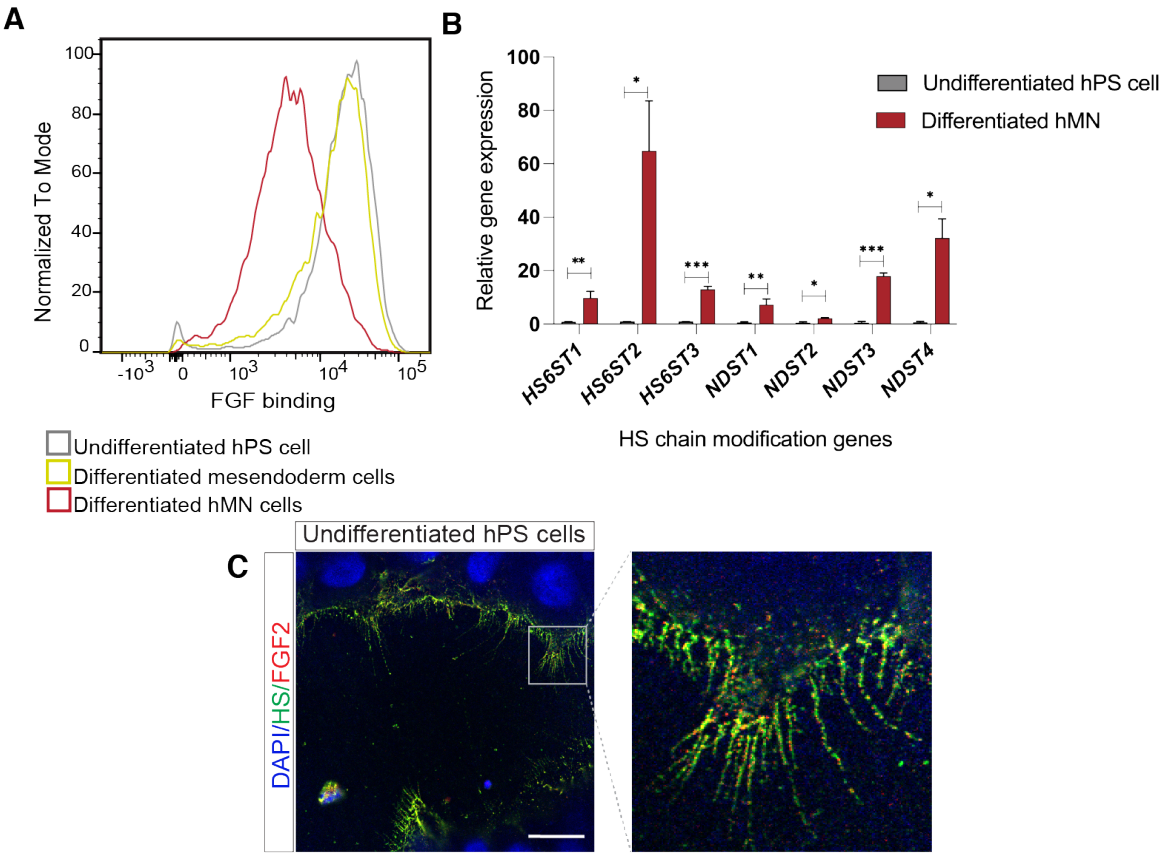

Fig. 2.5. FGF binding to hMN cells and expression of HS modification enzymes. (A) A comparison of the levels of FGF-2 bound to HS as hPS cells differentiate toward the neural lineage (hMN). Flow cytometry analysis of FGF-2 binding to undifferentiated hPS, hPS-derived mesendoderm, and hMN cells using an anti-FGF2 primary antibody and fluorophore-conjugated secondary antibody. (B) Quantitative real-time PCR analysis of HS modification enzymes in hPS-derived hMN cells compared to undifferentiated hPS cells. (n=3, biological replicate). An unpaired t-test between hPS and hMN cells was used for data analysis. An asterisk denotes a statistically significant difference *(*****p<0.000000xx, **p<0.05) between hPS and hMN cells. (C) Representative pro-ExM images of FGF2 bound to HS chain on the surface of undifferentiated hPS cells. DAPI (blue), HS (green), FGF2 (red). Scale bar 30 µm.

2.3.5 Visualizing heparan sulfate *in situ*

We applied pro-ExM to isolated tissue to determine whether the HS morphologies observed in hPS-derived hMN cells are recapitulated in primary neurons. We imaged brain slices collected from a transgenic mouse producing yellow fluorescent protein (YFP) expressed from a

Thy1 promoter. The YFP identifies the excitatory neurons in the cortex (*24*). We stained parvalbumin-positive (PV^+) interneurons for HS to assess whether the level of this glycan varies between excitatory and inhibitory neurons. In an unexpanded brain slice, we observed stark differences in HS expression distribution in $Thy1^+$ and PV^+ neurons in the cortex. PV^+ neurons have significant HS coverage around the cell body, while $Thy1^+$ neurons appeared to lack HS (**Fig. 2.6A**). Still, we posited these standard conditions might afford low resolution images, in which the HS nanostructure would not be apparent. Indeed, expansion of the brain slices revealed HS puncta in a wide range of cell types, including Thy1+ and PV+ neurons (**Fig. 2.6B and 2.6C**). Thus, pro-ExM afforded a HS signal that was otherwise invisible and confirmed that the HS morphology in neuronal culture resembles that in the mouse cortex.

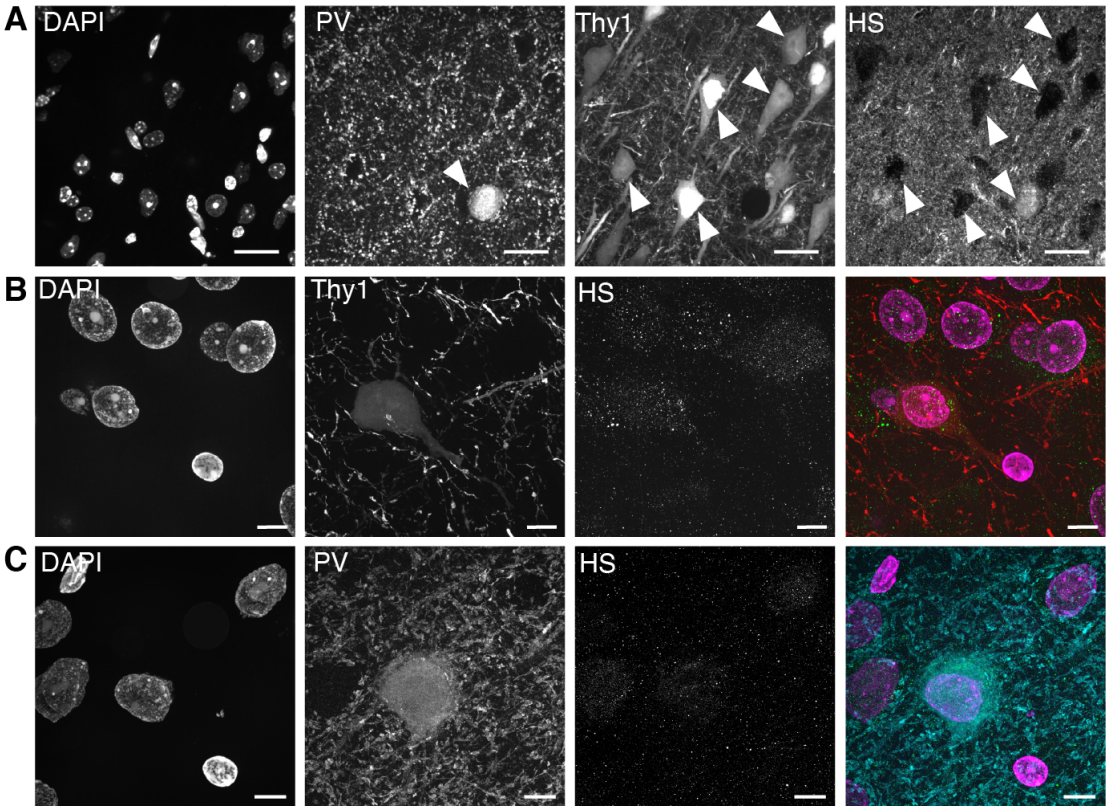

Fig. 2.6. *In situ* expansion imaging reveals puncta HS in excitatory and inhibitory neurons. (A) Imaging unexpanded brain slice shows HS on PV^+ inhibitory neurons but not in Thy^+ cells.

(B, C) Pro-ExM reveals HS puncta both on excitatory (Thy^+) and inhibitory (PV^+) neurons. (A-C) Scale bar, 30 μm.

2.4 Discussion

The spatial distribution and localization of macromolecules underlie their roles as signaling factors. Historically, characterization of cell surface glycans has relied on methods that require extraction and separation of polysaccharides from other cellular components. Few approaches have allowed for detailed analysis of glycans in their native environment (*37*). Even the most powerful strategies, such as mass spectrometry imaging, require the release of the glycan where the saccharide ultrastructure and localization are not fully preserved. We found that ExM can be used to reveal HS cell surface localization and ultrastructure in different cell states during hPS cell differentiation. Our findings showed that the ability of hPS cells to bind growth factor correlates with the changes in HS ultrastructure.

No significant changes in HS were detected when hPS cells were differentiated to multipotent mesendoderm cells. In contrast, stark differences were observed between hPS cells and the ectoderm lineage. Previous reports using LC-MS/MS analysis indicated that the HS sulfation pattern varies between differentiated and undifferentiated cell states (*1, 38, 39*). Our data suggest that the physical structure of HS changes dramatically in ectoderm lineage-specific multipotent neural crest or neural progenitor cells. Upon further differentiation towards terminal hMN cells, the overall content of HS on the cell surface decreases significantly. By imaging the glycan ultrastructure during differentiation, we uncovered lineage-specific morphological changes of HS. We postulate that these structural changes contribute to the HS function, including its ability to engage specific growth factors and facilitate growth factor signaling. In support of this hypothesis, cells with punctate HS are less capable of fibroblast growth factor (FGF) binding than undifferentiated cells that present longer, protruding chains of HS.

HS acts as a coactivator of signaling molecules, including FGF, to modulate cellular signaling pathways underlying multiple developmental processes. We found that cells at the pluripotent state show robust FGF2 binding. As they differentiate towards hMN, their ability to bind FGF2 decreases significantly. The propensity of hPS cells to bind FGF2 is consistent with studies indicating that FGF signaling is needed to maintain pluripotency (*9, 40-42*). In the early neural progenitor state, FGF2 promotes induction of the differentiation and survival. Therefore, enhanced FGF2 signaling at the onset of neural differentiation is a prerequisite, whereas inhibiting this signal at subsequent stages promotes the transition into differentiated neurons (*32, 43, 44*). These findings highlight the complex control of HS – growth factor interactions.

Given that hMN express higher levels of sulfotransferase genes compared to undifferentiated cells and that sulfate groups are required for FGF2 binding (*41*), the finding that hMN cells bind more poorly to FGF2 is unexpected. In contrast, FGF signaling is an important regulator of mesendoderm differentiation (*45*), and differentiated mesendoderm and hPS cells display HS with similar ultrastructure. Both cell types bind readily to FGF2. These findings underscore the difficulty of linking the genetic fingerprint to glycan-protein interactions and highlight the importance of HS morphology in signaling. Changes in HS ultrastructure on the cell surface could modulate the binding of a variety of growth factors (e.g., FGF, BMP, TGFß) during stem cell differentiation.

The utility of ExM for visualizing FGF2 binding on the protruding cell-surface HS chains of undifferentiated cells paves the way for further identifying growth factor binding. To use high-resolution imaging of complex glycans such as HS to visualize the location of different HS sequences, we need access to highly specific antibodies. Improving the expansion strategy to achieve even higher resolution would be crucial to resolve the locations of growth factor binding.

By applying pro-ExM to visualize HS *in situ* in murine brain slices, we could correlate HS ultrastructure observed in cell culture to that occurring in tissue. Pre-expansion imaging cannot distinguish HS nanostructure but can detect variations in HS expression levels across cell types. In particular, the signal from the cell body of PV^+ interneurons were significantly higher than that of $Thy1^+$ excitatory neuron cell bodies in the cortex. In contrast, post-expansion imaging revealed the puncta-like structure of HS across all the cell types, a finding that recapitulates the morphology observed in culture-differentiated neurons. We found the punctate HS nanostructure was conserved across various cell types in brain tissue, including $Thy1^+$ neurons whose HS signal was not visible using conventional microscopy. Thus, the HS structure we observed in human cell culture is conserved in primary mouse brain tissue.

The morphology shift of HS between pluripotent and neural cells corresponds to a functional shift in growth factor interactions. A recent study found that ablation of HS in mouse hippocampal neuron cultures results in a decrease of inhibitory synapse density without affecting excitatory synapse density (*46*). These findings suggest a significant role for HS in inhibitory synapse development. Our observation of elevated HS expression around interneuron soma supports this conclusion. These findings indicate that further exploration of HS ultrastructure can shed light on HS roles during mammalian neural development to address questions such as how HS expression level is regulated in different cell types and how HS contributes to synapse plasticity in the brain.

A lack of methods to visualize the ultrastructure of polysaccharides has hindered our understanding of their role in physiological and disease processes. In the case of heparan sulfate, this has led to a focus on how polysaccharide sequence influences binding. Here, using super-resolution imaging by ExM, we found that the glycans' spatial distribution and ultrastructure

correlates with growth factor recruitment. Intriguingly, the observation of cell surface protrusions that can present HS to engage growth factors was unexpected but highlights another mechanism by which cells can use glycosaminoglycans to control signaling. Our findings provide an alternative mechanism by which the cell surface polysaccharide HS regulates cell fate.

2.5 Conclusion and future directions

To the best of our knowledge, this is the first report showing the high-resolution visualization of heparan sulfate ultrastructure in human pluripotent stem cells and the associated changes during stem cell differentiation. Our findings suggest that the nanostructure of complex glycans, such as heparan sulfate on the cell surface can be modified in response to the cues from the microenvironment. These findings provide the foundation for high-resolution glycan imaging to understand their structure-function relationship.

This work lays the foundation for using expansion microscopy for *in situ* complex glycan imaging. Herein, we showed we can visualize the HS puncta structure in a mouse brain slice and recognize the ultrastructure of HS in both the inhibitory and excitatory neurons, which was not visible using conventional microscopy. We can further extend this visualization for other complex glycans. A big caveat, in this case, is an effective glycan labeling strategy that can recognize biologically important glycan epitopes. This challenge can be addressed by the recent advancements in glycan labeling through metabolic labeling. Multifunctional chemical probes or naturally occurring glycan-specific lectins can also be used to label glycan structure for ExM-based high-resolution visualization.

With this advancement, this strategy can be further applied to understand the sequence information of complex glycans. With novel binders to specific complex glycan structures, we would be able to map unique sequence information of glycans in culture or tissue. This would

significantly help to identify the sequence specificity of glycan for specific growth factor binding. Furthermore, there is the potential to multiplex this strategy which would be crucial for complex and heterogeneous sugar, such as heparan sulfate. This information will reveal how heterogenous HS sequence is across different cell types and locations. However, to map the specific sequence of complex glycan in it is native environment we may need an even higher resolution. This can be achieved by an iterative expansion strategy where samples are expanded iteratively (*47*). However, these strategies are yet to be tested to visualize complex glycan. Further investment in improving the gel chemistry to expand the resolution of ExM-based imaging could also be a strategy in this regard.

Moving further, these would aid the investigation of the role of HS in complex neurological disorders, such as amyotrophic lateral sclerosis (ALS), Alzheimer's disease, or autism spectrum disorders (ASD). Although numerous studies identified the involvement of heparan sulfate in several neurodevelopmental disorders as well as complex neurodegenerative diseases (*48-51*), it is still unclear how HS is interacting with other components of these microenvironments, what are the specificities of these interactions, and how they are modulated. ExM-based high-resolution imaging could be particularly important to address these questions since it preserves the native composition of the sugar. Imaging the interaction of different binding partners to HS in patient-derived samples or organoids will help to address these questions.

2.6 Methods and Materials

2.6.1 Cell culture

H9 (WiCell) human pluripotent stem (hPS) cells were grown with E8 medium (Thermo Fisher Scientific) on tissue culture plates coated with vitronectin (Thermo Fisher Scientific). Cells were

maintained at 37 °C in a 5% CO2 incubator. Cells were passaged manually using EDTA (1 mM in PBS, pH 7.4) every 4-5 days, with the addition of 5 μM ROCK inhibitor (Y-27632 dihydrochloride, Tocris) on the first day to prevent the cell death after dissociation. The cells were routinely tested for mycoplasma contamination (Lookout Mycoplasma PCR Detection Kit, Sigma Aldrich).

2.6.2 Differentiation of hPS cells into different lineage-specific derivatives

The cells were differentiated to mesendoderm using an established protocol (*29*). Briefly, the cells were dissociated with EDTA and plated at a density of 100,000 cells per cm^2 on vitronectin-coated plates with E8 media supplemented with 5 μM ROCK inhibitor (Y-27632 dihydrochloride, Tocris). The E8 medium was changed every day for the next two days. On day three, the media was changed to RPMI-1640 medium (Thermo Fisher Scientific) supplemented with 6 μM CHIR-99021 (Tocris). Following a 24 h treatment with the differentiation media, the cells were collected for analysis.

Neural crest differentiation was achieved using a chemically defined protocol described previously (*31*). In brief, hPS cells were dissociated into single cells using accutase (Thermo Fisher Scientific) and plated at a density of 10,000 cells per cm^2 on vitronectin-coated plates with E8 medium supplemented with 5 μM ROCK inhibitor. The cells were grown for 24 h, and then the medium was changed into the differentiation medium each of the next five days. The differentiation media was prepared by supplementing DMEM-F12 (Life Technologies) with 1x N-2 supplement (Gibco), 1.0 μM CHIR99021 (Tocris), 2.0 μM SB431542 (Tocris), 1.0 μM DMH1 (Tocris), and 15 ng/ml BMP4 (Tocris).

Motor neuron differentiation was effected using a modified 14-day protocol described previously (*33*). In brief, hPS cells were dissociated to single cells using accutase and plated at a

density of 40,000 cells per cm^2 on vitronectin-coated culture plates with E8 media supplemented with 5 μM ROCK inhibitor. As the cells reached >95% confluency, the medium was changed to d0-d5 differentiation media every day for the next five days. The d0-d5 differentiation medium was prepared by supplementing the basal medium with 10 μM SB431542 (Tocris), 100 nM dorsomorphin (Tocris), 1 μM retinoic acid (Sigma) and 1 μM smoothened agonist (Tocris). On the day six of differentiation, the medium was changed to d6-d14 differentiation media every day. The d6-d14 medium was prepared by supplementing the basal medium with 5 μM DAPT (Tocris), 4 μM SU-5402 (Tocris), 1 μM retinoic acid (Sigma), and 1 μM smoothened agonist (Tocris). The basal medium contained a 1:1 mixture of Neurobasal media (Life Technologies) and DMEM-F12 (Life Technologies) and was supplemented with 1x B-27 supplement (Gibco), 1x N-2 supplement (Gibco), and 1x Gibco GlutaMAX (Life Technologies).

2.6.3 Immunofluorescence staining and imaging

For immunocytochemistry analysis, cells were stained live or after fixation. The cells were rinsed with DMEM/F12 or basal media for live staining, followed by incubation in a blocking buffer (2% BSA in DMEM/F12) for 30 min on ice. The cells were further exposed to anti-HS 10E4 (US Biological, catalog# H1890) at 1:200 in a blocking buffer for 1 h at 4 °C. Then, the cells were exposed to the secondary antibody, IgM-Alexa Fluor 488 (Invitrogen), for 1 h at 4 °C. The stained cells were rinsed twice with cold buffer and fixed with 4% formaldehyde for 10 min at room temperature.

For the staining of internal markers, the fixed samples were permeabilized and blocked with PBS containing 0.1% Triton X-100 and 2% bovine serum albumin (BSA)s. All primary antibodies were incubated in a blocking buffer overnight at 4 °C or 1 h at room temperature. The primary antibodies and dilutions used are described in Table S1. The secondary antibody staining was

performed with Alexa Fluor 488, 594, 647 or Atto 647N conjugated anti-mouse, rabbit, chicken, or goat IgG antibodies (Invitrogen) diluted at 1:1000 in the blocking buffer and exposed to cells for one h at room temperature. For the samples for expansion, the secondary antibodies were used at 1:200 dilution. The cell nuclei were counterstained with DAPI dilactate (1:10000, Molecular Probes). Images were collected with the Nikon A1R Ultra-Fast Spectral Scanning Confocal Microscope. The 3D-SIM super resolution images were collected using Applied Precision DeltaVision-OMX Super-Resolution Microscope. Images were analyzed using Fiji.

2.6.4 Pro-ExM of stem cell culture

The following steps were performed as described previously (*24-26, 52*). Immunostained and fixed culture was incubated in 0.1 mg/mL Acryloyl-X, SE (Thermo Fisher Scientific) in PBS at 4 ˚C overnight. Cell culture was then washed twice with PBS for 15 min. Monomer solution (1x PBS, 2M NaCl, 8.625% (w/w) sodium acrylate, 2.5% (w/w) acrylamide, 0.15% (w/w) N,N'-methylenebisacrylamide), ammonium persulfate (APS) (10% w/w in water), and tetramethylethylenediamine (TEMED) (10% w/w in water) were stored frozen in aliquots. Upon thawing, monomer solution, water, TEMED solution, and APS solution were mixed in a ratio of 47:1:1:1 and kept on ice. The solution mixture was then dropped onto cell culture and covered with a parafilm-wrapped coverslip. The gelation chamber was then put under nitrogen and moved to a humidified 37 ˚C incubator for one h.

Gel was further incubated with Proteinase K at 8 units/mL (New England Biolabs) in digestion buffer (50 mM Tris pH 8.0, 1mM EDTA, 0.5% Triton X-100, 1 M NaCl) at room temperature for overnight. Digested gels were placed in large volumes of deionized water to expand. Water was replaced every 30 min until the gel no longer expanded.

2.6.5 Brain tissue preparation

All procedures involving Thy1-YFP-H transgenic mice (Jackson Laboratory) followed the US National Institute of Health Guide for the Care and Use of Laboratory Animals and were approved by the Massachusetts Institute of Technology Committee on Animal Care. Animals were housed in groups in standardized cages (temperature: 20-22˚C, humidity: 30-70%) with a 12-h light/12-h dark cycle with unrestricted access to food and water. Mice 2-4 months old were deeply anesthetized using isoflurane in room air. Mice were transcardially perfused at room temperature with ice-cold 10 mL of 4% paraformaldehyde in phosphate-buffered saline. Fixed brains were sectioned to 50 μm-thick slices with a vibrating microtome (Leica VT1000S) and stored in PBS at 4 ˚C.

2.6.6 Immunostaining of unexpanded tissue

Fixed brain slices were incubated in MAXblock Blocking Medium (Active Motif #15252) at 4˚C for overnight, followed by incubating with primary antibody (1:200) in MAXbind Staining Medium (Active Motif #15253) at 4˚C overnight. The slices were then washed with MAXwash Washing Medium (Active Motif #15254) four times for 30 min each at room temperature. The slices were incubated with secondary antibody (1:200) in MAXbind Staining Medium followed by four washes for 30 min with MAXwash washing buffer at room temperature.

2.6.7 Anchoring, gelation, digestion, and expansion of intact tissue

The following steps were performed as described previously (*24-26, 52*). Fixed and immunostained slices were incubated in 0.1 mg/mL Acryloyl-X, SE in PBS at 4 ˚C overnight. Monomer solution (1x PBS, 2 M NaCl, 8.625% (w/w) sodium acrylate, 2.5% (w/w) acrylamide, 0.15% (w/w) N,N’-methylenebisacrylamide), ammonium persulfate (APS) (10% w/w in water),

tetramethylethylenediamine (TEMED) (10% w/w in water), and 4-hydroxy-2,2,6,6-tetramethylpiperidin-1-oxyl (4-HT-TEMPO) inhibitor (0.5% w/w in water) were stored frozen in aliquots. Upon thawing, monomer solution, 4-HT-TEMPO solution, TEMED solution, and APS solution were mixed in a ratio of 47:1:1:1 and kept on ice. Tissue slices were incubated in the solution mixture for 30 min on ice and transferred to a humidified 37 ˚C incubator under nitrogen for two h.

The gel was then incubated with Proteinase K 8 units/mL (New England Biolabs) in digestion buffer (50 mM Tris pH 8, 1 mM EDTA, 0.5% Triton X-100, 1 M NaCl) at 37˚C overnight. Digested gels were placed in large volumes of deionized water to expand. Water was replaced every 30 min until the gel no longer expanded.

2.6.8 Detection of HS by flow cytometry

H9 hPS cells and the differentiated cells derived from hPS cells were analyzed by flow cytometry according to Holley *et al.* (*53*) with slight modifications. Briefly, cells were dissociated using warm accutase and resuspended in cold DMEM/F12 supplemented with 5 μM ROCK inhibitor. Cells were washed twice with cold PBS followed by incubation with 500 μL Ghost Dye™ Violet 450 cell stain (1:1000, Tonbo Biosciences) on ice for 30 min. Cells were then rinsed with cold buffer (PBS, pH 7.4 supplemented with 0.1% BSA). Cells were further incubated with anti-HS 10E4 at 1:200 dilution for one h, at 4 °C, followed by fixation with 1% formaldehyde in cold PBS. Data were collected using the Attune NxT Flow Cytometer (Thermo Fisher Scientific) and analyzed using FlowJo software. The percentage of positive cells was established by comparing wild-type cells to HS knockout cells.

2.6.9 Distribution of HS per chain detected by flow cytometry

Undifferentiated H9 hPS cells and hPS derived hMN cells were treated with Heparinase enzymes cocktail composed of *Bacteroides* Heparinase I (New England Biolabs, #P0735), Heparinase II (New England Biolabs, #P0736), and Heparinase III (New England Biolabs, #P0737). Each enzyme was used at 4 unit/ml concentration in the cocktail. Cells were incubated for 2 -2.5 h at the 37 °C in a 5% CO_2 incubator. After the heparinases treatment, cells were dissociated using warm accutase and rinsed with cold PBS followed by incubation with 500 µL Ghost Dye™ Violet 450 cell stain on ice for 30 min. Cells were then rinsed with cold buffer (PBS, pH 7.4 supplemented with 0.1% BSA). Cells were further incubated with anti-HS 10E4 at 1:200 or anti-HS 3G10 (Amsbio # 370260-S) for 1 h, at 4 °C. After two rinses with cold buffer, cells were incubated with IgM-PE (Santa Cruz) or IgM-Alexa Fluor 488 (Invitrogen) for one h, at 4 °C. The stained cells were rinsed twice with cold buffer and fixed with 1% formaldehyde in cold PBS. Data were collected using the Attune NxT Flow Cytometer and analyzed using FlowJo software. HS KO hPS cells were used as a negative control.

2.6.10 bFGF cell surface binding detected by flow cytometry

H9 hPS cells and differentiated derivatives were dissociated using warm accutase and rinsed three times with cold buffer (DMEM/F12 containing 1% BSA and 5 µM Y-27632) to remove excess growth factors from the media. The cells were then incubated with 1 µg/mL bFGF (Waisman Biomanufacturing) and Ghost Dye™ Violet 450 cell stain (1:1000) in ice for 30 min. Cells were then rinsed with cold buffer (PBS, pH 7.4 supplemented with 0.1% BSA). Bound bFGF was detected by anti-bFGF (1:100, LifeSpan Biosciences) labeled with a secondary antibody (mouse IgG_{2a+b}, BD Biosciences). Data were collected using the Attune NxT Flow Cytometer (Thermo Fisher Scientific) and analyzed using FlowJo software.

2.6.11 GAG preparation and disaccharide analysis

Cells were proteolyzed at 55 °C with 300 μL of 20-mg/mL actinase E for 24 h and followed by actinase E deactivation at 100 °C for 30 min. The amount of the above solution containing one million cells was transferred to a 3-kDa molecular weight cut-off (MWCO) spin tube. The filter unit was washed three times with 400 μL distilled water and then added to 300-μL digestion buffer (50 mM ammonium acetate containing 2 mM calcium chloride adjusted to pH 7.0). Recombinant heparin lyase I, II, III (pH optima 7.0−7.5) and recombinant chondroitin lyase ABC (pH optimum 7.4, 10 mU each) were added to each filter unit containing sample and incubated at 37 °C for 24 h. The enzymatic digestion was terminated by ultrafiltration through the 3-kDa spin tube. The filtrate was collected, and the filter unit was washed twice with 200 μL distilled water. All the filtrates containing the disaccharide products were combined and dried via freeze dry. The dried samples were AMAC-labeled by adding 10 μL of 0.1 M AMAC in DMSO/acetic acid (17/3, V/V) incubating at rt for 10 min, and then10 μL of 1 M aqueous sodium cyanoborohydride and incubating for 1 h at 45 °C. A mixture containing all 17-disaccharide standards prepared at 0.5 ng/μL was similarly AMAC-labeled and used as an external standard for each run. After the AMAC-labeling reaction, the samples were centrifuged, and each supernatant was recovered.

LC was performed on an Agilent 1200 LC system at 45 °C using an Agilent Poroshell 120 ECC18 (2.7 μm, 3.0 × 50 mm) column. Mobile phase A (MPA) was a 50 mM aqueous ammonium acetate solution, and mobile phase B (MPB) was methanol. The mobile phase passed through the column at a flow rate of 300 μL/min. The gradient was 0-10 min, 5-45% B; 10-10.2 min, 45-100% B; 10.2-14 min, 100% B; 14-22 min, 100-5% B. Injection volume is 5 μL.

A triple quadrupole mass spectrometry system equipped with an ESI source (Thermo Fisher Scientific) was used as a detector. The online MS analysis was at the Multiple Reaction Monitoring

(MRM) mode. MS parameters: negative ionization mode with a spray voltage of 3000 V, a vaporizer temperature of 300°C, and a capillary temperature of 270°C.

2.6.12 Polyacrylamide gel electrophoresis (PAGE)

The proteolyzed cell solution containing 10-16 million cells was subjected to chondroitin lyase ABC digestion. The chondroitin sulfate disaccharides were removed by ultrafiltration through a 3-kDa molecular weight cut-off (MWCO) spin tube. The filter unit was washed twice with 200 μL distilled water. The HS GAG that remained in the filter was collected and lyophilized. The lyophilized samples were then dissolved in 400 μL of a solution of denaturing buffer (8 M urea containing 2% wt. CHAPS), bound to Vivapure Q Mini H spin column, washed twice with 400 μL of denaturing buffer and washed three times with 400 μL of 0.2 M sodium chloride solution. The HS GAG components were then eluted from the spin column with three 400 μL volumes of 16% aqueous sodium chloride solution and collected by ultrafiltration through a 3-kDa molecular weight cut-off spin tube. The filter unit was washed twice with 400 μL distilled water to remove salt, and the HS GAG in the filter was collected and freeze-dried. The lyophilized samples were dissolved in 30 μL of loading buffer for PAGE. Three microliters of the above solution were loaded in native PAGE using 0.75 mm × 6.8 cm × 8.6 cm mini gels cast from 15% resolving gel monomer solution and 5% stacking gel monomer solution. Heparin partially digested was used as molecular markers (ladder). The mini gels were subjected to electrophoresis at a constant 190 V for 30 min and visualized with 0.5% (w/v) Alcian blue in a 2% (v/v) aqueous acetic acid solution. Molecular weight analysis was performed with UNSCANIT software (Silk Scientific) using the logarithmic relationship between the GAG molecular weight and its migration distance.

2.6.13 RNA preparation and qRT-PCR

Total RNA was extracted from undifferentiated hPS and d13 motor neurons using TRIzol (Life Technologies) and Direct-zol™ RNA MiniPrep kit (Zymo Research) per manufacturer instructions. RNA (1 µg) from each sample was reverse transcribed to cDNA using iScript cDNA Synthesis Kit (Bio-Rad). The qPCR was performed on the CFX Connect (Bio-Rad) using iTaq Universal SYBR Green Supermix (Bio-Rad) and gene-specific primers. GAPDH was used as a reference gene for normalization. The primer sequences used are described in Table S2. The relative gene expression levels were determined using the delta-delta CT (ddCt) method, and the error bars were determined from the standard deviation of at least three biological replicates.

2.7 Supplementary information

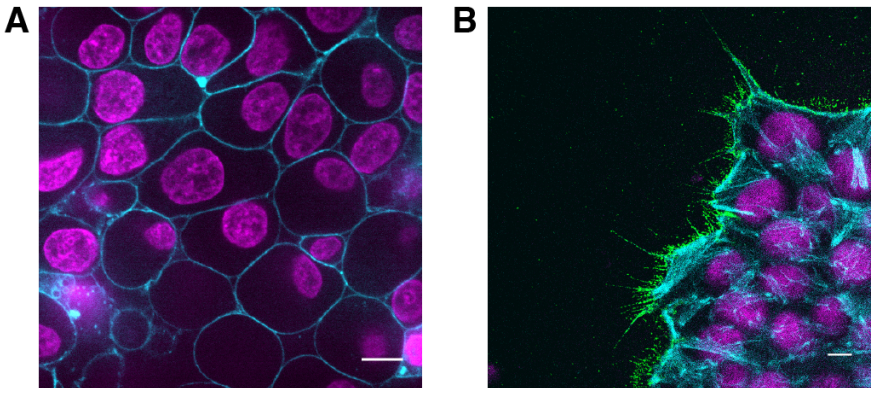

Supp. Fig. 2.1. Visualization of heparan sulfate on the hPS cell surface. (A) Membrane staining to detect filopodia structures on the hPS cell colony. Scale bar 10 µm. Nuclear stain by DAPI (magenta), membrane stain by CellBrite® Fix membrane dyes (cyan) (B) F-actin filament staining of the hPS cell colonies HS is extended from the base of the actin cytoskeleton. Nucleus (magenta), F-actin (cyan), HS (green). Scale bar is 30 µm.

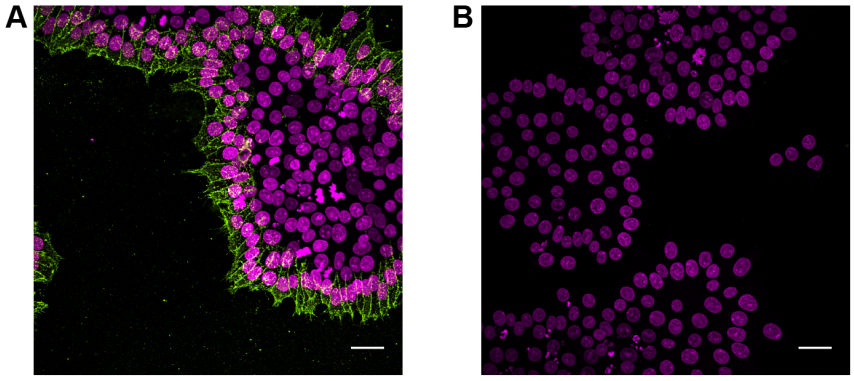

Supp. Fig. 2.2. Heparan sulfate staining after heparinase treatment. (A) Visualization of heparan sulfate (10E04 antibody) in an hPS cell colony without heparinase treatment. (B) Visualization of hPS cells colony after heparinase treatment. Nucleus by DAPI (magenta), HS (green) The scale bar is 30 μm.

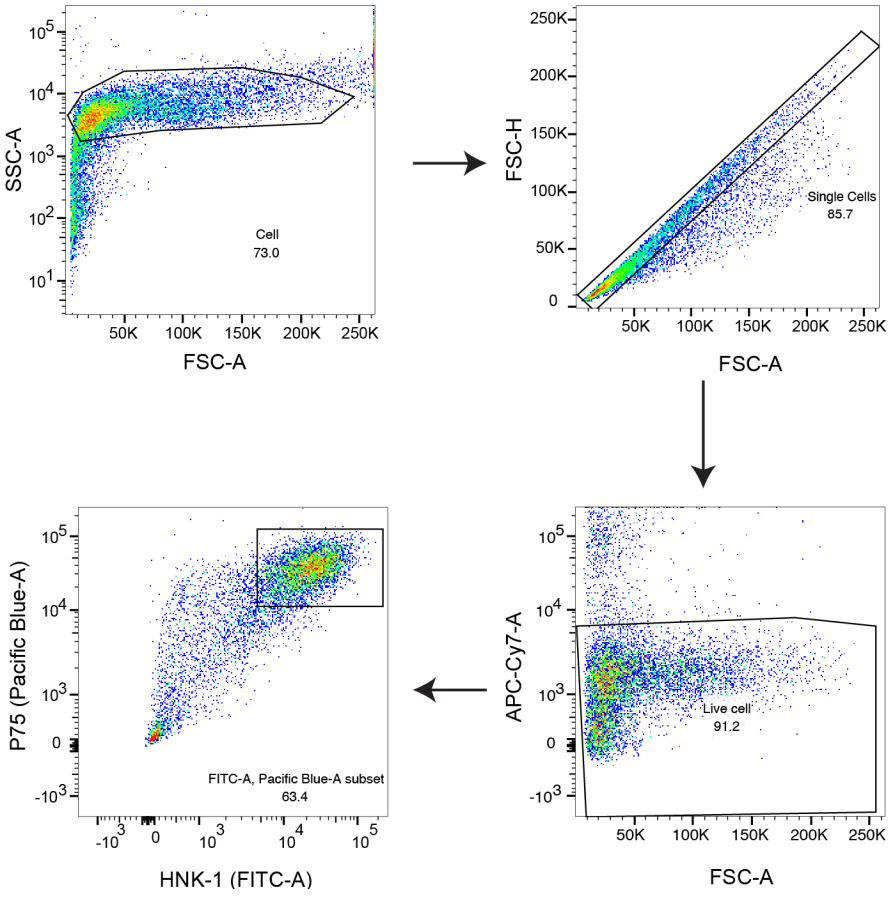

Supp. Fig. 2.3. Flow cytometry gating strategy for neural crest (NC) cells.

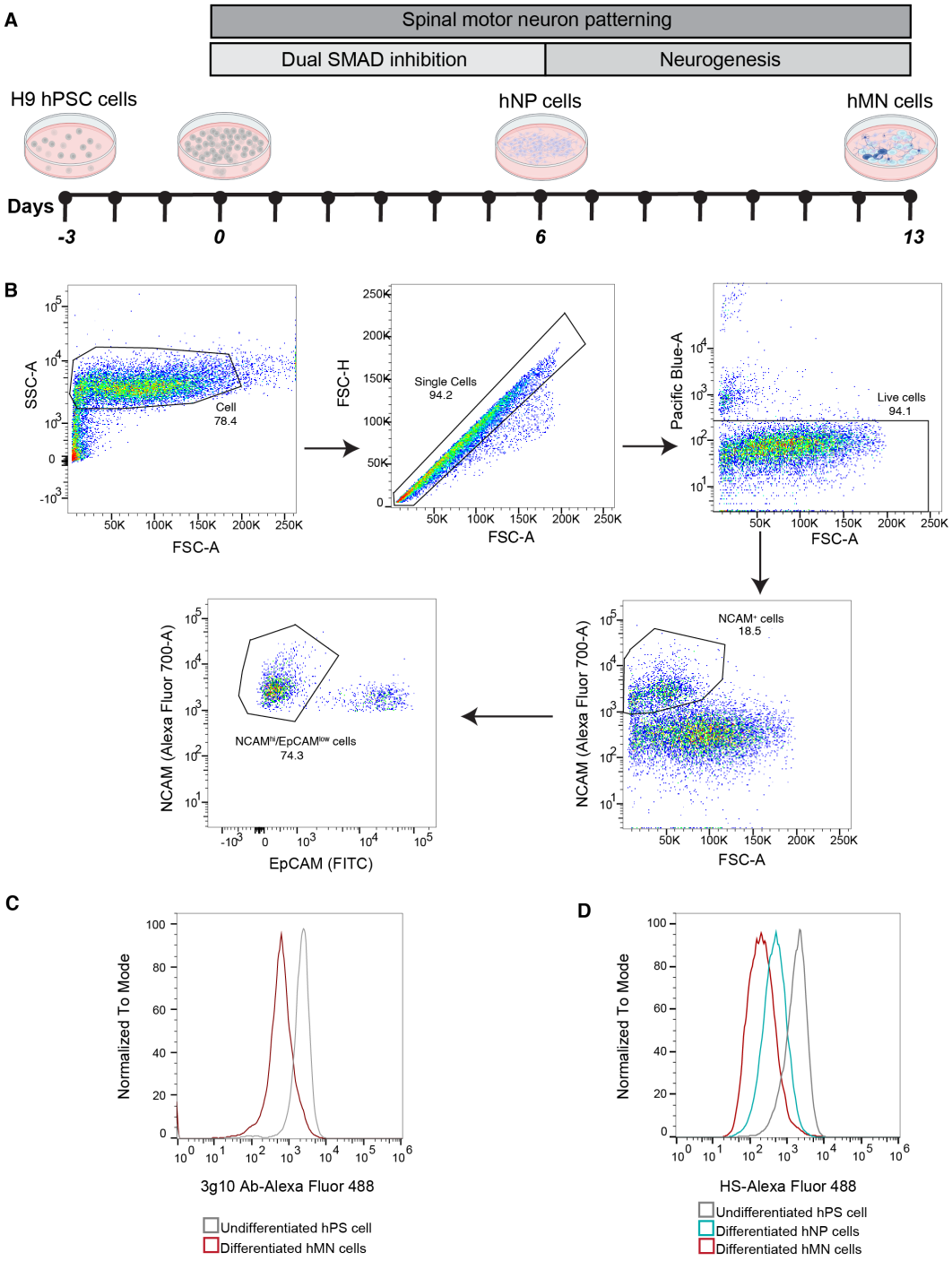

Supp. Fig. 2.4. Heparan sulfate decreased in hMN cells. (A) hMN differentiation strategy. (B) Flow cytometry gating strategy for hMN cells. (C) Binding of HS-3g10 Ab to the undifferentiated hPS and differentiated hMN cells. (D) Gradual decrease of cell surface HS during hMN differentiation.

Table 2.1. Primary antibodies

Antigen	Species	Source	Dilution
Heparan sulfate	Mouse	US Biological (H1890)	IHH 1:200, FC 1:200
Anti HS-3G10	Mouse	Amsbio (370260-S)	IHH 1:200
Basic FGF	Mouse	LifeSpan Biosciences (LS-C114423)	FC 1:100
Parvalbumin	Rabbit	Abcam (ab11427)	IHH 1:200
Pax6	Sheep	R&D system (AF8150)	IHH 1:100
Tuj-1	Rabbit	Abcam (ab229590)	IHH 1:200
NCAM	Mouse	BD Biosciences (561902)	FC 1:100
EpCAM	Mouse	BD Biosciences (565398)	FC 1:50
P75	Mouse	BD Biosciences (562562)	FC 1:100
HNK-1	Mouse	BD Biosciences (347393)	FC 1:100

Table 2.2. qPCR primer sequences

Enzyme	Gene Symbol	Forward Primer (5′-3′)	Reverse Primer (5′-3′)
N-deacetylase/*N*-sulfotransferase 1	*NDST1*	GGG CTA CTC AGG GAA ATT CTT C	CCA CCA GAA CTC CTT CAC ATA C
N-deacetylase/*N*-sulfotransferase 2	*NDST2*	GGT CCT TGT GTT TGT GGA GA	GGT GCC AAC TCA GTG CTA TAA
N-deacetylase/*N*-sulfotransferase 3	*NDST3*	GGG TCC TAA AGA GCT GGA TAA G	CAG TCG GTC ATT CCC ATA GTT
N-deacetylase/*N*-sulfotransferase 4	*NDST4*	GCT GCT CTG AGG TTC AAT TTC	CAT CCA GGT ACT AGG CAT CTT C
6-*O*-sulfotransferase 1	*HS6ST1*	CTA CTA CAT CAC CCT GCT ACG A	CCC ATC ACA CAT ATG CAA CGA
6-*O*-sulfotransferase 2	*HS6ST2*	AGC GTA TTG AGG GAC TGA ATT T	CTG ATG CTC TTT CTG CCT CAT A
6-*O*-sulfotransferase 3	*HS6ST3*	CTT GCG GGA GTT TAT GGA TTG	GGT GTT TCT TTC ACT CTC GTT C

2.8 Acknowledgment

I would like to thank Dr. Sayaka Masuko and Shiwei Wang for their help in this research. I would like to thank Dr. Jeffrey Kuhn, from the microscopy facility of Koch institute for integrative cancer research at MIT for the support in super-resolution imaging. Special thanks to Deepsing Syangtan, Dr. Amanda Dugan and Victoria Marando for editing this section.

2.9 References

1. J. Turnbull, A. Powell, S. Guimond, Heparan sulfate: decoding a dynamic multifunctional cell regulator. *Trends Cell Biol* **11**, 75-82 (2001).
2. H. E. Bulow, O. Hobert, The molecular diversity of glycosaminoglycans shapes animal development. *Annu Rev Cell Dev Biol* **22**, 375-407 (2006).
3. J. D. Esko, S. B. Selleck, Order out of chaos: assembly of ligand binding sites in heparan sulfate. *Annu Rev Biochem* **71**, 435-471 (2002).
4. A. V. Nairn, A. Kinoshita-Toyoda, H. Toyoda, J. Xie, K. Harris, S. Dalton, M. Kulik, J. M. Pierce, T. Toida, K. W. Moremen, R. J. Linhardt, Glycomics of proteoglycan biosynthesis in murine embryonic stem cell differentiation. *J Proteome Res* **6**, 4374-4387 (2007).
5. C. E. Johnson, B. E. Crawford, M. Stavridis, G. Ten Dam, A. L. Wat, G. Rushton, C. M. Ward, V. Wilson, T. H. van Kuppevelt, J. D. Esko, A. Smith, J. T. Gallagher, C. L. Merry, Essential alterations of heparan sulfate during the differentiation of embryonic stem cells to Sox1-enhanced green fluorescent protein-expressing neural progenitor cells. *Stem Cells* **25**, 1913-1923 (2007).
6. R. A. Smith, K. Meade, C. E. Pickford, R. J. Holley, C. L. Merry, Glycosaminoglycans as regulators of stem cell differentiation. *Biochem Soc Trans* **39**, 383-387 (2011).
7. R. J. Baldwin, G. B. ten Dam, T. H. van Kuppevelt, G. Lacaud, J. T. Gallagher, V. Kouskoff, C. L. Merry, A developmentally regulated heparan sulfate epitope defines a subpopulation with increased blood potential during mesodermal differentiation. *Stem Cells* **26**, 3108-3118 (2008).
8. G. B. Ten Dam, S. Kurup, E. M. van de Westerlo, E. M. Versteeg, U. Lindahl, D. Spillmann, T. H. van Kuppevelt, 3-O-sulfated oligosaccharide structures are recognized by anti-heparan sulfate antibody HS4C3. *J Biol Chem* **281**, 4654-4662 (2006).
9. S. Sarrazin, W. C. Lamanna, J. D. Esko, Heparan sulfate proteoglycans. *Cold Spring Harb Perspect Biol* **3**, (2011).
10. J. Kreuger, L. Kjellen, Heparan sulfate biosynthesis: regulation and variability. *J Histochem Cytochem* **60**, 898-907 (2012).
11. J. Zaia, Glycosaminoglycan glycomics using mass spectrometry. *Mol Cell Proteomics* **12**, 885-892 (2013).
12. J. E. Turnbull, J. J. Hopwood, J. T. Gallagher, A strategy for rapid sequencing of heparan sulfate and heparin saccharides. *Proc Natl Acad Sci U S A* **96**, 2698-2703 (1999).
13. G. Venkataraman, Z. Shriver, R. Raman, R. Sasisekharan, Sequencing complex polysaccharides. *Science* **286**, 537-542 (1999).
14. J. Kreuger, M. Salmivirta, L. Sturiale, G. Gimenez-Gallego, U. Lindahl, Sequence analysis of heparan sulfate epitopes with graded affinities for fibroblast growth factors 1 and 2. *J Biol Chem* **276**, 30744-30752 (2001).
15. B. Yang, K. Solakyildirim, Y. Chang, R. J. Linhardt, Hyphenated techniques for the analysis of heparin and heparan sulfate. *Anal Bioanal Chem* **399**, 541-557 (2011).
16. M. Horton, G. Su, L. Yi, Z. Wang, Y. Xu, V. Pagadala, F. Zhang, D. A. Zaharoff, K. Pearce, R. J. Linhardt, J. Liu, Construction of heparan sulfate microarray for investigating the binding of specific saccharide sequences to proteins. *Glycobiology* **31**, 188-199 (2021).
17. E. Tian, K. G. Ten Hagen, O-linked glycan expression during Drosophila development. *Glycobiology* **17**, 820-827 (2007).

18. L. D. Truong, V. T. Phung, Y. Yoshikawa, C. A. Mattioli, Glycoconjugates in normal human kidney. A histochemical study using 13 biotinylated lectins. *Histochemistry* **90**, 51-60 (1988).
19. J. A. Prescher, C. R. Bertozzi, Chemistry in living systems. *Nat Chem Biol* **1**, 13-21 (2005).
20. V. M. Marando, D. E. Kim, P. J. Calabretta, M. B. Kraft, B. D. Bryson, L. L. Kiessling, Biosynthetic Glycan Labeling. *J Am Chem Soc*, (2021).
21. T. L. Hsu, S. R. Hanson, K. Kishikawa, S. K. Wang, M. Sawa, C. H. Wong, Alkynyl sugar analogs for the labeling and visualization of glycoconjugates in cells. *Proc Natl Acad Sci U S A* **104**, 2614-2619 (2007).
22. L. C. Paessens, J. J. Garcia-Vallejo, R. J. Fernandes, Y. van Kooyk, The glycosylation of thymic microenvironments. A microscopic study using plant lectins. *Immunol Lett* **110**, 65-73 (2007).
23. B. R. Gallagher, Y. Zhao, Expansion microscopy: A powerful nanoscale imaging tool for neuroscientists. *Neurobiol Dis* **154**, 105362 (2021).
24. P. W. Tillberg, F. Chen, K. D. Piatkevich, Y. Zhao, C. C. Yu, B. P. English, L. Gao, A. Martorell, H. J. Suk, F. Yoshida, E. M. DeGennaro, D. H. Roossien, G. Gong, U. Seneviratne, S. R. Tannenbaum, R. Desimone, D. Cai, E. S. Boyden, Protein-retention expansion microscopy of cells and tissues labeled using standard fluorescent proteins and antibodies. *Nat Biotechnol* **34**, 987-992 (2016).
25. F. Chen, P. W. Tillberg, E. S. Boyden, Optical imaging. Expansion microscopy. *Science* **347**, 543-548 (2015).
26. A. T. Wassie, Y. Zhao, E. S. Boyden, Expansion microscopy: principles and uses in biological research. *Nat Methods* **16**, 33-41 (2019).
27. D. E. Sun, X. Fan, Y. Shi, H. Zhang, Z. Huang, B. Cheng, Q. Tang, W. Li, Y. Zhu, J. Bai, W. Liu, Y. Li, X. Wang, X. Lei, X. Chen, Click-ExM enables expansion microscopy for all biomolecules. *Nat Methods* **18**, 107-113 (2021).
28. L. Gasimli, A. M. Hickey, B. Yang, G. Li, M. dela Rosa, A. V. Nairn, M. J. Kulik, J. S. Dordick, K. W. Moremen, S. Dalton, R. J. Linhardt, Changes in glycosaminoglycan structure on differentiation of human embryonic stem cells towards mesoderm and endoderm lineages. *Biochim Biophys Acta* **1840**, 1993-2003 (2014).
29. X. Lian, X. Bao, M. Zilberter, M. Westman, A. Fisahn, C. Hsiao, L. B. Hazeltine, K. K. Dunn, T. J. Kamp, S. P. Palecek, Chemically defined, albumin-free human cardiomyocyte generation. *Nat Methods* **12**, 595-596 (2015).
30. N. Volpi, F. Galeotti, B. Yang, R. J. Linhardt, Analysis of glycosaminoglycan-derived, precolumn, 2-aminoacridone-labeled disaccharides with LC-fluorescence and LC-MS detection. *Nat Protoc* **9**, 541-558 (2014).
31. J. O. S. Hackland, T. J. R. Frith, P. W. Andrews, Fully Defined and Xeno-Free Induction of hPSCs into Neural Crest Using Top-Down Inhibition of BMP Signaling. *Methods Mol Biol* **1976**, 49-54 (2019).
32. S. M. Chambers, C. A. Fasano, E. P. Papapetrou, M. Tomishima, M. Sadelain, L. Studer, Highly efficient neural conversion of human ES and iPS cells by dual inhibition of SMAD signaling. *Nat Biotechnol* **27**, 275-280 (2009).
33. J. R. Klim, L. A. Williams, F. Limone, I. Guerra San Juan, B. N. Davis-Dusenbery, D. A. Mordes, A. Burberry, M. J. Steinbaugh, K. K. Gamage, R. Kirchner, R. Moccia, S. H. Cassel, K. Chen, B. J. Wainger, C. J. Woolf, K. Eggan, ALS-implicated protein TDP-43

sustains levels of STMN2, a mediator of motor neuron growth and repair. *Nat Neurosci* **22**, 167-179 (2019).
34. M. Maccarana, B. Casu, U. Lindahl, Minimal sequence in heparin/heparan sulfate required for binding of basic fibroblast growth factor. *J Biol Chem* **268**, 23898-23905 (1993).
35. N. Sugaya, H. Habuchi, N. Nagai, S. Ashikari-Hada, K. Kimata, 6-O-sulfation of heparan sulfate differentially regulates various fibroblast growth factor-dependent signalings in culture. *J Biol Chem* **283**, 10366-10376 (2008).
36. F. Teixeira, A. Vijaya Kumar, S. Kumar Katakam, C. Cocola, P. Pelucchi, M. Graf, L. Kiesel, R. Reinbold, M. S. G. Pavao, B. Greve, M. Gotte, The Heparan Sulfate Sulfotransferases HS2ST1 and HS3ST2 Are Novel Regulators of Breast Cancer Stem-Cell Properties. *Front Cell Dev Biol* **8**, 559554 (2020).
37. T. W. Powers, B. A. Neely, Y. Shao, H. Tang, D. A. Troyer, A. S. Mehta, B. B. Haab, R. R. Drake, MALDI imaging mass spectrometry profiling of N-glycans in formalin-fixed paraffin embedded clinical tissue blocks and tissue microarrays. *PLoS One* **9**, e106255 (2014).
38. T. Kunath, M. K. Saba-El-Leil, M. Almousailleakh, J. Wray, S. Meloche, A. Smith, FGF stimulation of the Erk1/2 signalling cascade triggers transition of pluripotent embryonic stem cells from self-renewal to lineage commitment. *Development* **134**, 2895-2902 (2007).
39. X. Lin, G. Wei, Z. Shi, L. Dryer, J. D. Esko, D. E. Wells, M. M. Matzuk, Disruption of gastrulation and heparan sulfate biosynthesis in EXT1-deficient mice. *Dev Biol* **224**, 299-311 (2000).
40. W. J. Kuo, M. A. Digman, A. D. Lander, Heparan sulfate acts as a bone morphogenetic protein coreceptor by facilitating ligand-induced receptor hetero-oligomerization. *Mol Biol Cell* **21**, 4028-4041 (2010).
41. J. R. Bishop, M. Schuksz, J. D. Esko, Heparan sulphate proteoglycans fine-tune mammalian physiology. *Nature* **446**, 1030-1037 (2007).
42. K. Symes, E. M. Smith, M. Mitsi, M. A. Nugent, Sweet cues: How heparan sulfate modification of fibronectin enables growth factor guided migration of embryonic cells. *Cell Adh Migr* **4**, 507-510 (2010).
43. A. J. Joannides, C. Fiore-Heriche, A. A. Battersby, P. Athauda-Arachchi, I. A. Bouhon, L. Williams, K. Westmore, P. J. Kemp, A. Compston, N. D. Allen, S. Chandran, A scaleable and defined system for generating neural stem cells from human embryonic stem cells. *Stem Cells* **25**, 731-737 (2007).
44. S. M. Chambers, Y. Qi, Y. Mica, G. Lee, X. J. Zhang, L. Niu, J. Bilsland, L. Cao, E. Stevens, P. Whiting, S. H. Shi, L. Studer, Combined small-molecule inhibition accelerates developmental timing and converts human pluripotent stem cells into nociceptors. *Nat Biotechnol* **30**, 715-720 (2012).
45. G. M. Morrison, I. Oikonomopoulou, R. P. Migueles, S. Soneji, A. Livigni, T. Enver, J. M. Brickman, Anterior definitive endoderm from ESCs reveals a role for FGF signaling. *Cell Stem Cell* **3**, 402-415 (2008).
46. P. Zhang, H. Lu, R. T. Peixoto, M. K. Pines, Y. Ge, S. Oku, T. J. Siddiqui, Y. Xie, W. Wu, S. Archer-Hartmann, K. Yoshida, K. F. Tanaka, A. R. Aricescu, P. Azadi, M. D. Gordon, B. L. Sabatini, R. O. L. Wong, A. M. Craig, Heparan Sulfate Organizes Neuronal Synapses through Neurexin Partnerships. *Cell* **174**, 1450-1464 e1423 (2018).

47. J. B. Chang, F. Chen, Y. G. Yoon, E. E. Jung, H. Babcock, J. S. Kang, S. Asano, H. J. Suk, N. Pak, P. W. Tillberg, A. T. Wassie, D. Cai, E. S. Boyden, Iterative expansion microscopy. *Nat Methods* **14**, 593-599 (2017).
48. D. Papy-Garcia, M. Christophe, H. Minh Bao, S. Fernando, S. Ludmilla, S. Diaz Julia Elisa, R.-V. Rita, Glycosaminoglycans, protein aggregation and neurodegeneration. *Current Protein and Peptide Science* **12**, 258-268 (2011).
49. C. Iannuzzi, G. Irace, I. Sirangelo, The effect of glycosaminoglycans (GAGs) on amyloid aggregation and toxicity. *Molecules* **20**, 2510-2528 (2015).
50. N. F. Liachko, A. D. Saxton, P. J. McMillan, T. J. Strovas, C. D. Keene, T. D. Bird, B. C. Kraemer, Genome wide analysis reveals heparan sulfate epimerase modulates TDP-43 proteinopathy. *PLoS Genet* **15**, e1008526 (2019).
51. A. Maiza, S. Chantepie, C. Vera, A. Fifre, M. B. Huynh, O. Stettler, M. O. Ouidja, D. Papy-Garcia, The role of heparan sulfates in protein aggregation and their potential impact on neurodegeneration. *FEBS Lett* **592**, 3806-3818 (2018).
52. S. M. Asano, R. Gao, A. T. Wassie, P. W. Tillberg, F. Chen, E. S. Boyden, Expansion Microscopy: Protocols for Imaging Proteins and RNA in Cells and Tissues. *Curr Protoc Cell Biol* **80**, e56 (2018).
53. R. J. Holley, C. E. Pickford, G. Rushton, G. Lacaud, J. T. Gallagher, V. Kouskoff, C. L. Merry, Influencing hematopoietic differentiation of mouse embryonic stem cells using soluble heparin and heparan sulfate saccharides. *J Biol Chem* **286**, 6241-6252 (2011).

Chapter 3

Heparan sulfate is indispensable for the neuronal differentiation of human pluripotent stem cells

3.1 Abstract

Heparan sulfate proteoglycans (HSPGs) are cell-surface glycans that regulate the cell fate decisions of embryonic stem cells. This long-chain polysaccharide can modulate developmental signals critical for stem cell pluripotency and differentiation efficiency. Still, the biological function of HS in human pluripotent stem (hPS) cell lineage commitment is largely unknown. To advance the understanding of its roles in human development, we generated a heparan sulfate-deficient cell line derived from human pluripotent stem (hPS) cells by targeting *EXT1* via CRISPR. This study shows that heparan sulfate-deficient *EXT1*$^{-/-}$ cells can self-renew and proliferate under standard hPS cell culture conditions. We showed that in absence of HS, the hPS cells cannot differentiate into primitive streak or mesendoderm lineage; however, the early ectoderm commitment of hPS cells remains intact. Lack of HS downregulates BMP and Nodal/TGF-β signaling pathway that facilitates the differentiation towards the early ectodermal lineage. However, despite being able to differentiate into progenitor cells of neural lineages, the HS-deficient hPS cells cannot develop proper neuronal projections or synaptic vesicles. Several critical genes for axonogenesis (*ROBO1, SLIT2, POU4F1)* are downregulated in the *EXT1*$^{-/-}$ cells-derived neurons. Overall, our data indicate that HS has a critical role in neurophysiological development; therefore, defects in its production are likely relevant for neurological disorders. This study identified a conserved and unique role of HS in hPS cell lineage commitment. Leveraging this advancement paves the way further for a better understanding of heparan sulfate's role in early human development.

3.2 Introduction

Heparan sulfate (HS) is an essential cell surface polysaccharide for mammalian development and is implicated in many critical processes including; morphogenesis, growth regulation, and differentiation. Genetic studies using model organisms (*Drosophila*, *C. elegans,* mouse, zebrafish), have demonstrated that HS has specific functions in the signaling of many morphogens and mitogens, such as fibroblast growth factors (FGFs), wingless (Wnt), hedgehog/sonic hedgehogs, bone morphogenetic protein (BMP), and transforming growth factor (TGF)-β (*1-4*). HS has ubiquitous expression, suggesting it may play a multitude of important biological roles. Though it is known that this expression is controlled in a developmentally regulated manner, the physiological importance and functional specificities of HS are yet to be elucidated in human development. Addressing this knowledge gap is essential for advancing our understanding of human development and diseases where HS plays a pivotal role.

Previous studies in *Drosophila* showed that HS is crucial for embryonic development, a finding that is further supported by conclusions from genetic studies in hamster and mice (*5-7*). Though these studies revealed the committed function of heparan sulfate proteoglycan (HSPG) in cell differentiation and morphogenesis in these models, its role in human development is still largely unexplored. Specifically, studying HS in a human context is important as mouse and human embryo developmental trajectories diverge substantially upon implantation, with the mouse forming a cup-shaped embryo while the human gives rise to a flat bilaminar disk structure. Therefore, the principles governing human morphogenesis cannot be extrapolated by the studies in mice or other mammals but urges the direct investigation of human embryonic development. However, the processes of primitive steak formation, patterning, and germ layer formation during gastrulation still present a challenge, as the 14-day rule prohibits the culture of human embryos

beyond this point (*8, 9*). Therefore, elucidation of the mechanisms governing the molecular and cellular events of human development vastly rely on stem cell-based models. Human pluripotent stem (hPS) cells derived either from the inner cell mass of blastocysts or reprogramed from somatic cells have the remarkable ability to self-renew and differentiate into multiple cell types in the body (*10, 11*). Therefore, they are excellent tools to probe fundamental biological questions about human development in a relevant context.

The stem cell microenvironment is a collection of intrinsic and extrinsic components that balance self-renewal and differentiation (*12*). The extracellular matrix (ECM), niche cells (supporting cells, stem cells), and the soluble factors derived from these cells are the three main components of this microenvironment (*13*). The cell fate choice of human embryonic stem (hES) cells is controlled by their interaction with both soluble and insoluble factors of this microenvironment. For example, a number of growth factors, including BMP, WNT and FGF are the critical soluble modulators in lineage specification. HS is present in the ECM and on the surface of cells, where it can interact with a number of these signaling molecules that govern cell fate choices (*14, 15*). However, despite residing in the stem cell niche, due to lack of efficient system and proper tools, the contribution of HS to cell fate decisions are not well understood.

HS is a long, linear polysaccharide belonging to the glycosaminoglycan family (GAG). HS biosynthesis is evolutionarily conserved across the animal kingdom *(16, 17)*. The primary biosynthesis of HS starts in the Golgi bodies with the exostosin glycosyltransferases (EXT1 and EXT2) enzymes (*14, 15, 18*) which initiate the chain elongation. Following chain elongation, this long polysaccharide undergoes several diverse modifications (sulfation, epimerization, and acetylation), allowing it to interact with different growth factors and chemokines to fine-tune their stability, bioavailability, and spatiotemporal distribution (*14, 15*). In humans, polymorphisms in

the HS biosynthetic genes (*EXT1* or *EXT2)* cause abnormal bone development, a condition known as hereditary multiple exostoses (HME). Targeted disruption of HS synthesis in mice results in embryonic lethality at E6.5 as they fail to undergo gastrulation (*7*). In contrast, HS is dispensable for mouse embryonic stem (mES) cell self-renewal but is required only for cell fate commitment (*19*), where lack of HS caused spontaneous differentiation into extraembryonic endoderm (*20*). Several other studies in mES cell indicate that HS is required for differentiation into ß3-tubulin-positive neuronal cells (*21*) , hematopoietic lineages (*22*), and for mesoderm differentiation, presumably for facilitating FGF and BMP signaling (*23*). However, mES and hPS cells represent different developmental stages (*24*), and therefore require different external cues for self-renewal and differentiation. Therefore, despite being studied in murin model, there is a need to explore the role of HS in hPS cell fate commitment in a human context.

Studies in mES and conditional knockout mice showed that HS has a role in neural development by modulation of neurogenesis, axonal guidance, and synaptogenesis (*25*). EXT KO mice (EXT^{CKO}) displayed behavior associated with autism (*26*). Human population genetic studies showed that individuals with clinical phenotype of HME also present autism or intellectual disability (*27*). More recent evidence demonstrated that HS expression modulates the differentiation of ES cells into specific neurons in rat models (*28*). Moreover, HS functions as an essential component of synaptic organizing complexes (neurexin and neuroligin) (*29*) and as a coactivator of FGF, BMP, and TGFβ signaling pathways, that together can modulate the proper synaptic connection in the brain. It is therefore of great interest to study how HS modulates hPS cells' differentiation specifically into a neural lineage to understand its role in human brain development.

We applied CRISPR/Cas9 to knock out the *EXT1* biosynthetic gene to engineer the first HS-deficient hPS cell line (*EXT1*$^{-/-}$ cells). While this specific cell line is able to maintain the pluripotency status in standard cell culture conditions, we showed that they are unable to differentiate into specific lineage under a directed differentiation condition. We observed that HS-deficient cells are able to differentiate to both the neural crest and neural progenitor cells, however, they cannot complete the neurogenesis and proper synapse formation due to lack of proper axonogenesis. Taken together these findings highlight that the lack of HS in hPS cells significantly perturbs the cellular signaling processes. Though this absence of HS favors the early ectodermal differentiation, it directly impairs the axonogenesis process, leading to defects in synaptic connection formation. We anticipate that this understanding of how HS modulates the signaling pathways and, therefore the cell fate choices of hPS, can help to identify the role of HS in human development and diseases, including various neurological conditions.

3.3 Results

3.3.1 CRISPR/Cas9-mediated generation of heparan sulfate-deficient hPS cells

To determine the functional roles of HS in hPS cells, we first set out to generate an HS-deficient hPS cell line by CRISPR-mediated targeting of the HS biosynthetic gene *EXT1* (Fig 3.1A). *EXT1* encodes exostosin glycosyltransferase 1, a polymerase that is required for the extension of the HS backbone chain. By knocking out the *EXT1* gene in mouse embryo (*7*) and mES cell line (*21*) the HS production is completely abolished. Therefore, we anticipated that *EXT1*$^{-/-}$ hPS cell line should result in a completely HS-deficient hPS cell line. Following CRISPR-mediated editing, we isolated and expanded a clone in which both alleles incorporated frameshift mutations at the targeted site (**Fig 3.1B**) indicating a homozygous mutation. To confirm that the HS biosynthesis is blocked, we assessed cell-surface HS levels by flow cytometry and

immunohistochemistry using the anti-HS antibody 10E4.

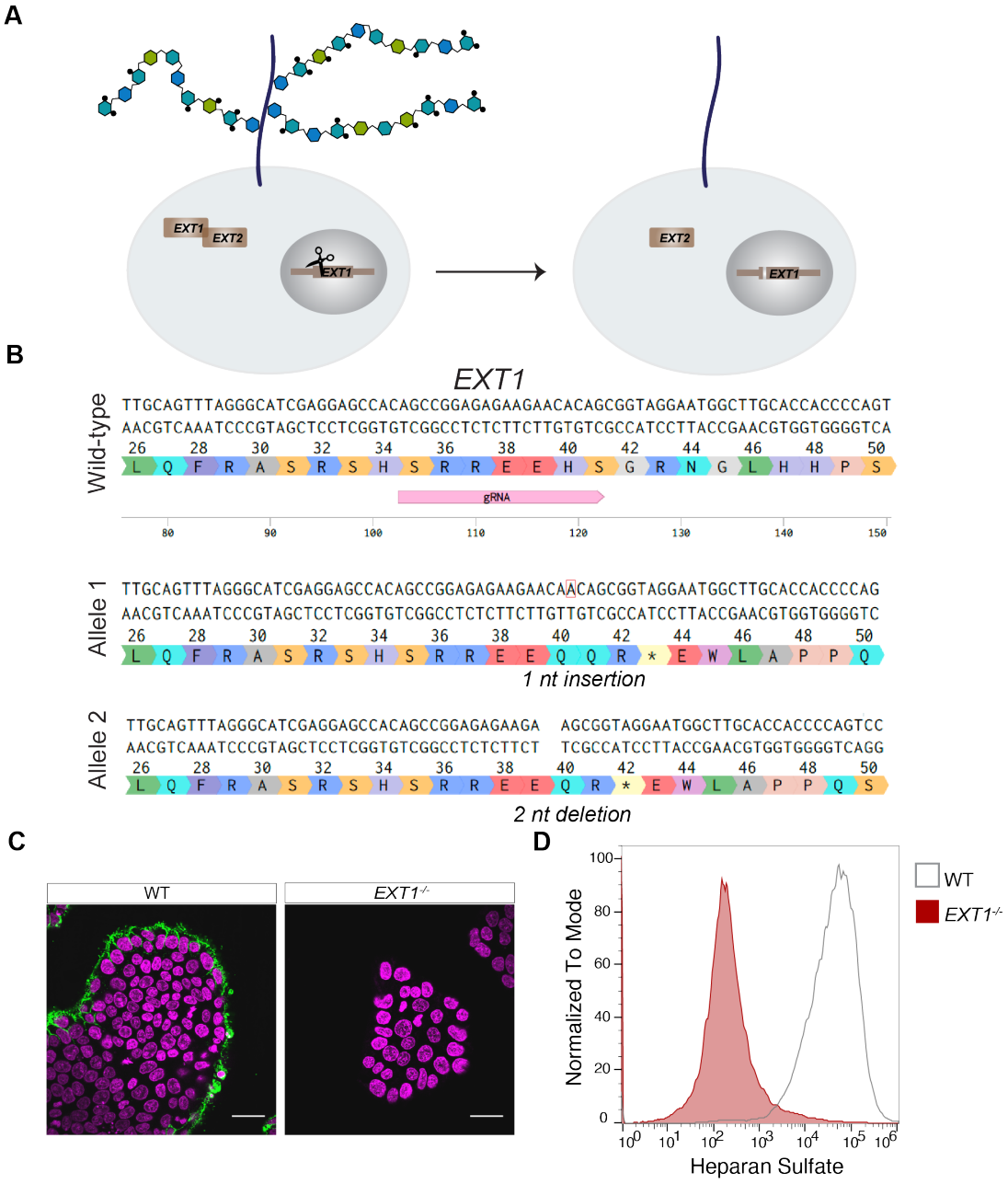

Fig. 3.1. Generation of an HS-deficient hPS cell line. (A) Scheme of generating the HS-deficient hPS cells via CRISPR-mediated targeting of *EXT1*. (B) Biallelic sequence in the sgRNA-targeted region of *EXT1* of an isolated H9 hPS cell clone following CRISPR editing. Frameshift mutations by CRISPR introduce a stop codon in both *EXT1* alleles (* denotes stop codon) early in the coding sequence of *EXT1*. (C) Wild-type (H9 cells) and *EXT1*$^{-/-}$ cells were immunostained for heparin sulfate (green) and counterstained with DAPI (magenta). Scale bar, 30 µm. (D) Histogram plot of HS fluorescence intensity measured by flow cytometry in WT and *EXT1*$^{-/-}$ cells using the anti-heparan sulfate antibody 10E4.

We detected HS expression in wildtype cells, whereas it was absent in the *EXT1*$^{-/-}$ cells (**Fig 3.1C, D**) indicating the successful generation of HS-deficient hPS cell line.

3.3.2 Assessing the pluripotency and differentiation potential of *EXT1*$^{-/-}$ cells

We next sought to assess the trilineage differentiation efficiency of the HS-deficient hPS cells. To address this, we employed an *in vitro* embryoid body (EB) assay. EBs are three-dimensional aggregates of cells that are an amalgam of the three different developmental germ layers (*30*). The EBs were collected from the 3D suspension culture and allowed to spontaneously differentiate as adherent cells. After 14 days of spontaneous differentiation the WT cells demonstrated the ability to differentiate into all three germ layers, However, the *EXT1*$^{-/-}$ cells expressed the ectoderm markers Nestin and Tuj-1 but not the mesoderm markers smooth muscle actin (SMA) or Brachyury, or the endoderm markers Sox-17 and alpha-fetoprotein (AFP) (**Fig 3.2)**. This embryoid body assay thus indicate that lack of HS almost completely abolishes the mesoderm and endoderm differentiation pathway of hPS cells, however interestingly may not affect the ectoderm lineage commitment. During development, mesoderm and endoderm layers are formed through a common transient structure represents the primitive streak called the mesendoderm. We speculated that the impaired ability of *EXT1*$^{-/-}$ cells to form mesoderm or endoderm is preceded by defective mesendoderm formation.

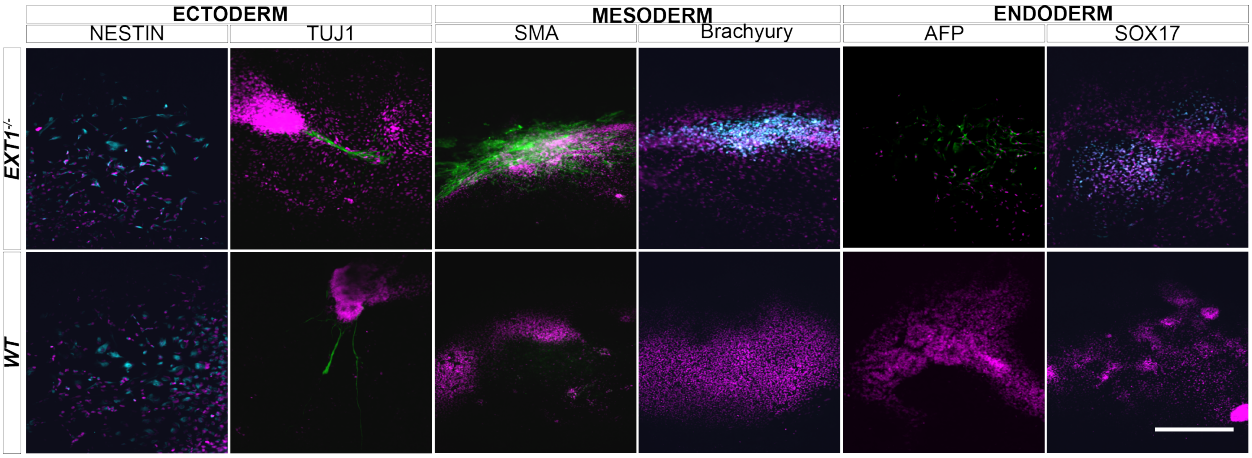

Fig. 3.2. The pluripotency and differentiation potential of *EXT1*$^{-/-}$cells. Spontaneously differentiated EBs derived from WT and *EXT1*$^{-/-}$ cells were immunostained for markers of ectoderm (Nestin [cyan] and Tuj-1 [green]), mesoderm (SMA [green] and Brachyury [cyan]), and endoderm (SOX17 [cyan] and AFP [green]) and counterstained with DAPI (magenta). Scale bar, 200 μm.

3.3.3 Ectoderm specific lineage commitment of *EXT1*$^{-/-}$ cells

Though embryoid body assay is considered as a gold standard for assessing pluripotency of pluripotent stem cells, the culture and differentiation condition is not fully defined and contains bovine serum which introduces external HS contamination to the differentiation condition of HS-deficient cells. Therefore, I sought to approach lineage-specific directed differentiation.

During the directed mesendoderm differentiation, we found that the *EXT1*$^{-/-}$ cells are not able to differentiate to the mesendoderm lineage defined by the number of Brachyury positive cells (**Fig. 3.3A**). However, from RNA-seq analysis we observed upregulation of multiple ectoderm lineage-specific genes including the *TFAP2A, HAND1, MSX1, PAX3, ZIC1, DLX5* (**Fig 3.3B**). This observation indicates that lack of HS in hPS cells directly suppresses the early mesendoderm lineage-specific differentiation, but it may not affect the ectodermal differentiation. We hypothesized that lack of HS may rather prime the hPS cells toward the ectodermal route.

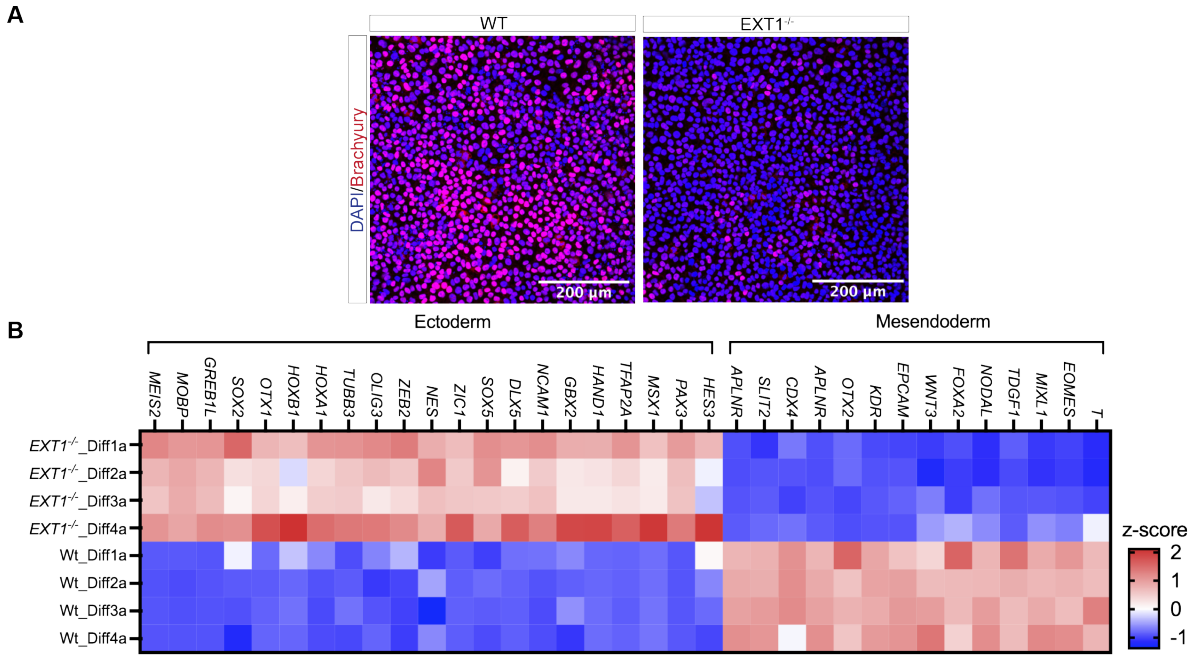

Fig 3.3. *EXT1*$^{-/-}$ cells are unable to differentiate to mesendoderm but upregulate ectodermal gene expression. (A) Directed differentiation to mesendoderm lineage. WT and *EXT1*$^{-/-}$ cells were immunostained for markers of mesendoderm (Brachyury) [red] and DAPI [blue], Scale bar 200 µm. (B) Heat map representing the expression of mesendodermal and ectodermal genes in WT versus *EXT1*$^{-/-}$ cells after 28 hours of mesendoderm induction (upregulated genes are red and downregulated genes are blue in the heatmap).

To test this hypothesis, I, therefore, differentiated the *EXT1*$^{-/-}$ cells towards the ectodermal lineage using a defined and directed differentiation protocol. I differentiated the *EXT1*$^{-/-}$ cells towards ectoderm specific non-neural line, neural crest (NC) by following a chemically defined protocol (*31*) (**Fig. 3.4A**). Upon differentiation, we measured the expression of SOX10 (Sry-related HMg-Box gene 10), a key nuclear transcription factor in the differentiation of neural crest. We detected a comparable expression of SOX10 in both wild-types (WT) has-derived NC and *EXT1*$^{-/-}$ cells-derived NC (**Fig. 3.4B**). Additionally, we also measured p75 and HNK1 double-positive NC cells using flow cytometry. Both the WT hPS cells and *EXT1*$^{-/-}$ cells exhibit a high level of differentiation efficiency (% of p75+/HNK1+ cells is 62.5% and 44.8% in WT and *EXT1*$^{-}$

$^{-/-}$ cells respectively (**Fig. 3.4C, 3.4D**). These results indicate that HS of hPS cells is not an essential requirement for ectoderm-specific multipotent neural crest differentiation.

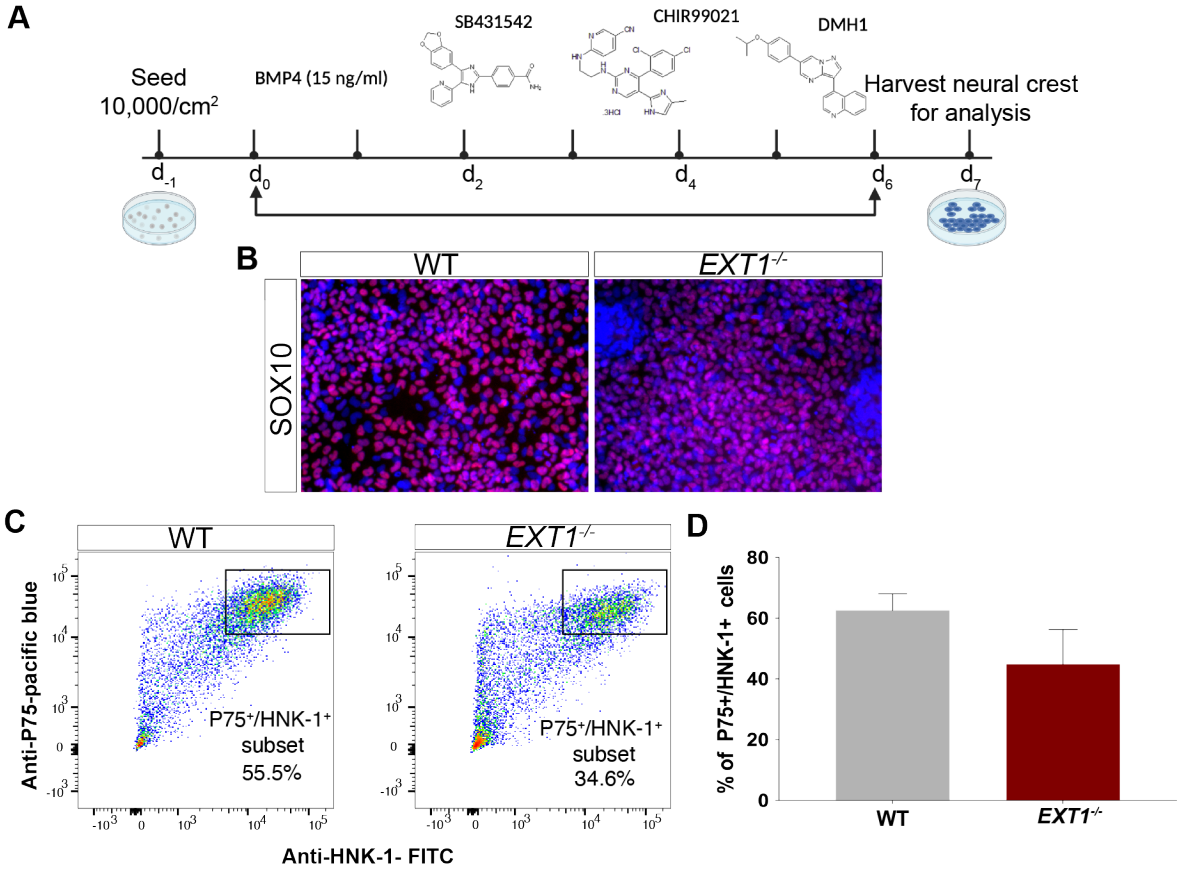

Fig 3.4. Neural crest differentiation of WT hPS cells and *EXT1*$^{-/-}$ cells. (A) Schematic representation of the procedure for neural crest differentiation of hPS cells. (B) Confocal microscopy images of wild-type and *EXT1*$^{-/-}$ cells upon directed differentiation into neural crest cells and immunostained for the neural crest marker SOX10 (red) and counterstained with DAPI (blue). Scale bar, 30 µm. Representative flow cytometry dot plot of P75^{+}/HNK-1^{+} cells in WT and *EXT1*$^{-/-}$ cells after neural crest differentiation. (D) Percentage of P75^{+}/HNK-1^{+} cells derived from WT and *EXT1*$^{-/-}$ cells after neural crest differentiation (n=4). Error bars indicate ±SD.

3.3.4 Heparan sulfate in neuronal differentiation of hPS cells

Ectoderm can give rise to both the neural and non-neural descendants (*32*). So, to determine whether HS is entirely dispensable for ectodermal differentiation of hPS cells beyond multipotent

neural crest differentiation, we differentiated the *EXT1*$^{-/-}$ cells towards neural lineage following a directed differentiation protocol (*33*). We differentiated the WT and *EXT1*$^{-/-}$ hPS cells into human motor neurons (hMN) under adherent culture conditions (**Fig. 3.5A**). This tailored dual-smad inhibition protocol has two steps; on day 6 of differentiation, the hPS cells differentiate into neural progenitor (NP) cells, which are further patterned to motor neurons. On day 14 of differentiation, the culture routinely comprises hMN cells with distinct neuronal morphology (**Fig. 3.5A**).

The cells are collected during and after the differentiation on day 6 and day 14. The expression of the postmitotic neuron-specific class III β-tubulin (*TUJ1*) gene was lower in the *EXT1*$^{-/-}$ derived neurons relative to WT suggesting a defect in neuron-specific differentiation in HS-deficient cell line (**Fig. 3.5B**). We also looked into the neuronal cell adhesion molecule (NCAM) and epithelial cell adhesion molecule (EpCAM) expression in the differentiated neurons. Based on unbiased immune profiling analysis of stem cell-derived neurons, it is known that NCAM^{high}/EpCAM^{low} is the antigenic signatures enriched on postmitotic neurons (*33*). When we investigated this in our system, we observed that most of the NCAM positive cells in WT-derived neurons lost their EpCAM expression, whereas for the *EXT1*$^{-/-}$ cells, a significant number of cells are positive for NCAM expression and they barely lost their EpCAM expression (**Fig. 3.5C**). Overall, the mean % of NCAM^{high}/EpCAM^{low} cells in the WT hPS cells-derived neurons is 66.8%, which is significantly lower (2.58%) in differentiated cells derived from *EXT1*$^{-/-}$ cells (**Fig. 3.5D**). Together these data suggest that the lack of HS affects neuronal differentiation.

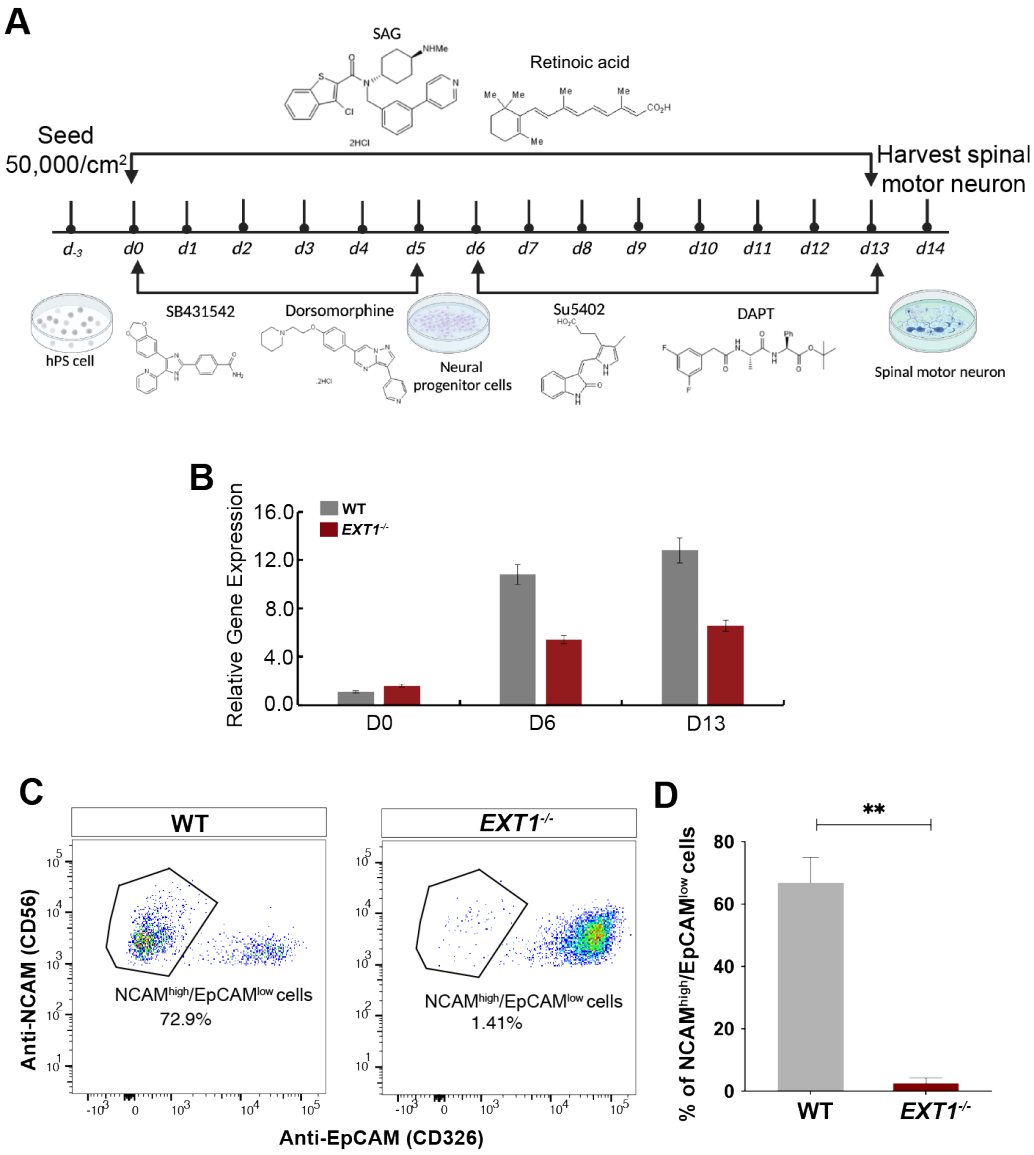

Fig 3.5. Lack of HS impairs motor neuron differentiation. (A) Schematic presentation of directed motor neuron differentiation procedure of hPS cells. (B) *TUJ1* gene expression during motor neuron differentiation of WT hPS and *EXT1*$^{-/-}$ cells (n=3) Error bars indicate ±SD. (C). Representative flow cytometry dot plot of NCAM^{high}/EpCAM^{low} cells in WT and *EXT1*$^{-/-}$ cells after thirteen days of neuronal differentiation. (D) Percentage of NCAM^{high}/EpCAM^{low} cells derived from WT and *EXT1*$^{-/-}$ cells after 13 days of differentiation (n=6). Error bars indicate ±SD. Mann Whitney t-test between WT hPS and *EXT1*$^{-/-}$ cells were used for data analysis. An asterisk denotes a statistically significant difference *(*****p<0.000000xx, **p<0.05) between WT hPS and *EXT1*$^{-/-}$ cells.

3.3.5 The morphology of differentiated neurons

Next, I sought to investigate the morphology of the WT and *EXT1*$^{-/-}$ derived neurons. Immunofluorescence imaging showed that the WT-derived neurons are positive for spinal motor neuron marker, ISLET1, and neuron-specific β III tubulin (TUJ1) signal and have long extended neuronal projection.

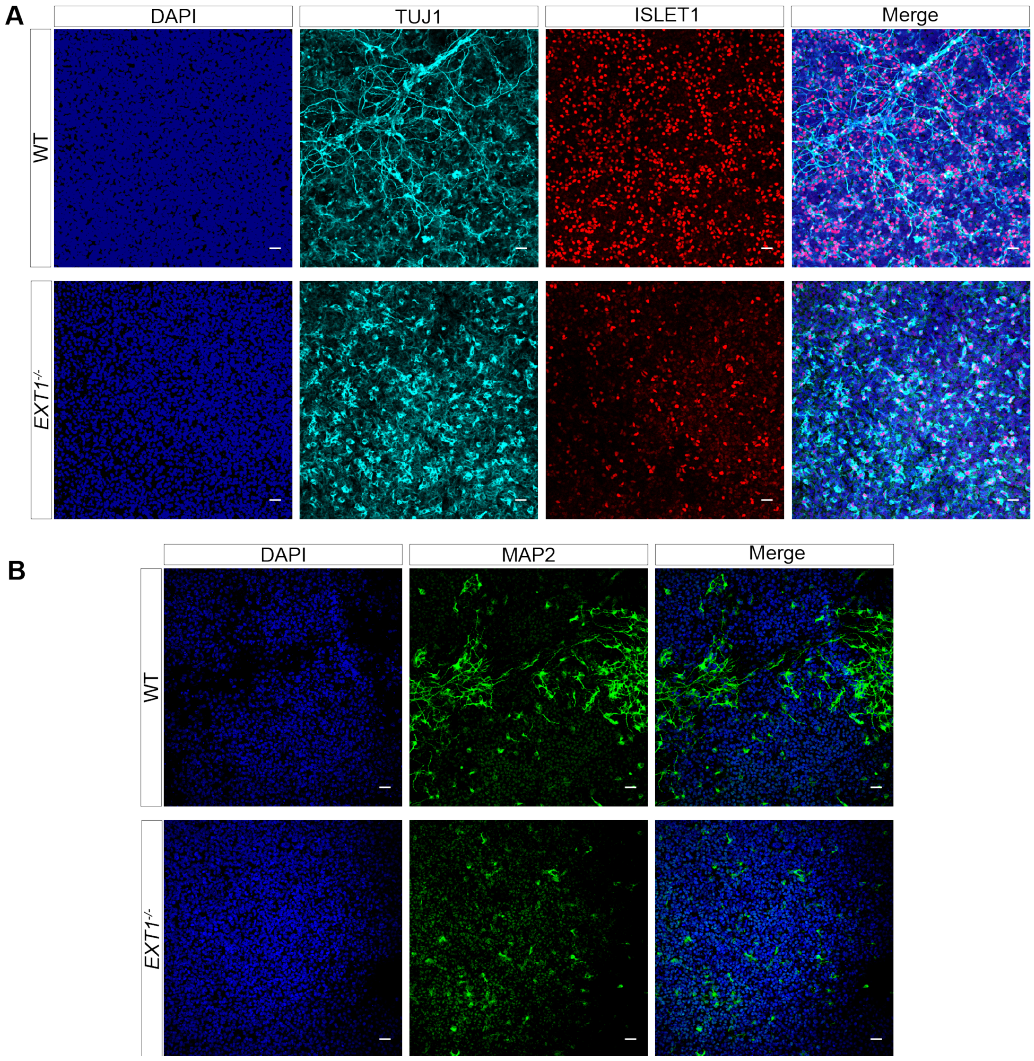

Fig 3.6. The *EXT1*$^{-/-}$ cells derivatives have defective neuronal projections. Confocal microscopy images of wild-type and *EXT1*$^{-/-}$ cells upon directed differentiation into spinal motor neuron cells and immunostained for neuron specific β III tubulin (TUJ1) (cyan), motor neuron marker, ISLET1 (red) (A) and dendritic marker MAP2 (green) (B). Counterstained with DAPI (blue). Scale bar, 30 μm.

In contrast, the *EXT1*$^{-/-}$ derivatives have short and truncated projections, though they are positive for the ISLET1 marker (**Fig. 3.6A**). Similarly, while stained for dendritic marker microtubule-associated protein 2 (MAP2), the *EXT1*$^{-/-}$ cells lack the extended neuronal projection morphology compared to the WT hPS cells derived neurons (**Fig. 3.6B**). These data suggest that even though the *EXT1*$^{-/-}$ hPS cells express some neuronal markers, they have a distinctive morphology that shows the defect in generating long extended neuronal projections.

Next, we sought to analyze the gene expression profile to understand the morphological defect that we observed.

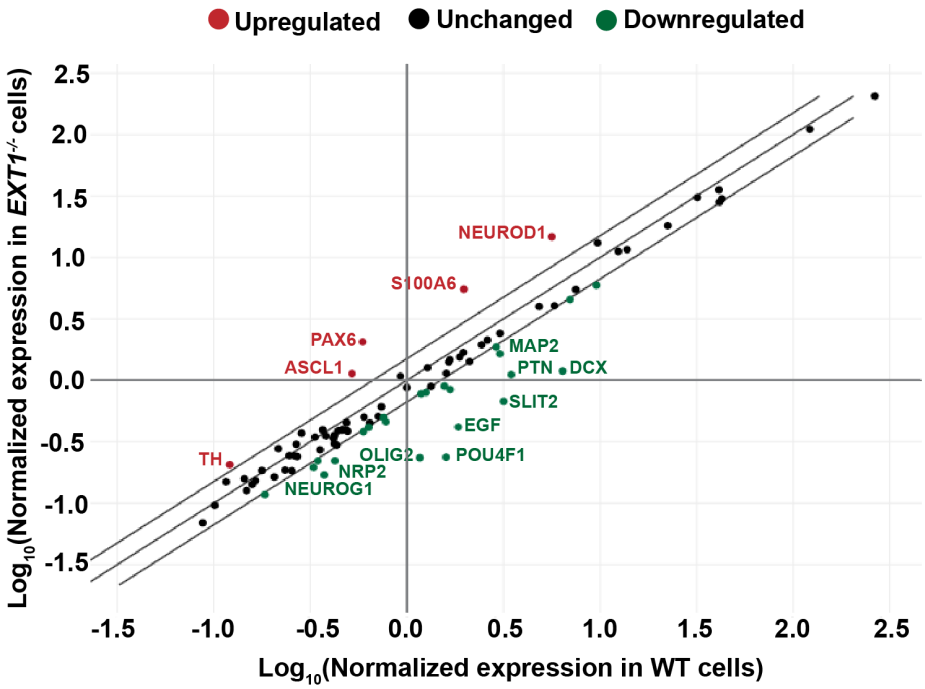

Fig 3.7. Gene expression analysis of motor neuron derived from WT hPS and *EXT1*$^{-/-}$ cells. The *EXT1*$^{-/-}$ cells were differentiated for 14 days following the motor neuron differentiation procedure, and their levels of neurogenesis markers were examined relative to WT hPS cells. Values shown are log10 of mean fold regulation in WT hPS cells (x axis) and log10 of mean fold regulation in *EXT1*$^{-/-}$ cells (y axis) (n=2). The cut-off value for the fold-difference is 1.5. The upregulated gene expression is shown as red and downregulated gene expression is shown as green.

We analyzed the gene expression profile of the WT and *EXT1*$^{-/-}$ hPS-differentiated cells by assessing the gene markers specific for the neurogenesis pathway (**Table: 3.1 and Table: 3.2**). After the 2 weeks of differentiation, most of the neurogenesis genes are significantly downregulated in *EXT1*$^{-/-}$ hPS-differentiated cells including *DCX, MAP2, NEUROG1, OLIG2*. Additionally, in these cells, expression levels were significantly decreased for the genes encoding essential proteins for proper axon formation (*ROBO1, SLIT2, POU4F1*) (**Fig. 3.7**).

Table 3.1: Genes under-expressed in *EXT1*$^{-/-}$ vs WT

Gene Description	Gene Symbol	Fold Regulation
Cyclin-dependent kinase 5, regulatory subunit 1 (p35)	*CDK5R1*	**-1.57**
CDK5 regulatory subunit associated protein 2	*CDK5RAP2*	**-1.74**
CAMP responsive element binding protein 1	*CREB1*	**-1.55**
Doublecortin	*DCX*	**-5.39**
Ephrin-B1	*EFNB1*	**-1.53**
Epidermal growth factor	*EGF*	**-4.43**
Fibroblast growth factor 2 (basic)	*FGF2*	**-1.52**
Filamin A, alpha	*FLNA*	**-1.52**
Hairy/enhancer-of-split related with YRPW motif 1	*HEY1*	**-1.56**
Microtubule-associated protein 2	*MAP2*	**-1.84**
Myeloid/lymphoid or mixed-lineage leukemia (trithorax homolog, Drosophila)	*KMT2A*	**-1.58**
Norrie disease (pseudoglioma)	*NDP*	**-1.57**
Neurogenin 1	*NEUROG1*	**-1.68**
Nuclear receptor subfamily 2, group E, member 3	*NR2E3*	**-2.2**
Neuregulin 1	*NRG1*	**-1.99**
Neuropilin 2	*NRP2*	**-1.92**
Neurotrophin 3	*NTF3*	**-1.69**
Oligodendrocyte lineage transcription factor 2	*OLIG2*	**-4.99**
POU class 4 homeobox 1	*POU4F1*	**-6.74**
Pleiotrophin	*PTN*	**-3.12**
Roundabout, axon guidance receptor, homolog 1 (Drosophila)	*ROBO1*	**-1.54**
Slit homolog 2 (Drosophila)	*SLIT2*	**-4.7**
Vascular endothelial growth factor A	*VEGFA*	**-1.61**

Table: 3.2 Genes over-expressed in *EXT1*$^{-/-}$ vs WT

Gene Description	Gene Symbol	Fold Regulation
Achaete-scute complex homolog 1 (Drosophila)	*ASCL1*	**2.18**
Neurogenic differentiation 1	*NEUROD1*	**2.61**
Paired box 6	*PAX6*	**3.49**
S100 calcium binding protein A6	*S100A6*	**2.8**
Tyrosine hydroxylase	*TH*	**1.7**

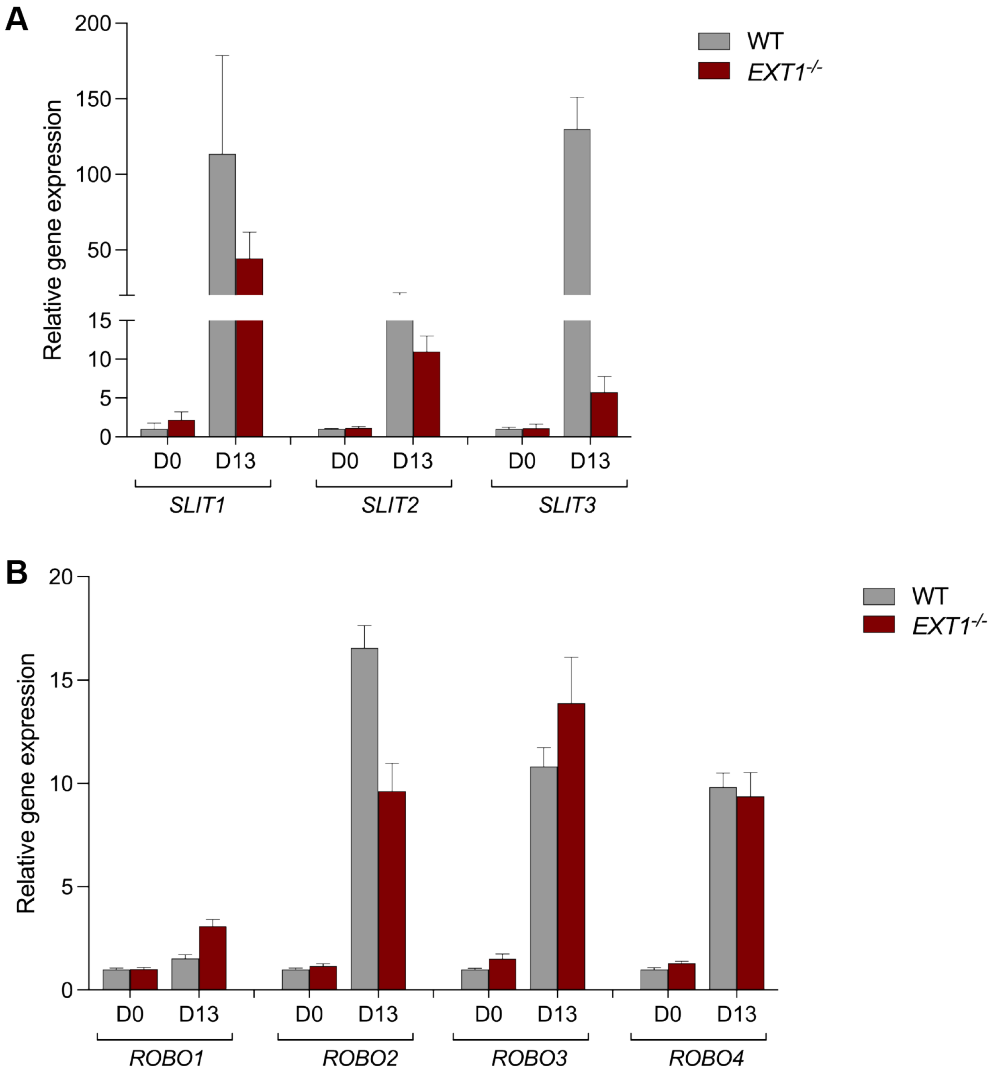

Fig 3.8. Expression of the ligands and receptors of the SLIT-ROBO signaling pathway. (A) All ligands of the SLIT-ROBO pathway have decreased expression in *EXT1*$^{-/-}$-derived neurons at day 13 of differentiation. (B) All receptors but ROBO2 have similar expression in *EXT1*$^{-/-}$-derived neurons compared to WT; (n=2) error bars indicate ±SD.

We next investigated the expression of the ligands and receptors of the SLIT-ROBO signaling pathway which is essential for proper axonal guidance (*34, 35*) . We found that, all the ligands (*SLIT1, SLIT2*, and *SLIT3*) have decreased expression in *EXT1*$^{-/-}$ derivatives. Although, the expression of all the receptors are either similar or higher in *EXT1*$^{-/-}$ -derived compared to WT-derived neurons (**Fig 3.8A, 3.8B**). These results are consistent with the morphological and immunocytochemical findings that the lack of heparan sulfate significantly hinders the axonogenesis of human pluripotent stem cells.

Next, we examined the ability of *EXT1*$^{-/-}$- derived neurons to form synapses. The immunofluorescence data showed that the *EXT1*$^{-/-}$ derivatives do not have synaptophysin expression, an integral membrane protein localized to synaptic vesicles. The absence of synaptic vesicle marker (**Fig. 3.9**) further confirms that the lack of HS disrupts the proper axon formation leading to a lack of proper synaptic connections.

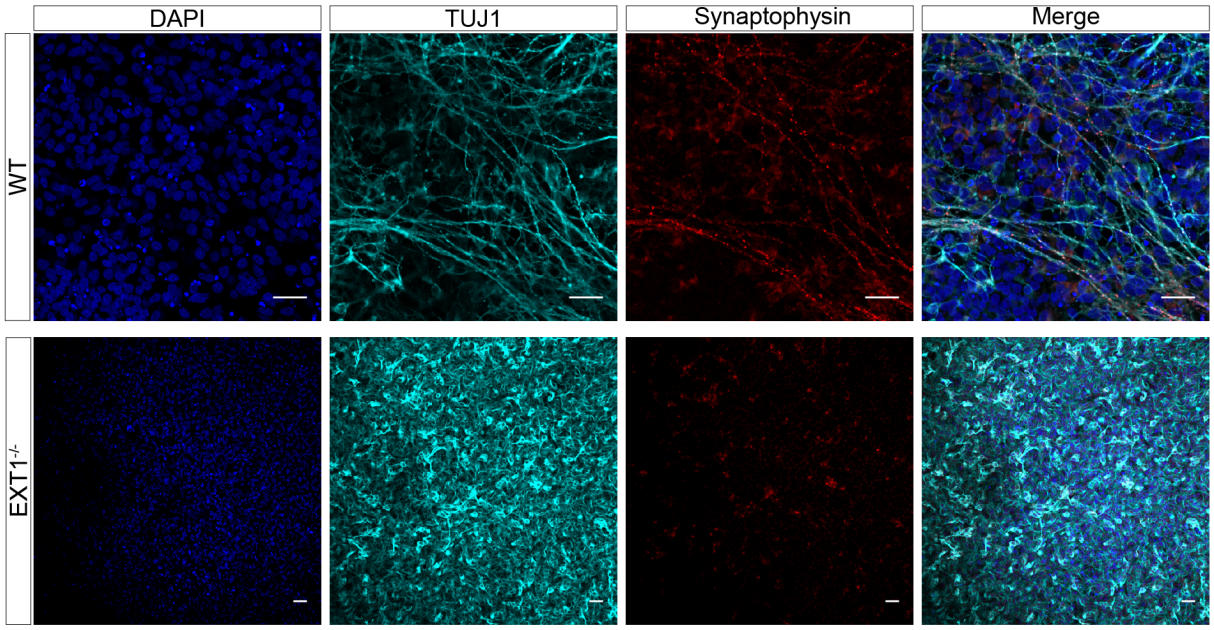

Fig 3.9. The *EXT1*$^{-/-}$ cells derivatives from no synaptic vesicle. (A) Confocal microscopy images of wild-type and *EXT1*$^{-/-}$ cells upon directed differentiation into spinal motor neuron cells and immunostained for neuron-specific β III tubulin (TUJ1) (cyan), Synaptophysin (red), Counterstained with DAPI (blue). Scale bar, 30 μm.

Though most of the neurogenesis genes are downregulated in *EXT1*$^{-/-}$ derived cells, two genes (*NEUROD1, PAX6*) (**Table:3.2**) explicitly related to the neural progenitor cell differentiation (*36*) are upregulated. This data intrigued us to investigate whether the *EXT1*$^{-/-}$ differentiated cells can go through the state of the neural progenitor (NPC). To test this, we investigated the expression of NPC marker PAX6 with immunohistochemistry (**Fig. 3.10A**) and this qualitative imaging data shows that the *EXT1*$^{-/-}$-derived neural progenitor cells have PAX6 expression. For further validation, we investigated the NCAM expression with flow cytometry in both WT and *EXT1*$^{-/-}$ (**Fig. 3.10B**) (*37*). This quantitative analysis shows that on day 6 of the differentiation, in fact, *EXT1*$^{-/-}$ derivatives express higher NCAM on the cell surface compared to WT derivatives.

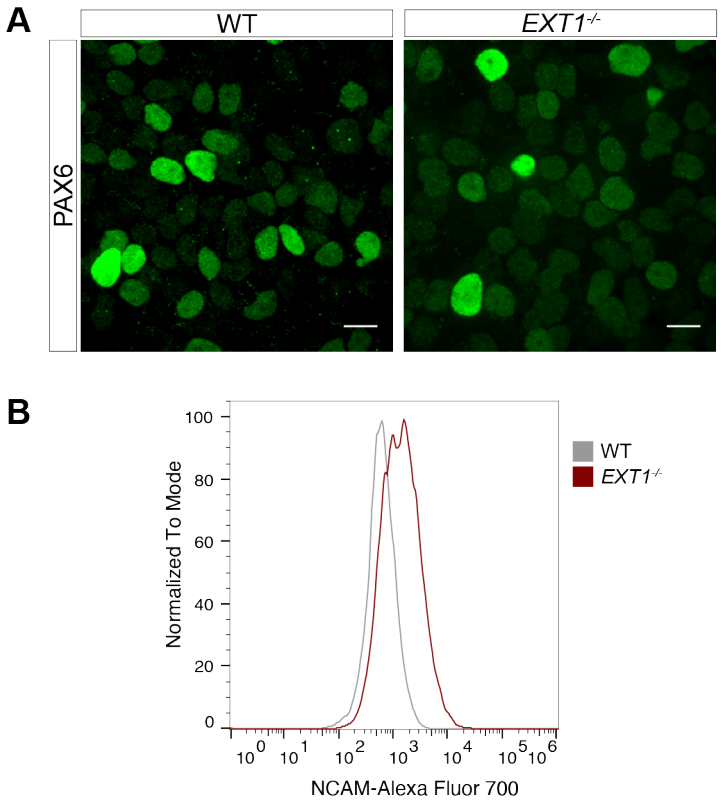

Fig 3.10. The *EXT1*$^{-/-}$ cells derivatives express neural progenitor markers. (A) Confocal microscopy images of wild-type and *EXT1*$^{-/-}$ cells after 6 days of neural differentiation and immunostained for neural progenitor cells (NPC) marker Pax6. Scale bar, 30 µm. (B) Histogram

plot of NCAM fluorescence intensity measured by flow cytometry in WT and *EXT1*$^{-/-}$ cells using the anti-NCAM antibody.

3.3.6 Key signaling pathways in *EXT1*$^{-/-}$ cells during the differentiation

Based on our data, we postulated that HS modulates the key signaling pathways mediating the fate decision between mesendoderm and ectoderm lineage. Mesendoderm differentiation is tightly regulated by the synergy between Wnt and TGFβ/Nodal signaling pathways (*38-41*). The Nodal pathway needs to be activated to direct mesendoderm differentiation. In contrast, directing the fate of hPS cells into ectodermal fate requires the inhibition of Activin/TGF-β and BMP signaling pathway, also referred as a dual-smad inhibition (*42*). Since the HS-deficient *EXT1*$^{-/-}$ cells do not undergo mesendoderm differentiation but express the early neuro-ectoderm marker PAX6, we hypothesized that these key signaling pathways (BMP TGFβ, and FGF) may be impacted during differentiation. We found that TGF-β/Nodal pathway was not robustly upregulated in *EXT1*$^{-/-}$ cells compared to the WT cells during mesendoderm differentiation (**Fig. 3.11A**). During the ectodermal differentiation the BMP and FGF signal was more downregulated in *EXT1*$^{-/-}$ cells relative to WT (**Fig. 3.11B, and 3.11C**). yet TGF- β inhibition was achieved at a similar level compared with the WT cells (**Fig. 3.11D**). These observations suggest that HS is required for both the Nodal, BMP pathways in addition to FGF pathways. Therefore, lack of HS impaired the activation of the Nodal pathway which hindered the mesendoderm differentiation. However, on the contrary, this HS-deficiency-induced downregulation of BMP and TGF-β/Nodal pathways made the *EXT1*$^{-/-}$ cells poised toward ectoderm lineage.

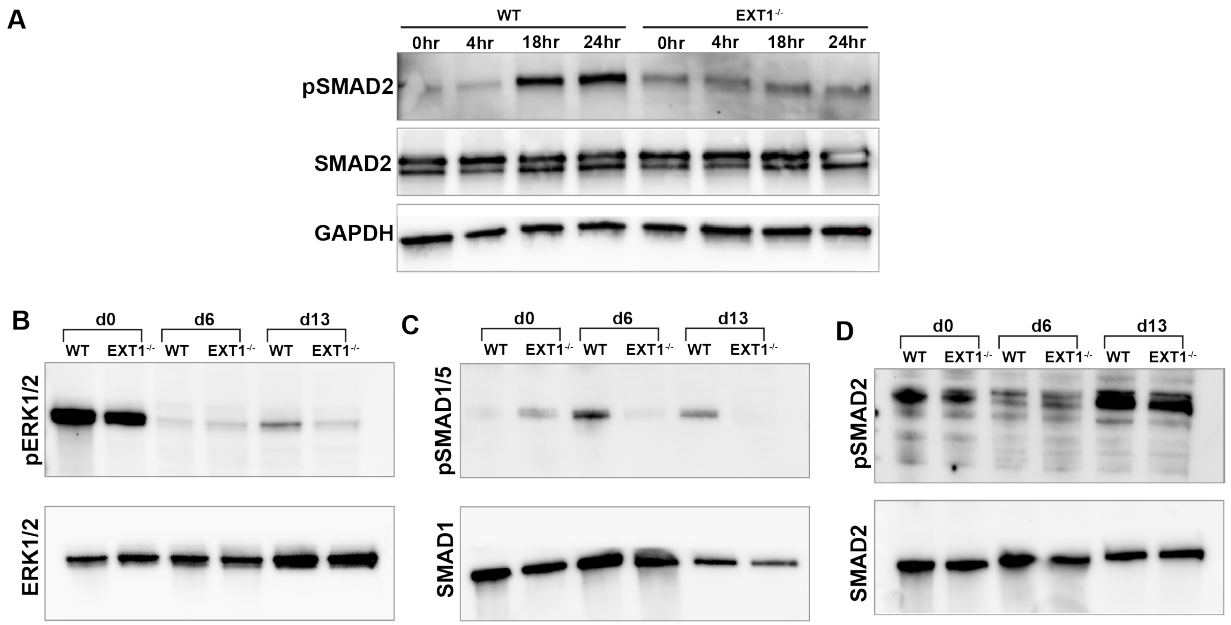

Fig 3.11. Key signaling pathways during mesendoderm and neuronal differentiation. Immunoblot analysis of TGFβ/Nodal pathway during mesendoderm differentiation (A). Wild-type and *EXT1*$^{-/-}$ cells are collected at different time point (0hr, 4hr, 18hr, 24hr) during differentiation. Immunoblot analysis of FGF pathway (B), BMP pathway (C), TGFβ/Nodal (D), pathway in response to neuronal differentiation. Wild-type and *EXT1*$^{-/-}$ cells are collected at day0 (d0), day 6 (d6) and day 13 (d13) of neuronal differentiation (B-D).

3.3.7 External heparin rescues the morphological defect in *EXT1*$^{-/-}$ cells

To confirm that the effects we observed were specifically related to HS, we tested whether the defect in neuronal differentiation could be restored by the addition of exogenous heparin in the media. Heparin is an anticoagulant and a commercial analog of heparan sulfate. From day 0 of neuronal differentiation, the differentiation media was supplemented with varying concentrations of heparin (0-10 μg/mL). We observed the morphology of the differentiated cells and assessed NCAM^{high}/EpCAM^{low} expression by flow cytometry. Rescue of the morphology along with NCAM^{high}/EpCAM^{low} expression was observed in *EXT1*$^{-/-}$ cells treated with 2.5-10 μg/mL heparin in the media, peaking at 7.5 μg/mL (~25% relative NCAM^{high}/EpCAM^{low} expression) (**Fig. 3.12**).

Taken together, these results demonstrate that heparan sulfate is required for the proper neuronal differentiation and heparin can rescue the differentiation defect observed in *EXT1*$^{-/-}$ cells.

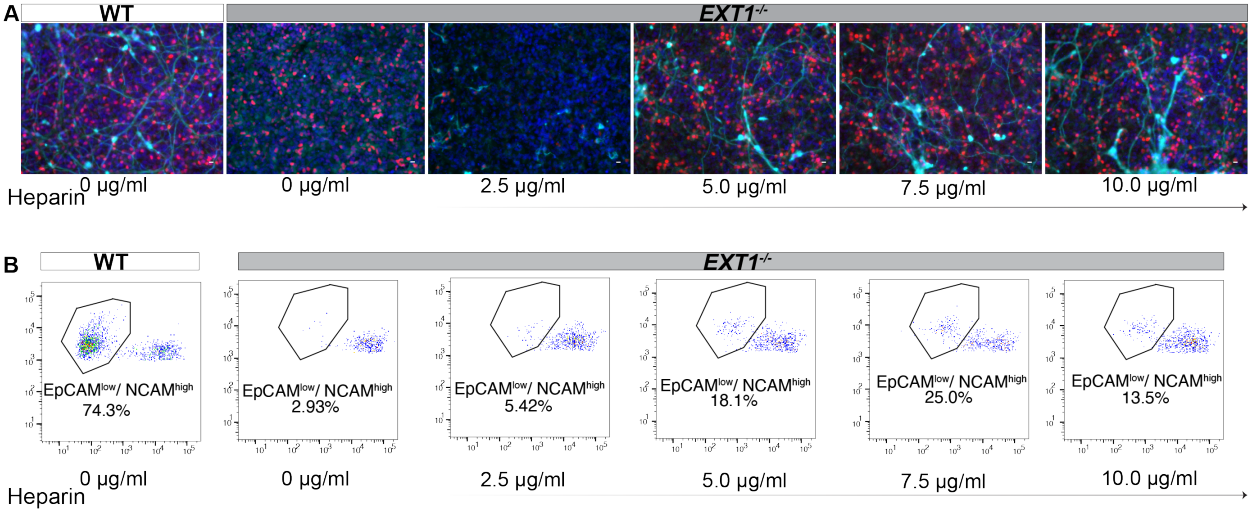

Fig 3.12 Exogenous heparin can rescue the morphological defect in *EXT1*$^{-/-}$ cell derivative. Heparin is added to the neuronal differentiation media each day of differentiation at 0, 2.5, 5.0, 7.5, or 10.0 µg/ml concentration. WT cells and *EXT1*$^{-/-}$ without any heparin stimulation (0 µg/ml) are used as the positive and negative control respectively. (A) Wild-type and *EXT1*$^{-/-}$ cells upon directed differentiation into motor neurons without or with varying amounts of heparin stimulation are immunostained for the neuronal marker, TUJ1 (cyan), ISLET1 (red) and counterstained with DAPI (blue). Scale bar, 30 µm. (B) Flow cytometry dot plot of NCAM^{high}/EpCAM^{low} cells in WT and *EXT1*$^{-/-}$ cells after 2 weeks of neuronal differentiation without or with varying amounts of heparin stimulation.

3.4 Discussion

Lack of cell surface HS is lethal for mouse embryos (*7*) . Both mES cells and drosophila serve as models which confirm that this long polysaccharide chain is essential for proper embryonic development. However, it is still unknown how HS modulates human developmental processes. We aimed to address this knowledge gap by establishing an hPS cell line that cannot biosynthesize HS to uncover the roles that HS plays in human biology. We showed that lack of HS significantly disrupts the primitive streak formation in hPS cells whereas HS is dispensable for

the early ectoderm commitment. Ultimately, we found that HS is an essential component in neural projection development and therefore for functional synapse formation. These findings uncovered, for the first time, a conserved role of HS in mammals and revealed a strikingly unique role HS plays in human neural development.

HSPG is an essential regulator of gastrulation and embryogenesis (*7*). Analysis of *Ext1*$^{-/-}$ mES cells *in vitro* showed that HS has an essential regulatory role in the exit of mES cells from pluripotency. Under the neural (*21*) (*43, 44*) or mesodermal (*22*) differentiation conditions, lack of HS hinders the mES cells from exiting the pluripotent state, retaining a high level of OCT4 expression (*19*). However, hES cells and mES cells differ significantly in their response to signaling pathways (*45*). For example, the FGF/ERK cascade promotes differentiation of mES cells and needs to be inactivated for mES cells self-renewal (*46, 47*) but in hES cells the FGF supplementation promotes self-renewal with enhanced survival, inhibiting the spontaneous differentiation (*48-52*). Therefore, it is difficult to extrapolate the findings from murine studies to exploit the role of HS in hES cell pluripotency.

We aimed to address how HS modulates the pluripotency and differentiation efficiency of human pluripotent stem cell model. We showed that HS is dispensable for the self-renewal of hPS cells in presence of high concentration of bFGF of standard stem cell maintenance conditions. Through the embryoid body assay, we showed that even in a spontaneous differentiation condition, HS-deficiency severely impairs the differentiation efficiency of hPS cells, specifically in mesendoderm lineage commitment highlighting the role of HS for primitive streak formation in hPS cells. It corroborates the findings from Kraushaar *et.al.* showing that *Ext1*$^{-/-}$ mES cells failed to upregulate the mesendoderm marker Brachyury during differentiation due to disrupted FGF and

BMP signaling (*23*). Thus, our findings highlight the conserved role of HS across the mammalian lines.

The HS-deficient hPS cell-derived EB showed that HS is not required for ectoderm differentiation of hPS cells. Moreover, the directed differentiation to non-neural ectoderm lineage derivative, neural crest showed that without any HS, the hPS cells are still able to differentiate into multipotent neural crest cells. These data indicate that HS is dispensable for the early ectoderm commitment in hPS cells. This observation significantly differs from the findings in mES cells study. Kraushaar *et al*. reported that HS is required for ectoderm commitment of *Ext1*$^{-/-}$ mES cell-derived EBs (*19*) and differentiation into neural progenitor cells in adherent culture (*23*). With HS deficient hPS cells, we further showed that although the early ectoderm commitment is not impaired in the absence of HS, during the directed differentiation towards the terminally differentiated motor neurons HS is required for proper neuronal projection formation. We discovered that, without HS, the hPS cells cannot form long extended axons or dendrites which also leads to no synaptic vesicle formation. Finally, we showed that the addition of exogenous heparin to the differentiation media can rescue the defective phenotype during the neuroectodermal differentiation in *EXT1*$^{-/-}$ cells. This further validates that our observation is a result of a lack of HS.

These findings corroborate the observations from genetic experiments in fly, worm, mouse (*53*), and zebrafish showing that HSPGs indeed have crucial roles *in vivo* axon guidance. Inatani *et al*. showed that loss of EXT1 can cause axon guidance errors in the major axon tracts in conditional knockout mice. Succeeding studies revealed that HS controls axon guidance through the binding and regulation of different axon guidance cues. In absence of HS in hPS cells the crucial axonogenesis genes expressions are downregulated, including major axon guidance ligand-

receptor expression, such as Slits and Robos. Slit-Robo signaling pathway for proper axon growth requires HS as a coactivator (*34, 35, 54*). These findings highlight the specific role of HS in the axonogenesis process in human neural development where the early ectodermal commitment of hPS cells does not require HS. This observation further indicates the role of HS as s synaptic organizer in human brain development. In 2018, Zhang *et al.* identified HS as a part of central synaptic organizers, neurexin using conditional knockout mice (*29*). They showed HS modulates the synaptic development by connecting with the other synaptic molecule, neuroligin and LRRTM (*29, 55*). Therefore, the role of HS as a synaptic modulator in human brain development needs to be evaluated. Further exploration of HS at the molecular level can shed light on HS roles in modulating human neural connections, specifically to answer questions such as how does HS help to regulate synapse plasticity in the human brain or how does HS function in the context of neurological diseases, such as, amyotrophic lateral sclerosis (ALS), Alzheimer's disease (AD).

To understand how HS is modulating the signaling pathways during these differentiation defects, we investigated the key signaling pathways (FGF, BMP, TGFβ/Nodal) during the mesendoderm and ectoderm differentiation. We found that the Nodal signal was not robustly upregulated in *EXT1*$^{-/-}$ cells during the mesendoderm differentiation. During the ectoderm specific differentiation, the FGF, BMP and Nodal signal were also downregulated in *EXT1*$^{-/-}$ cells, either at a comparable or higher level relative to WT cells. For the mesendoderm differentiation, a tightly regulated synergy between Wnt and Nodal signal is required where upregulation of Nodal signal direct toward mesendoderm differentiation (*56, 57*). Therefore, the *EXT1*$^{-/-}$ hPS cells are unable to differentiate into mesendoderm cells due to the absence of an adequate Nodal signal. In retrospect, the downregulation of BMP and TGFβ/Nodal signal induces the differentiation into the neurectoderm and neural crest cells, both derived from the ectoderm. Therefore, in absence of HS

and in dual smad inhibition condition, *EXT1*$^{-/-}$ cells shows reduced smad signals which are sufficient to promote the cells towards the early ectodermal lineage.

HS is a ubiquitous cell surface signaling polysaccharide that can modulate a number of developmental signaling routes. Prior to this work, the lack of a relevant tool to study the role of HS in human development hindered our understanding of how HS modulates the human stem cell fate choices as well as the human neuronal development. Therefore, we developed HS-deficient hPS cells as a tool to explore HS's role in regulating lineage commitment. We identified that HS affects the cellular differentiation of hPS cells in all three different germ layers. Specifically, in neural lineage differentiation, HS is essential for proper axonal development leading to effective synaptic connections. These findings also set the stage for future studies investigating the role of HS in patients-derived induced pluripotent stem cells (iPSCs) and brain organoids to explore the role of HS in neurodegeneration and neurological disease progressions. Therefore, by leveraging the advancement made in this study, we will pave the way for a better understanding of HS's role and its molecular and cellular contribution in early human development, leading to pinpointing the role of glycans in the human nervous system and associated neurological diseases.

3.5 Conclusion and future directions

To the best of our knowledge, this is the first report of a novel heparan sulfate deficient-cell line derived from human pluripotent stem cells. Our findings suggest that HS is essential for the late stages of neuronal development including proper axon formation. We showed that lack of HS causes downregulation of the Slit-Robo signaling molecule, similarly it would be interesting to investigate its effect on other critical signals, such as Netrin-DCC and Eph-ephrin signaling which are critical for proper axonal guidance. Identifying how HS modulates these signaling pathways would be useful to identify the specific role of HS in the axonogenesis

process. Similarly, our findings indicate a possible role of HS in the Nodal signaling pathway in hPS cells which is crucial for mesendoderm lineage-specific differentiation. This warrants further biochemical investigation to understand how HS is modulating nodal signaling, specifically, the interaction between HS and Nodal ligands and receptors.

Our data suggest that HS has a critical role in synapse formation in human brain development which is corroborated by previous findings that in the vertebrate brain excitatory synapse HS bridges the presynaptic and postsynaptic molecules (*58*). However, it is still unclear how HS modulates the synapse organization. HS may regulate the signal strength of synapse organizing molecules. Since HS has structural variation, it may allow HS to regulate the affinity strength between synapse organizing proteins. This may introduce diversity in the strength of signaling between pre-and post-synaptic regions which in turn can lead to differentiation of specific and diverse synapses. Moreover, the structural heterogeneity and flexibility of HS make it a better regulatory molecule to modulate multiple synapse organizing molecules at a time which indicates a possible role of HS as a functional hub that determines the synaptic specificity. Further investigation in this direction would be very useful to understand how HS acts as a synapse organizer in human brain.

To understand the differentiation defect that we observed in HS-deficient hPS cells, further examinations of the specific underlying molecular mechanisms will be necessary. To this end, I propose to do single-cell transcriptomics using next-generation transcript sequencing analysis on the *EXT1* $^{-/-}$ derivatives. This will be particularly informative since the dual-smad differentiation gives rise to a heterogeneous population, therefore, this single-cell RNA-seq will allow us to profile the cell-to-cell variability at the genomic scale. Examining the global transcriptome of ISLET1+ cells will help us to identify the variation in their molecular

components causing the defect that we are observing. Moving further, I propose to develop brain organoids with this *EXT1*$^{-/-}$ hPS cell. Though *in vitro* neurodevelopmental models mimic the organogenesis processes, they also present higher homogeneity but much lower complexity compared to human brain development. Therefore, brain organoids are valuable alternatives that provide more advanced cell composition, maturation, and tissue architecture (*59*). This will help us to understand the contribution of HS in the complex scheme of neuronal development through a monogenic approach.

Our findings also indicate the association of HS with diseases. A future goal of this project would be to understand human diseases based on our findings. Mutation in heparan sulfate biosynthetic genes, EXT1 or EXT2 cause a genetic condition called hereditary multiple exostoses (HME) that affects the regular bone growth. Defects in bone development and nervous system dysfunctions are the prominent features of HME patients. We also showed that lack of HS in hPS cells abolishes the mesendoderm differentiation and late stage of neuronal development which corroborates to these. I propose to develop the HME patient-derived iPSC cell line to investigate the direct connection between HS and these disease phenotypes. The ultimate goal here would be to understand the role of HS in complex neurological and genetic diseases to find a better stem cell-based regenerative medicine.

3.6 Methods and Materials

3.6.1 Cell culture

H9 (WiCell) and *EXT1*$^{-/-}$ human pluripotent stem (hPS) cells were grown with E8 medium (Thermo Fisher Scientific) on tissue culture plates coated with Vitronectin (Thermo Fisher Scientific). Cells were maintained at 37 °C in 5% CO_2 incubator. Cells were passaged manually using EDTA (1 mM in PBS, pH 7.4) every 4-5 days, with the addition of 5μM ROCK inhibitor

(Y-27632 dihydrochloride, Tocris) on the first day to prevent the cell death after dissociation. The cells were routinely tested for mycoplasma contamination (LookOut® Mycoplasma PCR Detection Kit, Sigma Aldrich).

3.6.2 Generation of *EXT1*$^{-/-}$ cells using CRISPR

Cas9 Nuclease 3NLS (Integrated DNA Technologies) was complexed with 2.4 μM gRNA (AGCCGGAGAGAAGAACACAG) in nucleofection buffer. H9 cells were nucleofected with the ribonucleoprotein complex using the Amaxa Nucleofector II (Lonza) as per manufacturer instructions. Cells were allowed to recover for one day in mTeSR1 medium supplemented with 1X RevitaCell (Gibco) and another day in mTeSR1 medium supplemented with 5 μM Y-27632. Clones were derived by serial dilution and analyzed by PCR amplification and Sanger sequencing for mutations in both alleles.

3.6.3 Differentiation of hPS cells into different lineage specific derivatives

The cells were differentiated to mesendoderm using established protocol (*60*). Briefly, the cells were dissociated with EDTA and plated at a density of 100,000 cells per cm^2 on vitronectin-coated plates with E8 media supplemented with 5 μM ROCK inhibitor. The E8 media was changed every day for the next 2 days. On day 3, the media was changed to RPMI-1640 medium (Thermo Fisher Scientific) supplemented with 6 μM CHIR-99021 (Tocris). Following a 24 h treatment with the differentiation media, the cells were collected for analysis.

Neural crest differentiation was achieved using a chemically defined protocol as described previously (*31*). In brief, hPS cells were dissociated to single cells using accutase (Thermo Fisher Scientific) and plated at a density of 10,000 cells per cm^2 on vitronectin-coated plates with E8 media supplemented with 5 μM ROCK inhibitor. The cells were grown for 24 h and then the

medium was changed into the differentiation media every day for the next 5 days. The differentiation media was prepared by supplementing DMEM-F12 (Life Technologies) with 1x N-2 supplement (Gibco), 1.0 μM CHIR99021 (Tocris), 2.0 μM SB431542 (Tocris), 1.0 μM DMH1 (Tocris), and 15 ng/ml BMP4 (Tocris).

Motor neuron differentiation was achieved using a modified 14-days protocol described previously (*33*). In brief, hPS cells were dissociated to single cells using accutase and plated at a density of 40,000 cells per cm^2 on vitronectin-coated culture plates with E8 media supplemented with 5 μM ROCK inhibitor. As the cells reached >95% confluency, the medium was changed to d0-d5 differentiation media every day for the next 5 days. The d0-d5 differentiation media was prepared by supplementing the basal medium with 10 μM SB431542 (Tocris), 100 nM dorsomorphin (Tocris), 1 μM retinoic acid (Sigma) and 1 μM Smoothend agonist (Tocris). On the day 6 of differentiation, the medium was changed to d6-d14 differentiation media every day. The d6-d14 medium was prepared by supplementing the basal medium with 5 μM DAPT (Tocris), 4 μM SU-5402 (Tocris), 1 μM retinoic acid (Sigma) and 1 μM Smoothend agonist (Tocris). The basal medium contained 1:1 mixture of Neurobasal media (Life Technologies) and DMEM-F12 (Life Technologies) and was supplemented with 1x B-27 supplement (Gibco), 1x N-2 supplement (Gibco), and 1x Gibco GlutaMAX (Life Technologies).

3.6.4 Immunofluorescence staining and imaging

For immunocytochemistry analysis, cells were stained live or stained after fixation. For live staining, the cells were rinsed with DMEM/F12 or basal media, followed by incubation in a blocking buffer (2% BSA in DMEM/F12) for 30 min in ice. The cells were further incubated with primary antibody at appropriate dilution in a blocking buffer for 1 h at 4 °C. Then, the cells were

exposed to the secondary antibody for 1 h at 4 °C. The stained cells were rinsed twice with cold buffer and fixed with 4% formaldehyde for 10-15 min at room temperature.

For the staining of internal markers, the fixed samples were permeabilized and blocked with PBS containing 0.1% Triton X-100 and 2% BSA. All primary antibodies were incubated in a blocking buffer overnight at 4 °C or 1 h at room temperature. The primary antibodies and dilutions used are described in Table S1. The secondary antibody staining was performed with Alexa Fluor 488, 594, 647 or Atto 647N conjugated anti-mouse, rabbit, chicken, or goat IgG antibodies (Invitrogen) which were diluted at 1:1000 in the blocking buffer and exposed to cells for 1 h at room temperature. For the samples for expansion, the secondary antibodies were used at 1:200 dilution. The cell nuclei were counterstained with DAPI dilactate (1:10000, Molecular Probes). Images were collected with the Nikon A1R Ultra-Fast Spectral Scanning Confocal Microscope. Images were analyzed using Fiji.

3.6.5 Flow cytometry

H9 hPS cells and the differentiated cells derived from hPS cells were analyzed by flow cytometry according to Holley *et al.* (*22*) with slight modifications. Briefly, cells were dissociated using warm accutase and resuspended in cold DMEM/F12 supplemented with 5 μM ROCK inhibitor. Cells were washed twice with cold PBS followed by incubation with 500 μL Ghost Dye™ Violet 450 cell stain (1:1000, Tonbo Biosciences) on ice for 30 min. Cells were then rinsed with cold buffer (PBS, pH 7.4 supplemented with 0.1% BSA). Cells were further incubated with anti-HS 10E4 at 1:200 dilution for 1 h, at 4 °C followed by fixation with 1% formaldehyde in cold PBS. Data were collected using the Attune NxT Flow Cytometer (Thermo Fisher Scientific) and analyzed using FlowJo software. The percentage of positive cells was established by comparing wildtype cells to HS knockout cells.

3.6.6 Immunoblotting

Cells were lysed in RIPA Buffer (Pierce) supplemented with 1x Halt Protease Inhibitor Cocktail (Thermo Fisher Scientific) and 1x Halt Phosphatase Inhibitor Cocktail (Thermo Fisher Scientific). Genomic DNA is removed from the Cell lysates by repeatedly running through a 27 gauge needle followed by spinning down at 14,000g for 15 min at 4 C. Cell lysate were then resolved by SDS-PAGE and transferred onto a PVDF membrane using a Trans-Blot® Turbo™ Transfer System (Bio-Rad). The membranes were blocked in 5% non-fat milk for 1 h at rt, then exposed to the primary antibody diluted in PBS containing 5% bovine serum albumin (US Biological) and 0.1% Tween-20 (Sigma) overnight at 4 C. The primary antibodies and dilutions used are described in Table S2. The PVDF membranes were then exposed to the secondary antibody, HRP-conjugated anti-rabbit IgG diluted at 1:10000 (Jackson ImmunoResearch) for 1 h at rt. ECL Prime (Amersham) was used for chemiluminescent detection, which was recorded using Chemi Doc imaging system (Bio Rad).

3.6.7 RNA preparation and qRT-PCR

Total RNA was extracted from undifferentiated hPS and d13 motor neurons using TRIzol (Life Technologies) and Direct-zol™ RNA MiniPrep kit (Zymo Research) as per manufacturer instructions. RNA (1 μg) from each sample was reverse transcribed to cDNA using iScript cDNA Synthesis Kit (Bio-Rad). The qPCR was performed on the CFX Connect (Bio-Rad) using iTaq Universal SYBR Green Supermix (Bio-Rad) and gene-specific primers. GAPDH was used as a reference gene for normalization. The primer sequences used are described in Table S2. The relative gene expression levels were determined using the ddCt method, and the error bars were determined from the standard deviation of at least three biological replicates.

3.6.8 Gene expression analysis by qPCR array

Human neurogensis RT^2 Profiler PCR Arrays (Qiagen) were performed using an iTaq Universal SYBR Green Supermix (Bio-Rad) on the CFX Connect (Bio-Rad) according to manufacturer protocol. Data were analyzed with the PCR array analysis web portal. The results represent the threshold cycle (Ct) for each gene normalized to the arithmetic mean of the Ct values ($2^{-\Delta Ct}$) of housekeeping genes. Black lines on scatter plots represent a 1.5-fold change between control and experimental conditions. Genes with Ct values that are greater than 35 under both experimental conditions were considered undetected and omitted.

Table 3.3. qPCR primer sequences

Gene Symbol	Forward Primer (5′-3′)	Reverse Primer (5′-3′)
SLIT1	GATGGCTTGAGGACCCTAAT	GGTGATCTGGTTGTCGTAGAG
SLIT2	CAACACCGAGAGACTGGATTTA	GATCCTGGAATGCTCCTCTTT
SLIT3	CCTTCACCCAGTACAAGAAACT	GACCAGCGATGTGAGTGATT
ROBO1	GAGTCTATGTCTGTGTAGCAAGG	CTGAAGTCATCCCGAAGTATGG
ROBO2	TTGACAGATAGACCTCCACCTA	GATCACCAGTGGCTTTACATTTC
ROBO3	ATTACAACGAAGCGGGAATCT	GCTGGGTCAATGGTGCTAT
ROBO4	TGGTTGGCAGACACTTGG	AAGGAGCGACGACAGTCTA
TUBB3	GTGCGGAAGGAGTGTGAAA	CATGATGCGGTCGGGATAC

Table 3.4. Primary antibodies

Antigen	Species	Source	Dilution
Heparan sulfate	Mouse	US Biological (H1890)	IHH 1:200, FC 1:200
Basic FGF	Mouse	LifeSpan Biosciences LS-C114423	FC 1:100
pERK1/2	Rabbit	Cell Signaling Technologies	IB 1:2000
ERK	Rabbit	Cell Signaling Technologies	IB 1:1000
SMAD2	Rabbit	Cell Signaling Technologies	IB 1:1000
pSMAD2	Rabbit	Cell Signaling Technologies	IB 1:1000
SMAD1	Rabbit	Cell Signaling Technologies	IB 1:1000
pSMAD1/5	Rabbit	Cell Signaling Technologies	IB 1:1000
GAPDH	Rabbit	Cell Signaling Technologies	IB 1:20,000
Nestin	Mouse	R&D Systems (1259)	IHH 1:3000
Tuj-1	Mouse	BioLegend (801201)	IHH 1:1000
SOX17	Goat	R&D Systems (1924)	IHH 1:250
AFP	Mouse	R&D Systems (MAB1368)	IHH 1:100
SMA	Mouse	Sigma (A2547)	IHH 1:400
Brachyury	Goat	R&D Systems (2085)	IHH 1:250
P75	Mouse	BD Biosciences (562562)	FC 1:100
HNK-1	Mouse	BD Biosciences (347393)	FC 1:100
NCAM	Mouse	BD Biosciences (561902)	FC 1:100
EpCAM	Mouse	BD Biosciences (565398)	FC 1:50
SOX10	Mouse	Santa Cruz Biotechnology (SC-374170)	IHH 1:100
ISLET1	Rabbit	Abcam (ab109517)	IHH 1:250
MAP2	Chicken	Abcam (ab5392)	IHH 1:200
Synaptophysin	Rabbit	Abcam (ab32127)	
PAX6	Sheep	R&D Systems (2085)	IHH 1:250

3.7 Acknowledgments

I would like to thank Dr. Sayaka Masuko for developing the HS-deficient hPS cells. I would like to thank my colleague Deepsing Syangtan for following up the role of HS in mesendoderm lineage commitment.

3.8 References

1. C. R. Blanchette, A. Thackeray, P. N. Perrat, S. Hekimi, C. Y. Benard, Functional Requirements for Heparan Sulfate Biosynthesis in Morphogenesis and Nervous System Development in C. elegans. *PLoS Genet* **13**, e1006525 (2017).
2. J. R. Bishop, M. Schuksz, J. D. Esko, Heparan sulphate proteoglycans fine-tune mammalian physiology. *Nature* **446**, 1030-1037 (2007).
3. U. Hacker, K. Nybakken, N. Perrimon, Heparan sulphate proteoglycans: the sweet side of development. *Nat Rev Mol Cell Biol* **6**, 530-541 (2005).
4. X. Lin, Functions of heparan sulfate proteoglycans in cell signaling during development. *Development* **131**, 6009-6021 (2004).
5. N. Perrimon, M. Bernfield, Specificities of heparan sulphate proteoglycans in developmental processes. *Nature* **404**, 725-728 (2000).
6. K. Lidholt, J. L. Weinke, C. S. Kiser, F. N. Lugemwa, K. J. Bame, S. Cheifetz, J. Massague, U. Lindahl, J. D. Esko, A single mutation affects both N-acetylglucosaminyltransferase and glucuronosyltransferase activities in a Chinese hamster ovary cell mutant defective in heparan sulfate biosynthesis. *Proc Natl Acad Sci U S A* **89**, 2267-2271 (1992).
7. X. Lin, G. Wei, Z. Shi, L. Dryer, J. D. Esko, D. E. Wells, M. M. Matzuk, Disruption of gastrulation and heparan sulfate biosynthesis in EXT1-deficient mice. *Dev Biol* **224**, 299-311 (2000).
8. J. B. Hurlbut, I. Hyun, A. D. Levine, R. Lovell-Badge, J. E. Lunshof, K. R. W. Matthews, P. Mills, A. Murdoch, M. F. Pera, C. T. Scott, J. Tizzard, M. Warnock, M. Zernicka-Goetz, Q. Zhou, L. Zoloth, Erratum: Revisiting the Warnock rule. *Nat Biotechnol* **35**, 1211 (2017).
9. A. T. Hertig, J. Rock, E. C. Adams, A description of 34 human ova within the first 17 days of development. *Am J Anat* **98**, 435-493 (1956).
10. K. Takahashi, K. Tanabe, M. Ohnuki, M. Narita, T. Ichisaka, K. Tomoda, S. Yamanaka, Induction of pluripotent stem cells from adult human fibroblasts by defined factors. *Cell* **131**, 861-872 (2007).
11. J. A. Thomson, J. Itskovitz-Eldor, S. S. Shapiro, M. A. Waknitz, J. J. Swiergiel, V. S. Marshall, J. M. Jones, Embryonic stem cell lines derived from human blastocysts. *Science* **282**, 1145-1147 (1998).
12. K. A. Moore, I. R. Lemischka, Stem cells and their niches. *Science* **311**, 1880-1885 (2006).
13. P. X. Wan, B. W. Wang, Z. C. Wang, Importance of the stem cell microenvironment for ophthalmological cell-based therapy. *World J Stem Cells* **7**, 448-460 (2015).
14. H. E. Bulow, O. Hobert, The molecular diversity of glycosaminoglycans shapes animal development. *Annu Rev Cell Dev Biol* **22**, 375-407 (2006).
15. J. D. Esko, S. B. Selleck, Order out of chaos: assembly of ligand binding sites in heparan sulfate. *Annu Rev Biochem* **71**, 435-471 (2002).
16. A. Feta, A. T. Do, F. Rentzsch, U. Technau, M. Kusche-Gullberg, Molecular analysis of heparan sulfate biosynthetic enzyme machinery and characterization of heparan sulfate structure in Nematostella vectensis. *Biochem J* **419**, 585-593 (2009).
17. G. F. Medeiros, A. Mendes, R. A. Castro, E. C. Bau, H. B. Nader, C. P. Dietrich, Distribution of sulfated glycosaminoglycans in the animal kingdom: widespread

occurrence of heparin-like compounds in invertebrates. *Biochim Biophys Acta* **1475**, 287-294 (2000).
18. J. Kreuger, L. Kjellen, Heparan sulfate biosynthesis: regulation and variability. *J Histochem Cytochem* **60**, 898-907 (2012).
19. D. C. Kraushaar, Y. Yamaguchi, L. Wang, Heparan sulfate is required for embryonic stem cells to exit from self-renewal. *J Biol Chem* **285**, 5907-5916 (2010).
20. N. Sasaki, K. Okishio, K. Ui-Tei, K. Saigo, A. Kinoshita-Toyoda, H. Toyoda, T. Nishimura, Y. Suda, M. Hayasaka, K. Hanaoka, S. Hitoshi, K. Ikenaka, S. Nishihara, Heparan sulfate regulates self-renewal and pluripotency of embryonic stem cells. *J Biol Chem* **283**, 3594-3606 (2008).
21. C. E. Johnson, B. E. Crawford, M. Stavridis, G. Ten Dam, A. L. Wat, G. Rushton, C. M. Ward, V. Wilson, T. H. van Kuppevelt, J. D. Esko, A. Smith, J. T. Gallagher, C. L. Merry, Essential alterations of heparan sulfate during the differentiation of embryonic stem cells to Sox1-enhanced green fluorescent protein-expressing neural progenitor cells. *Stem Cells* **25**, 1913-1923 (2007).
22. R. J. Holley, C. E. Pickford, G. Rushton, G. Lacaud, J. T. Gallagher, V. Kouskoff, C. L. Merry, Influencing hematopoietic differentiation of mouse embryonic stem cells using soluble heparin and heparan sulfate saccharides. *J Biol Chem* **286**, 6241-6252 (2011).
23. D. C. Kraushaar, S. Rai, E. Condac, A. Nairn, S. Zhang, Y. Yamaguchi, K. Moremen, S. Dalton, L. Wang, Heparan sulfate facilitates FGF and BMP signaling to drive mesoderm differentiation of mouse embryonic stem cells. *J Biol Chem* **287**, 22691-22700 (2012).
24. F. Lanner, J. Rossant, The role of FGF/Erk signaling in pluripotent cells. *Development* **137**, 3351-3360 (2010).
25. Y. Yamaguchi, Heparan sulfate proteoglycans in the nervous system: their diverse roles in neurogenesis, axon guidance, and synaptogenesis. *Semin Cell Dev Biol* **12**, 99-106 (2001).
26. F. Irie, H. Badie-Mahdavi, Y. Yamaguchi, Autism-like socio-communicative deficits and stereotypies in mice lacking heparan sulfate. *Proc Natl Acad Sci U S A* **109**, 5052-5056 (2012).
27. H. Li, T. Yamagata, M. Mori, M. Y. Momoi, Association of autism in two patients with hereditary multiple exostoses caused by novel deletion mutations of EXT1. *J Hum Genet* **47**, 262-265 (2002).
28. A. Fico, A. de Chevigny, C. Melon, M. Bohic, L. Kerkerian-Le Goff, F. Maina, R. Dono, H. Cremer, Reducing glypican-4 in ES cells improves recovery in a rat model of Parkinson's disease by increasing the production of dopaminergic neurons and decreasing teratoma formation. *J Neurosci* **34**, 8318-8323 (2014).
29. P. Zhang, H. Lu, R. T. Peixoto, M. K. Pines, Y. Ge, S. Oku, T. J. Siddiqui, Y. Xie, W. Wu, S. Archer-Hartmann, K. Yoshida, K. F. Tanaka, A. R. Aricescu, P. Azadi, M. D. Gordon, B. L. Sabatini, R. O. L. Wong, A. M. Craig, Heparan Sulfate Organizes Neuronal Synapses through Neurexin Partnerships. *Cell* **174**, 1450-1464 e1423 (2018).
30. R. Jaenisch, R. Young, Stem cells, the molecular circuitry of pluripotency and nuclear reprogramming. *Cell* **132**, 567-582 (2008).
31. J. O. S. Hackland, T. J. R. Frith, P. W. Andrews, Fully Defined and Xeno-Free Induction of hPSCs into Neural Crest Using Top-Down Inhibition of BMP Signaling. *Methods Mol Biol* **1976**, 49-54 (2019).

32. A. Achilleos, P. A. Trainor, Neural crest stem cells: discovery, properties and potential for therapy. *Cell Res* **22**, 288-304 (2012).
33. J. R. Klim, L. A. Williams, F. Limone, I. Guerra San Juan, B. N. Davis-Dusenbery, D. A. Mordes, A. Burberry, M. J. Steinbaugh, K. K. Gamage, R. Kirchner, R. Moccia, S. H. Cassel, K. Chen, B. J. Wainger, C. J. Woolf, K. Eggan, ALS-implicated protein TDP-43 sustains levels of STMN2, a mediator of motor neuron growth and repair. *Nat Neurosci* **22**, 167-179 (2019).
34. M. A. Manavalan, V. R. Jayasinghe, R. Grewal, K. M. Bhat, The glycosylation pathway is required for the secretion of Slit and for the maintenance of the Slit receptor Robo on axons. *Sci Signal* **10**, (2017).
35. H. Hu, Cell-surface heparan sulfate is involved in the repulsive guidance activities of Slit2 protein. *Nat Neurosci* **4**, 695-701 (2001).
36. W. Y. Choi, J. H. Hwang, A. N. Cho, A. J. Lee, I. Jung, S. W. Cho, L. K. Kim, Y. J. Kim, NEUROD1 Intrinsically Initiates Differentiation of Induced Pluripotent Stem Cells into Neural Progenitor Cells. *Mol Cells* **43**, 1011-1022 (2020).
37. M. Sundberg, P. H. Andersson, E. Akesson, J. Odeberg, L. Holmberg, J. Inzunza, S. Falci, J. Ohman, R. Suuronen, H. Skottman, K. Lehtimaki, O. Hovatta, S. Narkilahti, E. Sundstrom, Markers of pluripotency and differentiation in human neural precursor cells derived from embryonic stem cells and CNS tissue. *Cell Transplant* **20**, 177-191 (2011).
38. Q. Wang, Y. Zou, S. Nowotschin, S. Y. Kim, Q. V. Li, C. L. Soh, J. Su, C. Zhang, W. Shu, Q. Xi, D. Huangfu, A. K. Hadjantonakis, J. Massague, The p53 Family Coordinates Wnt and Nodal Inputs in Mesendodermal Differentiation of Embryonic Stem Cells. *Cell Stem Cell* **20**, 70-86 (2017).
39. K. Matulka, H. H. Lin, H. Hribkova, D. Uwanogho, P. Dvorak, Y. M. Sun, PTP1B is an effector of activin signaling and regulates neural specification of embryonic stem cells. *Cell Stem Cell* **13**, 706-719 (2013).
40. N. S. Funa, K. A. Schachter, M. Lerdrup, J. Ekberg, K. Hess, N. Dietrich, C. Honore, K. Hansen, H. Semb, beta-Catenin Regulates Primitive Streak Induction through Collaborative Interactions with SMAD2/SMAD3 and OCT4. *Cell Stem Cell* **16**, 639-652 (2015).
41. Z. Chng, A. Teo, R. A. Pedersen, L. Vallier, SIP1 mediates cell-fate decisions between neuroectoderm and mesendoderm in human pluripotent stem cells. *Cell Stem Cell* **6**, 59-70 (2010).
42. S. M. Chambers, C. A. Fasano, E. P. Papapetrou, M. Tomishima, M. Sadelain, L. Studer, Highly efficient neural conversion of human ES and iPS cells by dual inhibition of SMAD signaling. *Nat Biotechnol* **27**, 275-280 (2009).
43. C. E. Pickford, R. J. Holley, G. Rushton, M. P. Stavridis, C. M. Ward, C. L. Merry, Specific glycosaminoglycans modulate neural specification of mouse embryonic stem cells. *Stem Cells* **29**, 629-640 (2011).
44. K. A. Meade, K. J. White, C. E. Pickford, R. J. Holley, A. Marson, D. Tillotson, T. H. van Kuppevelt, J. D. Whittle, A. J. Day, C. L. Merry, Immobilization of heparan sulfate on electrospun meshes to support embryonic stem cell culture and differentiation. *J Biol Chem* **288**, 5530-5538 (2013).
45. B. Greber, G. Wu, C. Bernemann, J. Y. Joo, D. W. Han, K. Ko, N. Tapia, D. Sabour, J. Sterneckert, P. Tesar, H. R. Scholer, Conserved and divergent roles of FGF signaling in

mouse epiblast stem cells and human embryonic stem cells. *Cell Stem Cell* **6**, 215-226 (2010).
46. G. Guo, J. Yang, J. Nichols, J. S. Hall, I. Eyres, W. Mansfield, A. Smith, Klf4 reverts developmentally programmed restriction of ground state pluripotency. *Development* **136**, 1063-1069 (2009).
47. Q. L. Ying, J. Wray, J. Nichols, L. Batlle-Morera, B. Doble, J. Woodgett, P. Cohen, A. Smith, The ground state of embryonic stem cell self-renewal. *Nature* **453**, 519-523 (2008).
48. S. Yao, S. Chen, J. Clark, E. Hao, G. M. Beattie, A. Hayek, S. Ding, Long-term self-renewal and directed differentiation of human embryonic stem cells in chemically defined conditions. *Proc Natl Acad Sci U S A* **103**, 6907-6912 (2006).
49. C. Xu, E. Rosler, J. Jiang, J. S. Lebkowski, J. D. Gold, C. O'Sullivan, K. Delavan-Boorsma, M. Mok, A. Bronstein, M. K. Carpenter, Basic fibroblast growth factor supports undifferentiated human embryonic stem cell growth without conditioned medium. *Stem Cells* **23**, 315-323 (2005).
50. M. E. Levenstein, T. E. Ludwig, R. H. Xu, R. A. Llanas, K. VanDenHeuvel-Kramer, D. Manning, J. A. Thomson, Basic fibroblast growth factor support of human embryonic stem cell self-renewal. *Stem Cells* **24**, 568-574 (2006).
51. M. K. Furue, J. Na, J. P. Jackson, T. Okamoto, M. Jones, D. Baker, R. Hata, H. D. Moore, J. D. Sato, P. W. Andrews, Heparin promotes the growth of human embryonic stem cells in a defined serum-free medium. *Proc Natl Acad Sci U S A* **105**, 13409-13414 (2008).
52. P. Dvorak, D. Dvorakova, S. Koskova, M. Vodinska, M. Najvirtova, D. Krekac, A. Hampl, Expression and potential role of fibroblast growth factor 2 and its receptors in human embryonic stem cells. *Stem Cells* **23**, 1200-1211 (2005).
53. M. Inatani, F. Irie, A. S. Plump, M. Tessier-Lavigne, Y. Yamaguchi, Mammalian brain morphogenesis and midline axon guidance require heparan sulfate. *Science* **302**, 1044-1046 (2003).
54. C. Perez, D. Sawmiller, J. Tan, The role of heparan sulfate deficiency in autistic phenotype: potential involvement of Slit/Robo/srGAPs-mediated dendritic spine formation. *Neural Dev* **11**, 11 (2016).
55. T. J. Siddiqui, P. K. Tari, S. A. Connor, P. Zhang, F. A. Dobie, K. She, H. Kawabe, Y. T. Wang, N. Brose, A. M. Craig, An LRRTM4-HSPG complex mediates excitatory synapse development on dentate gyrus granule cells. *Neuron* **79**, 680-695 (2013).
56. P. Gadue, T. L. Huber, P. J. Paddison, G. M. Keller, Wnt and TGF-beta signaling are required for the induction of an in vitro model of primitive streak formation using embryonic stem cells. *Proc Natl Acad Sci U S A* **103**, 16806-16811 (2006).
57. S. J. Kattman, A. D. Witty, M. Gagliardi, N. C. Dubois, M. Niapour, A. Hotta, J. Ellis, G. Keller, Stage-specific optimization of activin/nodal and BMP signaling promotes cardiac differentiation of mouse and human pluripotent stem cell lines. *Cell Stem Cell* **8**, 228-240 (2011).
58. K. Kamimura, N. Maeda, Glypicans and Heparan Sulfate in Synaptic Development, Neural Plasticity, and Neurological Disorders. *Front Neural Circuits* **15**, 595596 (2021).
59. I. Chiaradia, M. A. Lancaster, Brain organoids for the study of human neurobiology at the interface of in vitro and in vivo. *Nat Neurosci* **23**, 1496-1508 (2020).

60. X. Lian, X. Bao, M. Zilberter, M. Westman, A. Fisahn, C. Hsiao, L. B. Hazeltine, K. K. Dunn, T. J. Kamp, S. P. Palecek, Chemically defined, albumin-free human cardiomyocyte generation. *Nat Methods* **12**, 595-596 (2015).

Chapter 4

Ligand-specific synthetic surfaces for label-free enrichment of cell subpopulations

4.1 Abstract

Cell enrichment and separation techniques are fundamental components of biological research yet these processes remain complicated and expensive. To address this technological gap, we present a synthetic, surface-based cell separation strategy that can isolate or enrich cells of interest in a simple and cost-effective way. Biocompatible materials can be tailored to present high affinity, selective small molecules to engage specific cell surface markers. We aimed to develop a small molecule-presenting, synthetic surface to isolate a subset of cells from a mixture. We hypothesized that we could achieve enrichment of a cell population without any exogenous labeling, at a much faster rate and with a very low cell loss. As a proof of this concept, we applied this strategy to isolate genetically engineered human pluripotent stem cells by engaging the cell surface polysaccharide, heparan sulfate. We next developed a synthetic surface presenting $\alpha_v\beta_3$ integrin-specific ligand. This display would be able to isolate the activated monocytes and T-cells from the whole blood PBMCs. This synthetic surface-mediated cell separation strategy is modular in nature and can be adapted to various systems by changing the small molecule structure. These initial studies can serve as a platform, and future studies can accomplish it further by expanding the library of small molecules to target specific cell surface markers. Overall, this strategy provides access to tailored surfaces that can provide a simple, efficient, and cost-effective way to enrich a subset of cells from a heterogeneous population.

4.2 Introduction

Cell separation technologies are fundamental in biomedical science by facilitating the isolation of cellular subpopulations for basic science or clinical application. From the first report of separating the red and white blood cells (*1*), cell separation/ enrichment techniques are now an integral component in bioresearch to isolate diseased tissue, identify the presence of specific cells during pathological conditions, or develop cell-based regenerative therapies (*2*). With such high impact applications, several strategies have evolved over the last several decades (*3*). Fluorescent-activated cell sorting (FACS) and magnetic-activated cell sorting (MACS) both use external labeling to identify target populations. FACS uses a fluorescent label to detect the cell type and can sort up to 50,000 cells per second (*4*). MACS, on the other hand, uses the magnetic microbeads conjugated antibodies which can extract the cell of interest using a magnetic field (*5*) and generally have a higher throughput. These cell sorting methods offer a high-speed cell separation, although this higher rate is often achieved at the cost of loss of cells and purity. They require an increased number of cells, as cell loss can exceed even half the population (*6*). In either case, adding these additional labels to the cells may limit the usefulness of these techniques, particularly for the downstream experiments in cases where the labels persist. Moreover, these also make cell preparation time-consuming and cumbersome. The other popular option is the density gradient method, a label-free separation technique that exploits differences in density between populations (*7*). However, it is also expensive and has very limited applicability (*7*).

To address this technological gap, we set out to develop a simple and cost-effective method to isolate a pure population using a modular synthetic surface. Synthetic small molecules have been found to engage specific cell surface molecules, including integrin, growth factor receptor or even cell surface polysaccharides (*8, 9*). We envisioned combining modern surface fabrication

methods with a highly selective ligand to probe ligand-presenting surfaces for an efficient and cost-effective way to capture a subset of cells from a heterogeneous population.

As a proof of concept, we applied this strategy to two different systems. First, we aimed to isolate genetically engineered human pluripotent stem cells based on the distinct expression of cell surface carbohydrates using a ligand-specific surface. Starting from basic research to clinical regenerative therapy, efficient cell separation methods are essential. However, the delicate nature of pluripotent stem cells and the stem cell-derived differentiated cells causes a significant cell loss with FACS or MACS due to long sample preparation and processing time. Moreover, it has been shown that MACS or FACS are unable to meet the required level of purification for cell therapy purposes (*10*). Our aim is to address this using a surface-based enrichment strategy, which would rely on the expressed cell surface molecules without any exogenous antibody/small molecule/fluorophore labeling. Moreover, we specifically targeted a cell surface glycan to isolate the cell of interest. Carbohydrates are the most prominent and outermost feature of the cells where they can serve as a cellular "identification card" (*11*). There are numerous pieces of evidence that confirmed that glycans remodel based on circumstances, such as alteration during the migratory phase of carcinoma cells (*12, 13*), modification of *N*-glycan, *O*-glycan during cellular senescence (*14*), even changes in glycan profile during active infection and inflammation (*15*). Therefore, using a modular, surface-presenting a glycan-specific ligand could be a critical tool to identify unique changes in cell surface glycans under developmental or pathological conditions.

The need for cell sorting is not limited to stem cells and thus we wanted to test the broad applicability of our approach. Towards this, we set out to purify the specific immune cells from the heterogeneous population. Currently, immune cell separation heavily relies on FACS (*16*). We hypothesized that we could target a cell surface integrin to capture desired cell types. The Integrin

family of receptors is expressed in virtually every cell in the human body except erythrocytes (*17*). This heterodimeric transmembrane protein is composed of one α and one β subunit (*18*). There are 18 α and 8 β subunits in humans that can form 24 unique compositions on the cell surface (*17*). Therefore, synthetic surfaces that can selectively engage specific integrin molecules could be useful to engage specific cell types from the mixed population.

Currently available cell sorting methods can multiplex the cell separation based on multiple cellular markers. Although the small molecule-ligand-specific surface we presented here is highly modular, it is yet to be adapted to multiplexing. This surface could be improved as a patterned surface presenting different ligands to engage different cell subtypes from the same cell mixture. This would allow separating different cell types from a heterogeneous population in a rapid, traceless, and inexpensive way. Moreover, the surface presenting highly selective small molecules could also be used to modulate the specific signal transduction downstream of a specific cell surface molecule, such as integrin, glycosaminoglycan, specific growth factors etc. This could further yield insights complementary to the findings obtained from traditional genetic experiments.

4.3 Results

4.3.1 Enrichment of genetically modified human pluripotent stem cells

Heparan sulfate deficient cells were engineered by CRISPR-mediated targeting of the HS biosynthetic gene *EXT1*. The CRISPR protocol yielded a mixed cell population containing the heparan sulfate-containing (WT) and -deficient ($EXT1^{-/-}$) cells. A modular surface was used to isolate the HS-deficient cells. Previously it was shown that a synthetic surface presenting heparin-binding peptide (GKKQRFRHRNRKG, FHRRIKA, and GWQPPARARI) can consistently mediate the hPS cell adhesion and allowed for hPS cell propagation in the undifferentiated state (*9*). Out of these three heparin-binding peptides, GKKQRFRHRNRKG which is derived from

vitronectin was shown to support the adhesion and propagation of the hPS cells at the lowest peptide substitution level. We reasoned that presenting this vitronectin heparin-binding domain (VHBD) as a surface to hPS cells would engage the cell surface heparan sulfate. Thus, HS-deficient hPS cells would not be able to bind to the surface and remain floating in the cell suspension allowing for separation (**Fig. 4.1**).

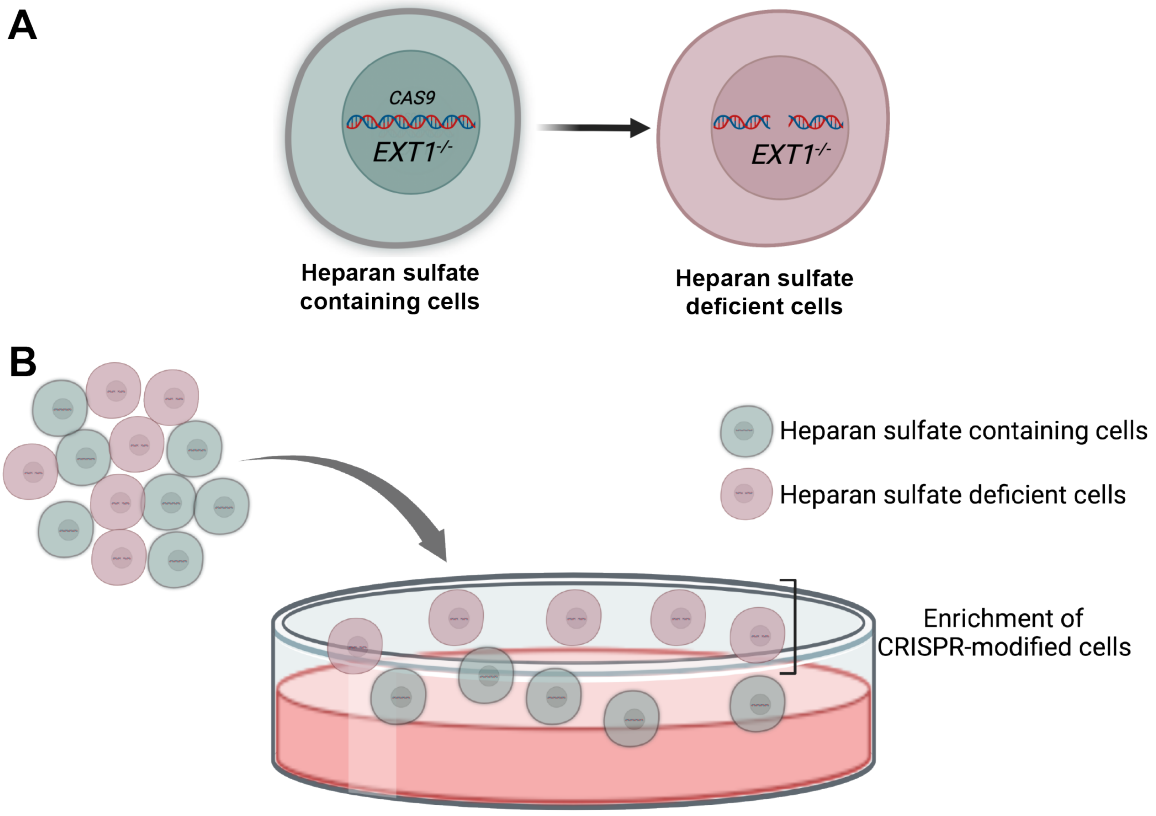

Fig. 4.1: Schematic plan to enrich the CRISPR-modified cells using a modular surface. A) Targeting the *EXT1* gene using CRISPR. B) Purification of cells that are engineered and lack the cell surface heparan sulfate.

The mixture of WT and *EXT1*$^{-/-}$ cells was presented to the VHBD peptide-presenting surface where the biotinylated peptide has adhered to the plastic surface of the culture plate through streptavidin. Cells were allowed to bind to the surface for 30 min incubation. After 30 min incubation, the media suspension was collected as the fraction of HS-deficient (*EXT1*$^{-/-}$) cells. This

enrichment was repeated for 3 more rounds and the collected cells were tested for the presence of HS-containing cells.

To assess the utility of this method, we tested the efficiency of this enrichment strategy. We tested the presence of glycosylated syndecan 4 (Sdc4) in the pre-and post-enrichment fractions by Western blot. Syndecan 4 is one of the core proteins of heparan sulfate glycoprotein (HSPG). We showed that after the enrichment there is significantly less glycosylated Sdc4 protein (**Fig. 4.2A**). This suggests that after the enrichment, the isolated cell fraction does not have cell surface heparan sulfate.

To confirm this further, we measured the HS expression of the pre-and post- enrichment cell fractions using flow cytometry. We showed that only after one round of enrichment, the isolated cell fraction contains 63.2% of HS deficient cells (**Fig. 4.2B)**. Moreover, after three rounds of enrichment using the modular cell culture surface, the isolated cell fraction increased to 76.7% (**Fig. 4.2C)**. We further confirmed with microscopy that the isolated cell fraction does not express any HS (**Fig. 4.3A)** on the cell surface but retains the pluripotency markers (**Fig. 4.3B)** Finally, we observed a normal karyotype, confirming the genomic integrity of the enriched cells (**Fig. 4.3C)**.

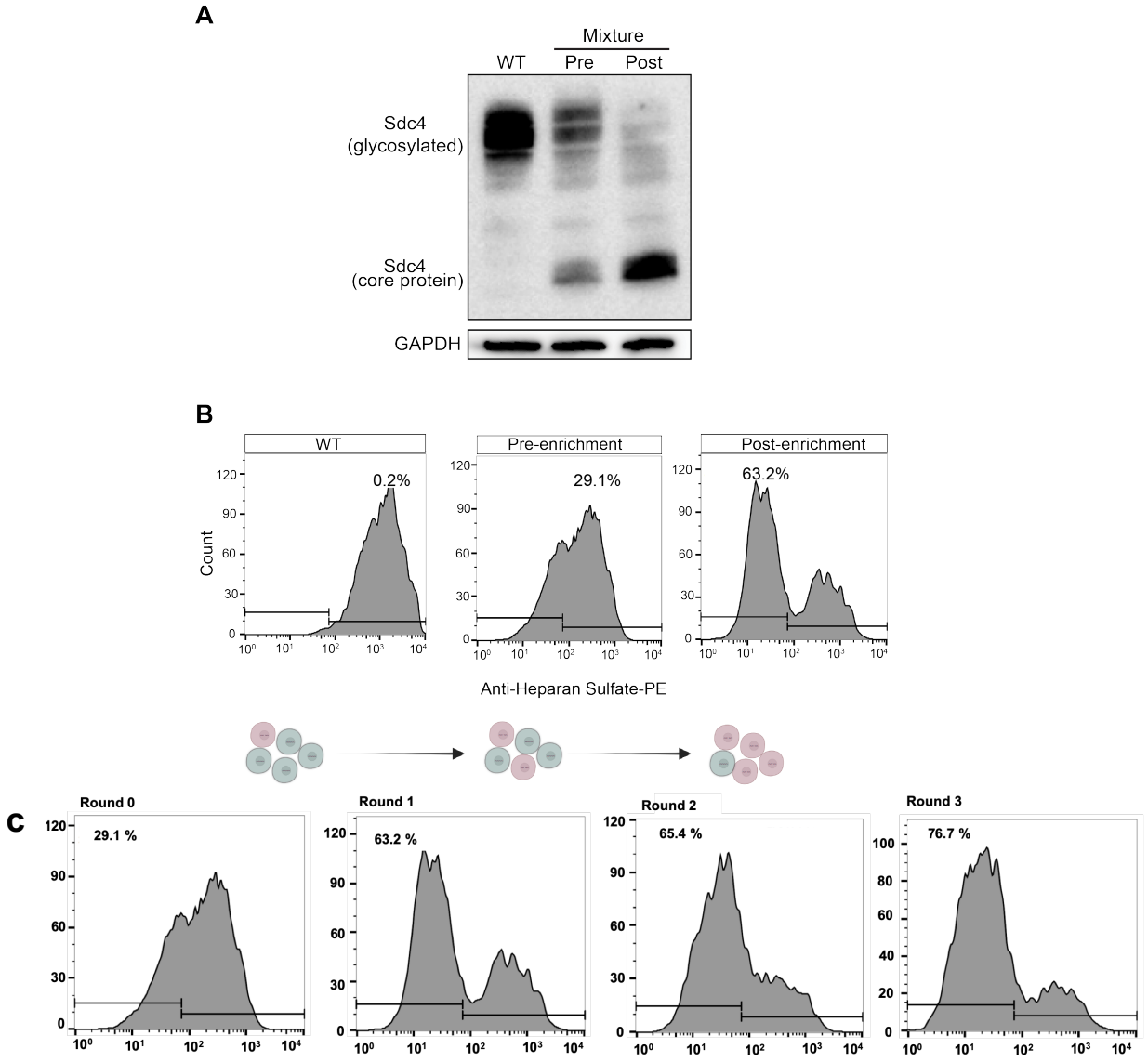

Fig. 4.2: Assessing the enrichment efficiency. A) The enrichment efficiency was measured by detecting the syndecan-4 (Sdc4) in wildtype (WT), pre-enrichment (Pre), and Post-enrichment (Post). The post enrichment mixture of cells significantly less Sdc4 expression. B) Heparan sulfate expression is detected in the pre-and post-enriched population. C) After 3 rounds of enrichment the mixture of cells are mostly composed of HS-deficient cells.

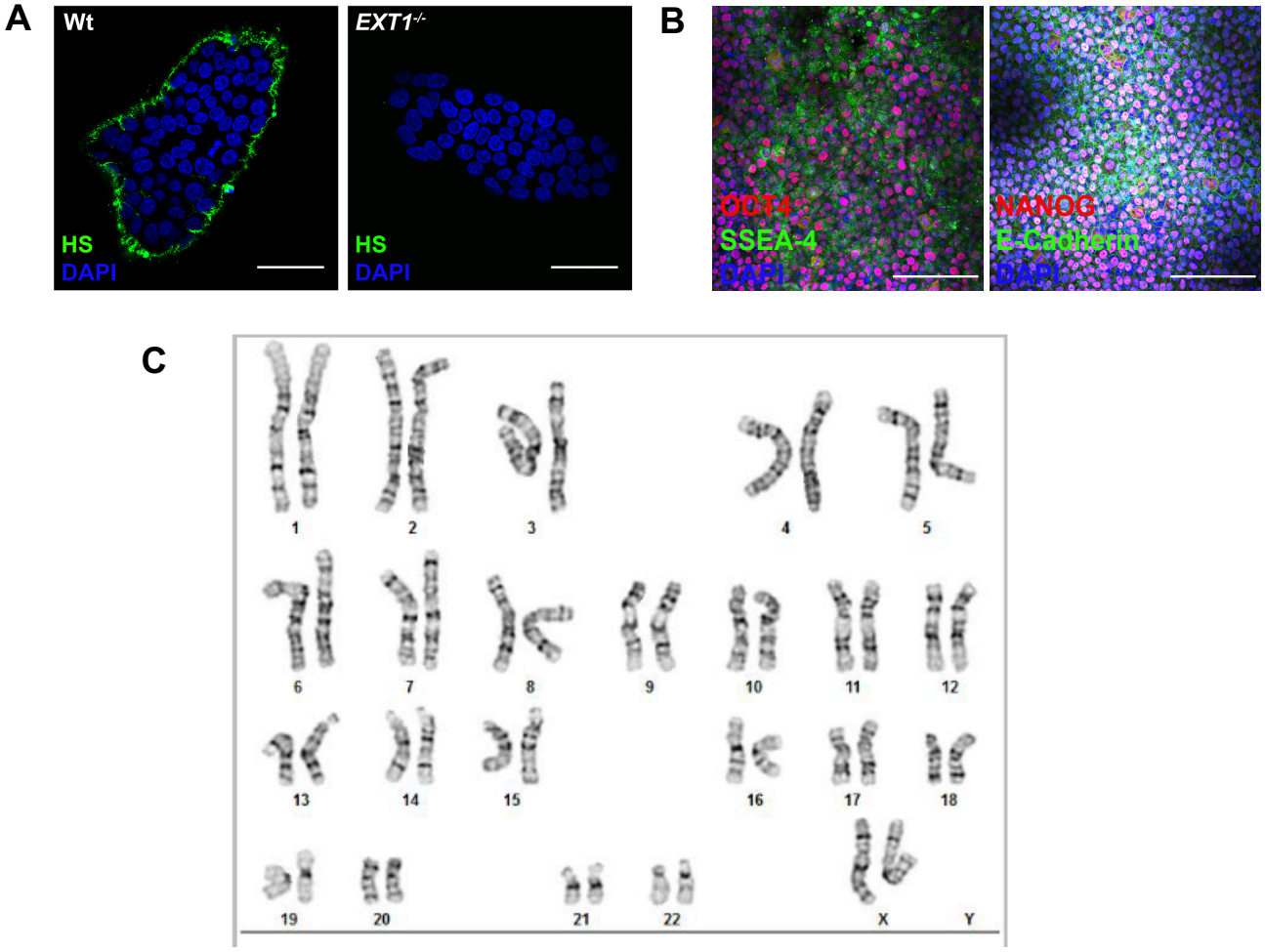

Fig 4.3: The enriched cell population were HS-deficient human pluripotent stem cells. A) Confocal microscopy images of wildtype (H9) and *EXT1*$^{-/-}$ cells immunostained for heparan sulfate (green) and counterstained with DAPI (blue). Scale bar, 50 µm. B) Confocal microscopy images of *EXT1*$^{-/-}$ cells immunostained for pluripotency markers Oct-4, SSEA-4, Nanog, and E-cadherin, and counterstained with DAPI (blue). Scale bar, 200 µm. C) G-banded karyotyping of *EXT1*$^{-/-}$ cells cultured in standard hPS cell culture conditions indicate a normal karyotype.

4.3.2 Strategy to separate the primary immune cells using the modular surface

Next, we sought to apply this strategy to isolate specific immune cells from the mixture of whole blood-derived peripheral blood mononuclear cell (PBMC). PBMC contains a mixture of many specialized immune cells. While activated, these specialized cells expressed specific surface markers. We reasoned that developing a modular surface that presents a specific ligand to bind to

a specific cell surface marker on these immune cells would allow us to do a rapid, traceless purification of immune cells.

Previously it has been shown that human monocytes can be activated in presence of hematopoietic growth factor- granulocyte-macrophage colony-stimulating factor (GM-CSF) and human T-cells can be activated in presence of phytohemagglutinin (PHA) and phorbol-12-myristate-13-acetate (PMA) (*19*). These activated blood cells express specific integrin $\alpha_v\beta_3$ on the cell surface. We envisioned that a biotinylated version of the $\alpha_v\beta_3$ antagonist could be presented on a surface to engage these specific activated blood cells and would allow isolating this subpopulation from the mixture **(Fig 4.4)**.

We first separated the PBMC from whole human blood using density-gradient centrifugation. The separated PBMCs were stimulated with GM-CSF or PHA+PMA for 48 hours. After stimulation, we tested the expression of $\alpha_v\beta_3$ integrin in the PBMC by flow cytometry. We showed that both of the stimulations significantly induced the expression of $\alpha_v\beta_3$ integrin in monocytes (**Fig. 4.5B**) and T-cells (**Fig. 4.5A**), respectively. Once we had confirmed the expression of specific integrin $\alpha_v\beta_3$, we aimed to isolate these subpopulations using our modular surface strategy. A bifunctional compound was developed previously (*8*) where a synthetic integrin antagonist targeting $\alpha_v\beta_3$ integrin was appended on a biotin moiety through an oligo (ethylene glycol) ((EG)4) linker (**Fig. 4.5C**) (*8*). This biotinylated $\alpha_v\beta_3$ antagonist can be presented on the polystyrene plates coated with streptavidin. This work is currently in progress. We anticipate that this modular surface would readily engage the $\alpha_v\beta_3$ integrin of the activated immune cells from the mixture and thus would allow isolating the subpopulation of the immune cells in a rapid and label-free way.

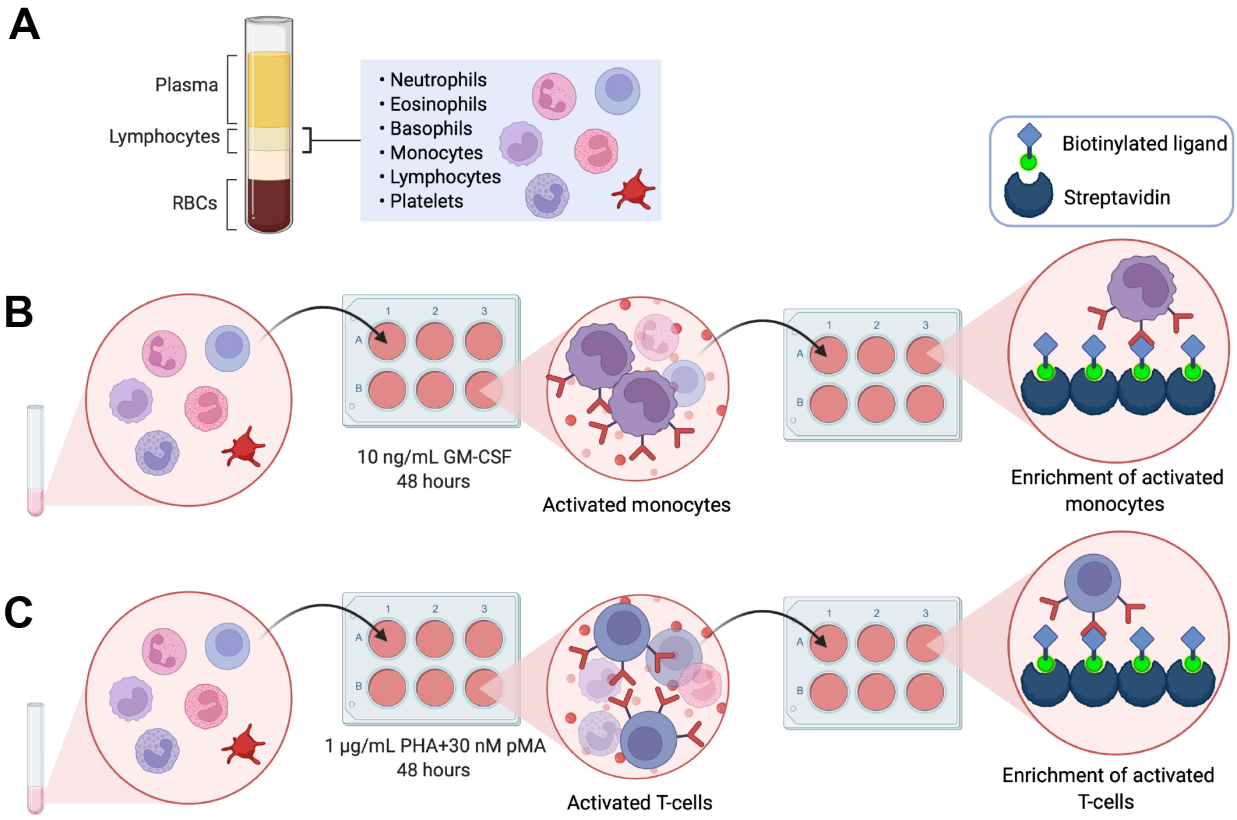

Fig. 4.4: Schematic plan to enrich the activated immune cells using a modular surface. A) Separation of PBMC from the whole human blood. B) Purification of the activated monocytes using modular surface presenting biotinylated ligand to bind specific ligand on the cell surface. C) Purification of the activated T-cells using modular surface presenting biotinylated ligand to bind specific ligand on the cell surface.

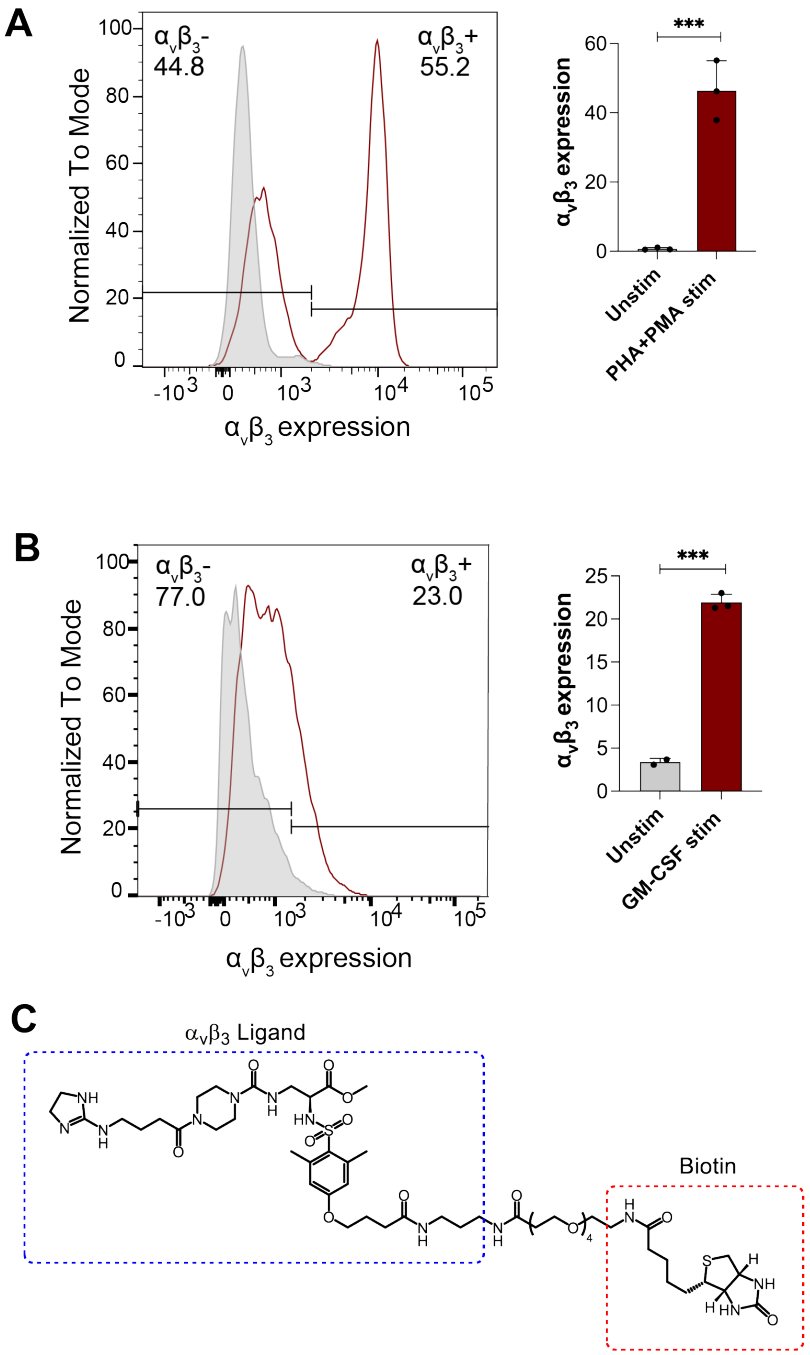

Fig. 4.5: Expression of αVβ3 ligand on the surface of activated monocytes and T-cells. The activated T-cells upon PHA and PMA stimulation (A), and the activated monocytes upon GM-CSF stimulation (B) express αVβ3 integrin on the surface. (C) Chemical structure of the bifunctional compound that binds specifically to the $\alpha_V\beta_3$ integrin. A biotin moiety with an oligo (ethylene glycol) ((EG)4) linker is appended to the amine 1 of the compound, specific for the $\alpha_V\beta_3$ integrin. Unpaired t-test between unstim and stimulated cells were used for data analysis. An asterisk denotes a statistically significant difference (*****p<0.000000xx, **p<0.05) between unstim and stimulated cells.

4.4 Discussion and future direction

Cell isolation or enrichment is a fundamental process in biomedical science, yet this process currently remains labor-intensive and expensive. Where rapid collection of pure live cells at the output is the final arbiter of the quality of the separation/enrichment method, existing separation methods, such as FACS, and MACS, sometimes fall short. Even these powerful tools require extensive and expensive labeling and the cells separation is biased by the effectiveness of labeling. Here we presented a strategy to separate/enrich a live-cell subpopulation in a rapid, label-free way. Unlike conventional methods for cell sorting, (*20*) our strategy relies only on the presence of endogenous cell-surface markers. This method advances usability, efficiency, purity, cell losses, and cost of the existing techniques. Developing this strategy into a benchtop practice would significantly contribute to biomedical research.

Biocompatible materials have diverse utilities in cell-cell/matrix interactions, cellular signaling, etc. A critical advantage of using synthetic material is that it can be tailored to a specific application. Herein, we reveal that the synthetic modular surface can be tailored and used to separate cellular subpopulations from a cell mixture. We showed that our small-peptide-modified surface can engage specific glycosaminoglycan, heparan sulfate on the cell surface and thus separate the HS-containing and HS-deficient cells. This label-free, fast method was specifically helpful since these isolated HS-deficient live cells can be further cultured and propagated as a human pluripotent stem cell line. We confirmed that after the separation, the cells are healthy, maintained genetic integrity, and maintained their pluripotency. This highlights the effectiveness of this method to separate the genetically engineered cell line after the modification. No labeling was required to identify the cells of interest, making it convenient for the downstream handling and further experiments, which is a caveat with other existing tools (e.g., FACS, MACS).

Isolating and controlling the differentiation of human pluripotent stem cells is still a challenging task in the field of stem cell biology. To separate the differentiated cells from their pluripotent counterpart or to enrich a specific type of cell upon differentiation; complex purification protocols, such as fluorescence or magnetic-activated cell sorting are used. Such separations are critical because if any 'contamination' of undifferentiated cells is remaining, it may cause teratoma formation (*10, 21*) in the culture. Using a modular surface that can engage specific cell-surface protein thus provides an alternative, rapid, and convenient method for isolating differentiating cells from their undifferentiated counterpart. This is specifically important for stem cell biology since, differentiated cells such as neuronal cells, organoids are needed to be handled very delicately. Moreover, expanding this modular surface to present a combination of small molecules, engaging specific adhesion molecules or growth factor receptors also has the potential to guide the subsequent differentiation of specific cell types after sequestering. Thus, this can be a powerful tool to modulate the functionality of cells.

We aimed to extend this strategy to other cell separation problems. Rapid, label-free purification of immune cells remains a challenge and heavily relies on flow cytometry-based cell sorting, which can be cumbersome and time-consuming. We identified a specific cell surface marker, $\alpha_v\beta_3$ integrin, expressed on surfaces of activated immune cells (monocytes and T-cells). We developed a small-molecule-based platform that can engage these $\alpha_v\beta_3$ positive cells and thus be able to separate them from a mixed population. Our preliminary results show a great potential of this strategy; however, it warrants further characterization and optimization to establish this technique for isolating immune cells from the mixture. This work is currently in progress.

While we showed $\alpha_v\beta_3$ integrin expression on specific immune cells, inflammatory Th17 cells also express $\alpha_v\beta_3$ integrin for pathogenic functions(*22*), moreover activated glioma (*23*),

melanoma cells (*24*) express $\alpha_v\beta_3$ integrin which correlates to the migratory property of the cancerous cells. In these cases, our small-molecule-based surface could also be used as a strategy to identify the presence of specific cells in tumors or cells collected from the site of infection. Therefore, the tailored surface could be used as a diagnostic tool even to detect the state of infection or cancer progression. There are multiple small molecule binders selective for integrins other than $\alpha_v\beta_3$ have been reported, specifically–targeting RGD recognizing integrins ($\alpha_{IIb}\beta_3$, $\alpha_v\beta_5$, $\alpha_5\beta_1$, $\alpha_v\beta_6$) (*25-27*). Therefore, this general, modular strategy can be readily adapted to isolate, enrich and identify specific sets of cells from a mixed population.

The modular strategy outlined here can be readily used to isolate specific cells from a mixture. It can be further expanded to unravel diseases state, developmental or inflammation progression. However, to accomplish these strategies, our ability to target cell surface markers with synthetic molecules needs to be further expanded. We anticipate that this selective ligand binding tailored surface has significant promise as a new standard benchtop laboratory technique that could augment or perhaps even replace existing purification protocols.

4.5 Method and Materials

4.5.1 Cell lines and cell culture

H9 (WiCell) and *EXT1*$^{-/-}$ human embryonic stem cells were maintained in E8™ medium (Stem Cell Technologies) on VTN-XF™ (Stem Cell Technologies)-coated non-tissue culture plates. Cells were maintained at 37 °C in 5% CO_2. Cells were passaged manually using EDTA (1 mM) every 4-5 days, with the addition of 5 μM Y-27632 dihydrochloride (Tocris) during the first day.

Human blood samples were purchased from a commercial vendor, RBC (Research Blood Components, Watertown, MA).

4.5.2 Immunostaining, immunoblotting, and flow cytometry assay

Immunofluorescence, immunoblotting, and flow cytometry assays were performed as described in previous chapters. The primary antibodies used are listed in Table 4.1.

4.5.3 Karyotyping

G-banded karyotyping is performed through Themo fischer scientific.

4.5.4 PBMC isolation and stimulation

Peripheral blood mononuclear cells from whole blood freshly drawn from healthy human volunteers were isolated via centrifugation using RosetteSep and Lymphoprep reagents (StemCell Technologies).

For cell activation studies PBMCs are stimulated with either 10 ng/ml human GM-CSF (R&D Systems) in RPMI media or a combination of 1 μg/ml PHA and 30 nm PMA for 48 hours. Control (unstimulated) cells were maintained in RPMI for equivalent times.

4.5.5 Synthesis of $\alpha_v\beta_3$ integrin-specific bifunctional molecule

$\alpha_v\beta_3$ integrin-specific bifunctional molecule was synthesized following the protocol published elsewhere (*8, 28*).

Table 4.1 Primary antibodies

Antigen	Species	Source	Dilution
Heparan sulfate	Mouse	US Biological (H1890)	IHH 1:200, FC 1:200
Syndecan-4	Rabbit	Abcam (ab74139)	IB 1:1000
GAPDH	Rabbit	Cell Signaling Technologies	IB 1:20,000
OCT4	Goat	R&D Systems (AF1759)	IHH 1:150
SSEA-4	Mouse	R&D Systems (MAB1435)	IHH 1:50
NANOG	Goat	R&D Systems (AF1997)	IHH 1:150
E-Cadherin	Mouse	R&D Systems (MAB1838)	IHH 1:100

4.6 Acknowledgments

I would like to thank my colleague Dr. Sayaka Masuko for engineering the *EXT1*$^{-/-}$ heparan sulfate deficient cell line and helping with the follow up work. I would like to thank Dr. Austin Kruger for synthesizing the $\alpha_v\beta_3$ integrin-specific bifunctional molecule. I would like to thank Dr. Mohammad Murshid Alam for helping me with whole blood sample handling. Thank you Victoria Marando for editing this chapter in such a short notice! All the schematic figures are created with BioRender.com

Research reported in the presentation was supported by the National Institute of General Medical Sciences of the National Institute of Health under award numbers F32GM111014 and R01049975.

4.7 References

1. D. English, B. R. Andersen, Single-step separation of red blood cells. Granulocytes and mononuclear leukocytes on discontinuous density gradients of Ficoll-Hypaque. *J Immunol Methods* **5**, 249-252 (1974).
2. M. J. Tomlinson, S. Tomlinson, X. B. Yang, J. Kirkham, Cell separation: Terminology and practical considerations. *Journal of tissue engineering* **4**, 2041731412472690 (2013).
3. S. A. Faraghat, K. F. Hoettges, M. K. Steinbach, D. R. van der Veen, W. J. Brackenbury, E. A. Henslee, F. H. Labeed, M. P. Hughes, High-throughput, low-loss, low-cost, and label-free cell separation using electrophysiology-activated cell enrichment. *Proc Natl Acad Sci U S A* **114**, 4591-4596 (2017).
4. W. A. Bonner, H. R. Hulett, R. G. Sweet, L. A. Herzenberg, Fluorescence activated cell sorting. *Rev Sci Instrum* **43**, 404-409 (1972).
5. S. Miltenyi, W. Muller, W. Weichel, A. Radbruch, High gradient magnetic cell separation with MACS. *Cytometry* **11**, 231-238 (1990).
6. J. Pan, J. Wan, Methodological comparison of FACS and MACS isolation of enriched microglia and astrocytes from mouse brain. *J Immunol Methods* **486**, 112834 (2020).
7. A. Emad, R. Drouin, Evaluation of the impact of density gradient centrifugation on fetal cell loss during enrichment from maternal peripheral blood. *Prenat Diagn* **34**, 878-885 (2014).
8. J. R. Klim, A. J. Fowler, A. H. Courtney, P. J. Wrighton, R. T. Sheridan, M. L. Wong, L. L. Kiessling, Small-molecule-modified surfaces engage cells through the alphavbeta3 integrin. *ACS Chem Biol* **7**, 518-525 (2012).

9. J. R. Klim, L. Li, P. J. Wrighton, M. S. Piekarczyk, L. L. Kiessling, A defined glycosaminoglycan-binding substratum for human pluripotent stem cells. *Nat Methods* **7**, 989-994 (2010).
10. K. Schriebl, S. Lim, A. Choo, A. Tscheliessnig, A. Jungbauer, Stem cell separation: a bottleneck in stem cell therapy. *Biotechnol J* **5**, 50-61 (2010).
11. L. L. Kiessling, Chemistry-driven glycoscience. *Bioorg Med Chem* **26**, 5229-5238 (2018).
12. S. Li, C. Mo, Q. Peng, X. Kang, C. Sun, K. Jiang, L. Huang, Y. Lu, J. Sui, X. Qin, Y. Liu, Cell surface glycan alterations in epithelial mesenchymal transition process of Huh7 hepatocellular carcinoma cell. *PLoS One* **8**, e71273 (2013).
13. D. Wang, L. Wu, X. Liu, Glycan Markers as Potential Immunological Targets in Circulating Tumor Cells. *Adv Exp Med Biol* **994**, 275-284 (2017).
14. Y. Itakura, N. Sasaki, D. Kami, S. Gojo, A. Umezawa, M. Toyoda, N- and O-glycan cell surface protein modifications associated with cellular senescence and human aging. *Cell Biosci* **6**, 14 (2016).
15. M. Galvan, K. Murali-Krishna, L. L. Ming, L. Baum, R. Ahmed, Alterations in cell surface carbohydrates on T cells from virally infected mice can distinguish effector/memory CD8+ T cells from naive cells. *J Immunol* **161**, 641-648 (1998).
16. X. Liao, M. Makris, X. M. Luo, Fluorescence-activated Cell Sorting for Purification of Plasmacytoid Dendritic Cells from the Mouse Bone Marrow. *J Vis Exp*, (2016).
17. M. S. Johnson, N. Lu, K. Denessiouk, J. Heino, D. Gullberg, Integrins during evolution: evolutionary trees and model organisms. *Biochim Biophys Acta* **1788**, 779-789 (2009).
18. M. Barczyk, S. Carracedo, D. Gullberg, Integrins. *Cell Tissue Res* **339**, 269-280 (2010).
19. S. Huang, R. I. Endo, G. R. Nemerow, Upregulation of integrins alpha v beta 3 and alpha v beta 5 on human monocytes and T lymphocytes facilitates adenovirus-mediated gene delivery. *J Virol* **69**, 2257-2263 (1995).
20. H. J. Tanke, M. van der Keur, Selection of defined cell types by flow-cytometric cell sorting. *Trends Biotechnol* **11**, 55-62 (1993).
21. C. Tang, A. S. Lee, J. P. Volkmer, D. Sahoo, D. Nag, A. R. Mosley, M. A. Inlay, R. Ardehali, S. L. Chavez, R. R. Pera, B. Behr, J. C. Wu, I. L. Weissman, M. Drukker, An antibody against SSEA-5 glycan on human pluripotent stem cells enables removal of teratoma-forming cells. *Nat Biotechnol* **29**, 829-834 (2011).
22. F. Du, A. V. Garg, K. Kosar, S. Majumder, D. G. Kugler, G. H. Mir, M. Maggio, M. Henkel, A. Lacy-Hulbert, M. J. McGeachy, Inflammatory Th17 Cells Express Integrin alphavbeta3 for Pathogenic Function. *Cell Rep* **16**, 1339-1351 (2016).
23. O. Schnell, B. Krebs, E. Wagner, A. Romagna, A. J. Beer, S. J. Grau, N. Thon, C. Goetz, H. A. Kretzschmar, J. C. Tonn, R. H. Goldbrunner, Expression of integrin alphavbeta3 in gliomas correlates with tumor grade and is not restricted to tumor vasculature. *Brain Pathol* **18**, 378-386 (2008).
24. E. B. Voura, R. A. Ramjeesingh, A. M. Montgomery, C. H. Siu, Involvement of integrin alpha(v)beta(3) and cell adhesion molecule L1 in transendothelial migration of melanoma cells. *Mol Biol Cell* **12**, 2699-2710 (2001).
25. A. Perdih, M. S. Dolenc, Small molecule antagonists of integrin receptors. *Curr Med Chem* **17**, 2371-2392 (2010).

26. T. Boxus, R. Touillaux, G. Dive, J. Marchand-Brynaert, Synthesis and evaluation of RGD peptidomimetics aimed at surface bioderivatization of polymer substrates. *Bioorg Med Chem* **6**, 1577-1595 (1998).
27. S. L. Goodman, G. Holzemann, G. A. Sulyok, H. Kessler, Nanomolar small molecule inhibitors for alphav(beta)6, alphav(beta)5, and alphav(beta)3 integrins. *J Med Chem* **45**, 1045-1051 (2002).
28. R. M. Owen, C. B. Carlson, J. Xu, P. Mowery, E. Fasella, L. L. Kiessling, Bifunctional ligands that target cells displaying the alpha v beta3 integrin. *Chembiochem* **8**, 68-82 (2007).